THE UNIVERSITY OF MANITOBA

INFLUENCE OF CHORD PRELOAD ON BEHAVIOUR OF TUBULAR TRUSS JOINTS WITH CROPPED WEBS

by

CHEUK FAI NG

A THESIS

SUBMITTED TO THE FACULTY OF GRADUATE STUDIES

IN PARTIAL FULFILMENT OF THE REQUIREMENTS FOR THE DEGREE OF

MASTER OF SCIENCE IN CIVIL ENGINEERING

WINNIPEG, MANITOBA

CANADA

APRIL 1980

INFLUENCE OF CHORD PRELOAD ON BEHAVIOUR OF TUBULAR TRUSS JOINTS WITH CROPPED WEBS

BY

CHEUK FAI NG

A thesis submitted to the Faculty of Graduate Studies of the University of Manitoba in partial fulfillment of the requirements of the degree of

MASTER OF SCIENCE

ABSTRACT

An experimental investigation of the influence of variation of combined compressive axial and bending loads in chords on the statical behaviour of cropped-web joints is described. The joints had square hollow sections as chord members and round hollow sections with cropped ends as web members. Chord compressive axial forces and bending moments were used to simulate the overall truss action. Tests of eight isolated joints with a Pratt-truss configuration are reported. Equations obtained by the use of the least square method to relate the strengths and stiffnesses of the joints to the additional loading in chords are presented. The joints failed due to excessive deformation of the chord face at the joint, accompanied by an in-plane buckling of the compression web member. The strengths of the joints decreased with an increase in chord preload. The yield strengths of the preloaded joints were approximately two to twenty-six percent lower than those of similar non-preloaded joints, while the ultimate strengths were about one to fifteen percent less. The compression stiffnesses of the joints were rarely affected by the chord preload, while the tension stiffnesses decreased with an increase in chord preload. The effect of preload was much more significant for joints involving thin chords than for those with thick chords.

ACKNOWLEDGEMENT

The author wishes to express his profound gratitude to Dr. Glenn Morris, Professor and Head of the Department of Civil Engineering, for his extensive guidance and assistance in this project.

Special appreciation goes to Dr. Y. Yoshida, Professor of Civil Engineering Department, Tokyo Institute of Technology (Tokyo Kogyo Daigaku), for his encouragement and generous provision of valuable information.

The author wishes to thank Mr. E. Lemke, Mr. M. McVey and the laboratory staff of the Civil Engineering Department for their assistance in the fabrication and testing of the specimens.

Thanks are due to Mrs. P. Giardino for her excellent work in typing the thesis.

The assistance of the Steel Company of Canada in the supply of materials is also gratefully acknowledged.

Special recognition is extended to the authors of the many excellent papers and books on tubular joints which sparked the author's ideas.

The author is deeply indebted to his mother, S.H. Wong, who has been a constant source of support and encouragement.

Finally, the author owes the deepest gratitude to his wife, T.T. Trinh, who has provided him a strong impetus toward continuing his efforts to further his studies in Canada. He is most grateful to her, not only for her unending patience, understanding, and encouragement during preparation of the work, but also for her services as draftsperson and photographer.

TABLE OF CONTENTS

		Page
ABSTRACT		i
ACKNOWLEDGEMENT		ii
LIST OF TABLES		vi
LIST OF FIGURES		vii
LIST OF SYMBOLS		xii
CHAPTER		
1	GENERAL INTRODUCTION	1
	1.1 Introduction	1
	1.2 Performance of H.S.S. Truss Joints	8
	1.2.1 Performance criteria	8
	1.2.2 Parameters affecting joint performance	9
	1.2.3 Modes and criteria of failure	13
	1.3 Previous Research on H.S.S. Truss Joints	15
	1.3.1 Behaviour of conventional and cropped-web tubular truss joints	15
	1.3.2 Effect of chord preload	17
	1.3.3 Comparison of behaviour of truss joints and isolated joint specimens	17
	1.4 Scope of Study	20
	1.5 Assumptions and Limitations	20
2	DESIGN AND FABRICATION OF TEST SPECIMENS	22
	2.1 Choice of Joint	22

CHAPTER Page

2.2 Specimen Designation 22
2.3 Materials 27
2.4 Joint Fabrication 27

3 TEST PROCEDURE 32
3.1 Test Equipment 32
3.1.1 Loading frame 32
3.1.2 Prestressing system 32
3.2 Instrumentation 35
3.2.1 Deformation measurement 35
3.2.2 Strain measurement 38
3.2.3 Data acquisition 38
3.3 Testing Procedures 38

4 TEST RESULTS AND DISCUSSIONS 46
4.1 Test Series 3B50-I to 3B50-IV 46
4.1.1 Local chord face deformation 46
4.1.2 Buckling of compression web members 51
4.1.3 Strains of chord faces 53
4.1.4 Strains in compression web members 57
4.1.5 Strains in tension web members 60
4.1.6 Failure modes 63
4.1.7 Joint strength 69
4.1.8 Joint stiffness 79

CHAPTER Page

4.2 Test Series 4B50-I to 4B50-IV 82

4.2.1 Local chord face deformation 82

4.2.2 Buckling of compression web members 86

4.2.3 Strains of chord faces 86

4.2.4 Strains in compression web members 90

4.2.5 Strains in tension web members 90

4.2.6 Failure modes 94

4.2.7 Joint strength 100

4.2.8 Joint stiffness 107

5 CONCLUSIONS AND RECOMMENDATIONS 111

5.1 Conclusions 111

5.2 Design Recommendations 114

5.3 Recommendations for Future Research 115

REFERENCES 116

APPENDIX A - COMPREHENSIVE REVIEW OF PREVIOUS RESEARCH ON TUBULAR TRUSS JOINTS 123

APPENDIX B - EXISTING DESIGN SPECIFICATIONS 138

APPENDIX C - MATERIAL TESTING 140

APPENDIX D - CALIBRATION OF PRESTRESSING BARS 148

APPENDIX E - MEASUREMENT OF TENSILE FORCES IN PRESTRESSING BARS 153

LIST OF TABLES

Table		Page
2.1	Specimen Properties	25
3.1	Magnitudes of Preload in Chord	45
4.1	Test Results - Test Series 3B50	73
4.2	Test Results - Test Series 4B50	102

LIST OF FIGURES

Figure		Page
1.1	A Tubular Truss Bridge	2
1.2	A Tubular Space Frame	2
1.3	A Profiled X-type Joint	3
1.4	A Profiled NK-type Joint	3
1.5	Joints with Gusset Plate	5
1.6	A Sawn N-type Joint	6
1.7	A Cropped N-type Joint	6
1.8	Various Types of Connectors	7
1.9	Parameters Affecting Joint Behaviour	10
1.10	Joint Eccentricity	12
1.11	A Typical Test Specimen	16
1.12	Chord Preload, P_o	18
2.1	Pratt-truss and Test Specimen	23
2.2	Test Specimen 3B50	24
2.3	Test Specimen 4B50	24
2.4	Cropping Machine	28
2.5	Cropping of Tension Web	28
2.6a	Welding Jig	30
2.6b	Welding Jig	30
2.7	Welding Specification	31
3.1	Loading Frame	33
3.2	Prestressing System	34

Figure		Page
3.3	Transducer Locations on Chord Wall	36
3.4	Transducer Locations on Compression Web	36
3.5	Transducer Assembly	37
3.6	Strain Gauge Locations on Specimens 3B50-I to 3B50-III and Specimens 4B50-I to 4B50-III	39
3.7	Strain Gauge Locations on Specimen 3B50-IV	40
3.8	Strain Gauge Locations on Specimen 4B50-IV	41
3.9a	Schematic Diagram of Data Acquisition System	42
3.9b	Data Acquisition System	43
4.1	Deflection Profiles of Loaded Chord Face of Specimen 3B50-I	47
4.2	Mechanism of Chord-wall Rotation	48
4.3	Comparison of Chord Face Deformation of Specimens 3B50-I to 3B50-IV at Ultimate Load	50
4.4	Load-deformation Behaviour Near the Extremities of Tension Webs of Specimens 3B50-I to 3B50-IV	52
4.5	Deflection Profiles of Compression Web of Specimen 3B50-I	54
4.6	Transverse Strains on Loaded Chord Face of Specimen 3B50-I	55
4.7	Transverse Strains on Loaded Chord Faces of Specimens 3B50-I to 3B50-IV	56
4.8	Longitudinal Strains on Loaded Chord Faces of Specimens 3B50-I to 3B50-IV	58
4.9	Longitudinal Strains on Compression Web Member of Specimen 3B50-IV	59
4.10	Longitudinal Strains on Tension Web Member of Specimen 3B50-IV	61

Figure		Page
4.11	Deformation Profiles of Tension Web Member of Specimen 3B50-IV	62
4.12	Failure Mode A - Local Deformation of Loaded Chord Face of Specimen 3B50-I	64
4.13	Failure Mode A - Local Deformation of Loaded Chord Face of Specimen 3B50-IV	64
4.14	Failure Mode B - Buckling of Compression Web Member of Specimen 3B50-I	66
4.15	Failure Mode B - Buckling of Compression Web Member of Specimen 3B50-IV	66
4.16	Failure Mode C - Fracture of Weld at the Toe of Tension Web Member or Tearing of Tension Web Member of Specimen 3B50-III	67
4.17	Failure Mode C - Fracture of Weld at the Toe of Tension Web Member or Tearing of Tension Web Member of Specimen 3B50-IV	67
4.18	Failure Mode D - Buckling of Chord Specimen 3B50-IV	68
4.19	The Author's Method of Finding Joint Yield Strength	70
4.20	Akiyama's Method of Finding Joint Yield Strength	70
4.21	Load-deformation Behaviour of Specimens 3B50-I to 3B50-IV	72
4.22	Reduction Coefficient of Joint Yield Strength	77
4.23	Reduction Coefficient of Joint Ultimate Strength	78
4.24	Joint Efficiency	80
4.25	Definition of Joint Stiffness	81

Figure		Page
4.26	Joint Stiffness	83
4.27	Deflection Profiles of Loaded Chord Face of Specimen 4B50-I	84
4.28	Comparison of Chord Face Deformation of Specimens 4B50-I to 4B50-IV at Ultimate Load	85
4.29	Deflection Profiles of Compression Web of Specimen 4B50-I	87
4.30	Deflection Profiles of Compression Web of Specimen 4B50-IV	88
4.31	Longitudinal Strains on Chord Face of Specimen 4B50-IV Due to Preload and Load Transfer Between Members	89
4.32	Transverse Strains on Loaded Chord Face of Specimen 4B50-IV Due to Preload and Load Transfer Between Members	91
4.33	Longitudinal Strains on Compression Web Member of Specimen 4B50-IV	92
4.34	Longitudinal Strains on Tension Web Member of Specimen 4B50-IV	93
4.35	Deformation Profiles of Tension Web Member of Specimen 4B50-IV	95
4.36	Failure Mode A - Excessive Local Chord Deformation of Specimen 4B50-I	96
4.37	Failure Mode A - Excessive Local Chord Deformation of Specimen 4B50-IV	96
4.38	Failure Mode B - Buckling of Compression Web Member of Specimen 4B50-II	97
4.39	Failure Mode B - Buckling of Compression Web Member of Specimen 4B50-IV	97
4.40	Failure Mode C - Fracture of Weld at the Toe of Tension Web Member or Tearing of Tension Web Member of Specimen 4B50-II	98

Figure		Page
4.41	Failure Mode C - Fracture of Weld at the Toe of Tension Web Member or Tearing of Tension Web Member of Specimen 4B50-III	98
4.42	Failure Mode D - Buckling of Chord of Specimen 4B50-IV	99
4.43	Failure Mode E - Fracture of Compression Web Member of Specimen 4B50-IV	99
4.44	Load-Deformation Behaviour of Specimens 4B50-I to 4B50-IV	101
4.45	Reduction Coefficient of Joint Yield Strength	105
4.46	Reduction Coefficient of Joint Ultimate Strength	106
4.47	Joint Efficiency	108
4.48	Joint Stiffness	109

LIST OF SYMBOLS

Symbol	
A	Cross-sectional area; or failure by excessive deformation of loaded chord face
A_o, A_1, A_2	Cross-sectional areas of chord, compression web, and tension web, respectively
B	Failure by buckling of compression web member
b_o	Outside width of chord
C	Fracture of weld at the toe of tension web or tearing of tension web
D	Buckling of chord
d	Average outside diameter of compression and tension webs
d_o, d_1, d_2	Outside diameters of chord, compression web, and tension web, respectively
E	Modulus of elasticity (207,000 MPa); or fracture of compression web at its toe
e	Eccentricity of joint, equal to distance between the point of intersection of the web axes and the chord axis
E_{ff}	Joint efficiency, equal to $N_{u2}/A_2\ \sigma_{e2}$
F_1, F_2, F_3, F_4	Tensile forces in prestressing bars
g	Gap between the compression and tension webs measured along the chord face
h_o	Outside depth of a rectangular chord
k_1, k_2	Stiffness of a cropped-web joint along the compression and tension web axis, respectively
kN	Kilo-Newton(s)
L_1, L_2, L_3	Member length
LVDT	Linear voltage displacement transducer(s)

Symbol	
m	Meter(s)
mm	Millimeter(s)
MPa	Megapascal(s)
M_o	Preload bending moment in chord
N	Newton(s)
n	Percentage of preload, equal to σ_o/σ_e
N_1, N_2	Linear forces along compression and tension web axes, respectively, at the loaded chord face
Nm	Newton-meter
N/mm^2	Newton(s) per square millimeter
N_{u1}, N_{u2}	Ultimate loads in compression and tension webs, respectively
O_g	Gap, equal to g/d_2
O_v	Overlap, equal to q/d_2
Pa	Pascal(s)
P_1, P_2	Axial forces in the chord on either side of the joint
P_o	Preload axial compressive force in chord
P_u	Ultimate strength of a preloaded joint
P_{uo}	Ultimate strength of a non-preloaded joint
P_y	Yield strength of a preloaded joint
P_{yo}	Yield strength of a non-preloaded joint
q	Overlap length of a tension web
RLC	Prestressing bar load cell
t	Average thickness of compression and tension webs
t_o,t_1,t_2	Thicknesses of chord, compression web, and tension web, respectively

Symbol	
α	Reduction coefficient of joint yield strength, equal to P_y/P_{yo}
β	Reduction coefficient of joint ultimate strength, equal to P_u/P_{uo}
δ_1, δ_2	Displacement along compression and tension web axes at loaded chord face
θ_1, θ_2	Angles of intersection of compression and tension webs with chord
σ_e	Yield stress (at 0.2% offset) of chords
σ_{e1}, σ_{e2}	Yield stresses (at 0.2% offset) of compression and tension webs, respectively
σ_o	Stress in chord due to preload
σ_{ult}	Ultimate stress of chord
$\sigma_{ult1}, \sigma_{ult2}$	Ultimate stress of compression and tension webs, respectively

CHAPTER 1

GENERAL INTRODUCTION

1.1 Introduction

In recent years, hollow structural sections (H.S.S.) have become increasingly popular in truss and space frame construction. This is because H.S.S. have many advantages over conventional rolled sections. H.S.S. have excellent buckling and torsional resistance compared to any conventional sections of the same cross-sectional area. Their small drag coefficients offer lower resistance to fluid flow and thereby reduce wind or wave loadings.

H.S.S. have other advantages. Their closed, smooth cross-sections minimize the costs of painting and maintenance, as well as fire and corrosion protection. Structures fabricated from H.S.S. offer an exceptionally neat and pleasing appearance, free of the usual mass of protruding rivets, gussets or bolts (see Fig. 1.1 and Fig. 1.2). This aesthetic appeal makes H.S.S. ideal for use where the exposing of structural members is essential.

However, a major disadvantage to the use of H.S.S. in trusses is the relatively high cost and difficulty of fabrication of the joints. The ends of the web members require careful and accurate profiling in order to match the chord face (see Fig. 1.3 and Fig. 1.4). This is especially difficult when circular webs connect directly to a circular chord. Moreover, the welding of the members is fairly difficult in the acute angles between web and chord members. In general, the number of man hours required for the fabrication of such tubular members is 50 percent greater than that required for conventional rolled sections (Tada 1961).

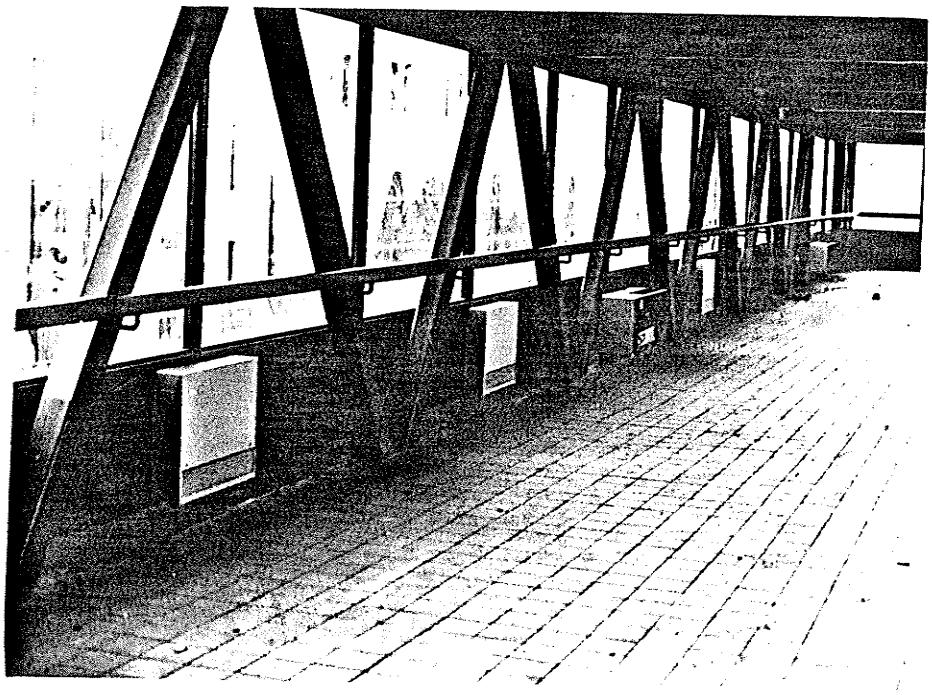

Fig. 1.1 A TUBULAR TRUSS BRIDGE

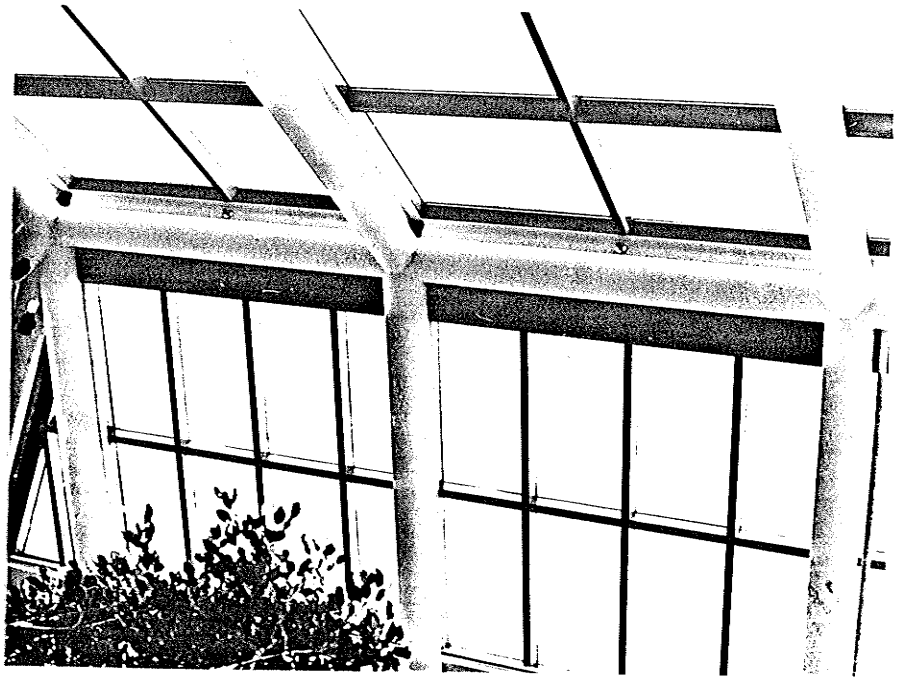

Fig. 1.2 A TUBULAR SPACE FRAME

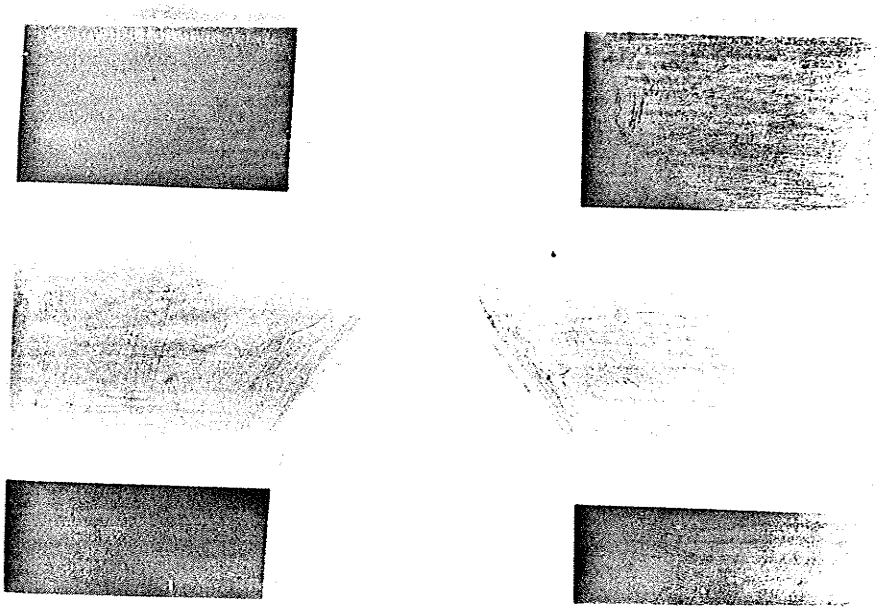

Fig. 1.3 A Profiled X-type Joint

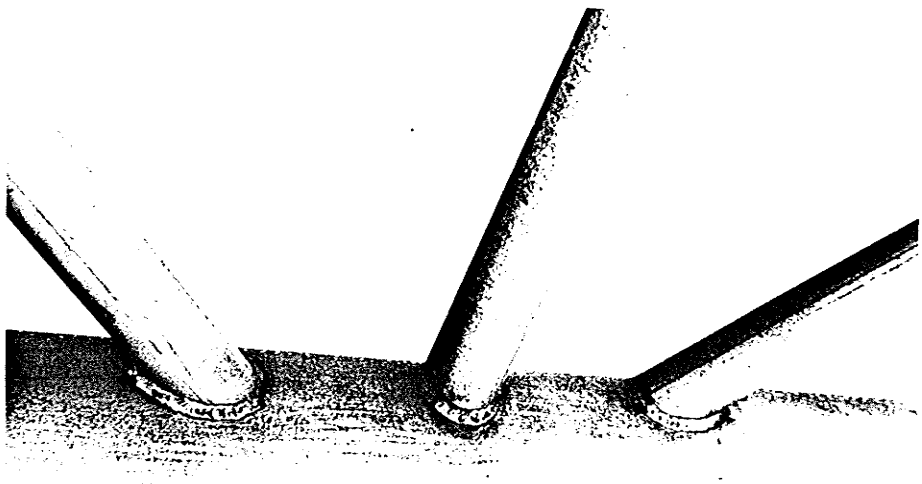

Fig. 1.4 A Profiled NK-type Joint

Several methods such as using automatic profiling machines, gusset plates, rectangular tubes, and connectors have been applied to solve the fabrication difficulties.

Automatic profiling can efficiently profile the ends of tubes, but such end preparation is not economical for members smaller than 4 inches in diameter and the machine cannot be used for a chord diameter smaller than 6 inches (Anonymous 1961).

As illustrated in Figure 1.5, gusset plates in the plane of a truss have been used to eliminate profiling. However, they tend to cause high stress concentrations in the tube wall near the ends of the gusset plate (Bouwkamp 1964), and extra welding for connecting the gusset plate to the chord member is required.

Profiling can be avoided by using rectangular H.S.S. as chord members. Their flat faces permit round or rectangular tubes to be welded directly to them (see Fig. 1.6). However, this is possible only if the webs do not overlap.

Connectors can also be used to eliminate profiling (see Fig. 1.8). The spherical or the short-tube connector selected are of sufficient diameter to accommodate the branches without difficult profiling. However, when connectors are used, the structure may lose part of its aesthetic appeal. Moreover, the weight and cost of the structure may thereby be increased.

A recent proposal to overcome the difficulty in fabricating tubular truss joints is end-cropping. Cropping is accomplished by means of a cropping tool which has two V-shaped steel blades that simultaneously flatten and cut a circular tube. The process is fast and simple. No special training of

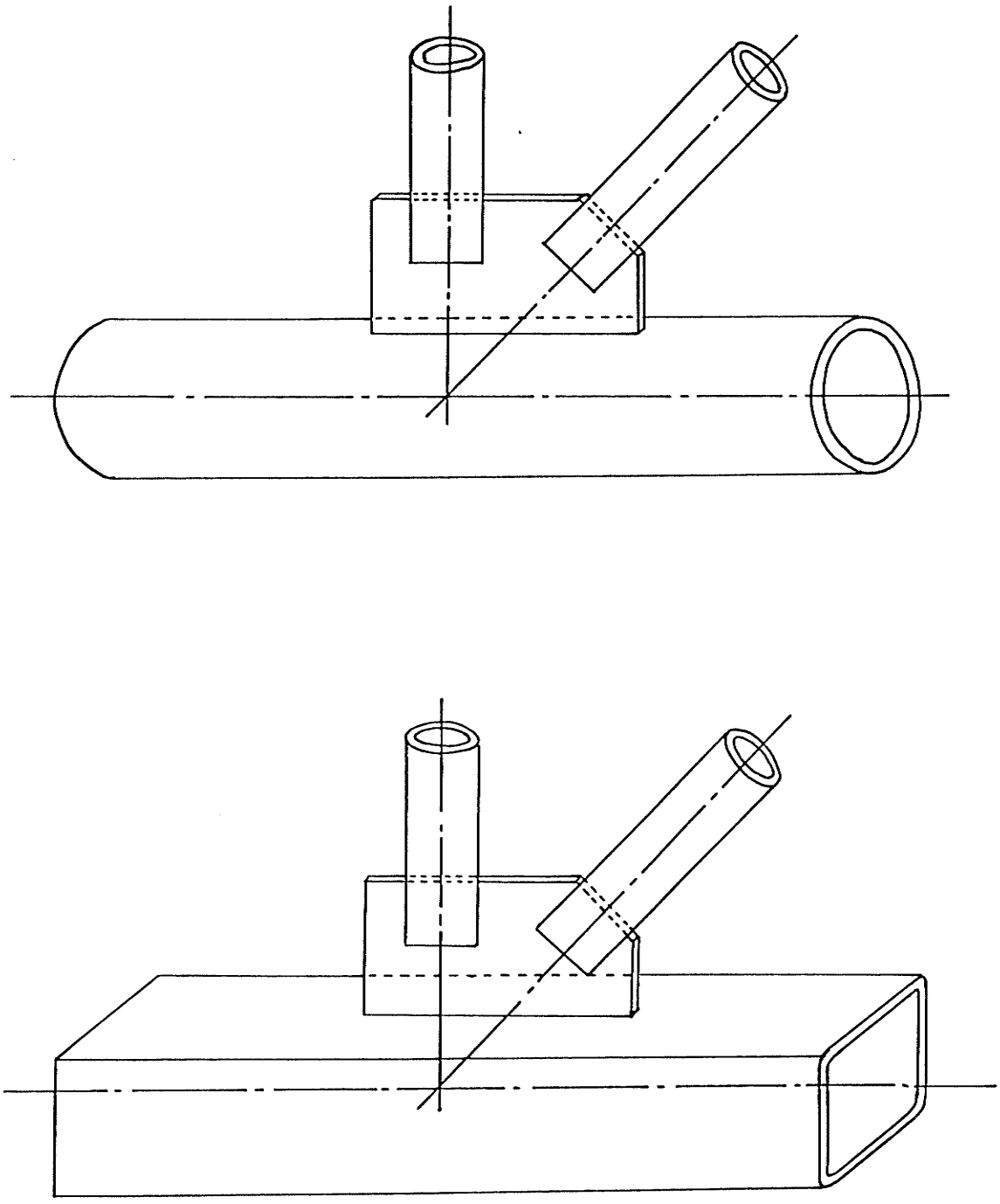

Fig. 1.5 Joints with Gusset Plate

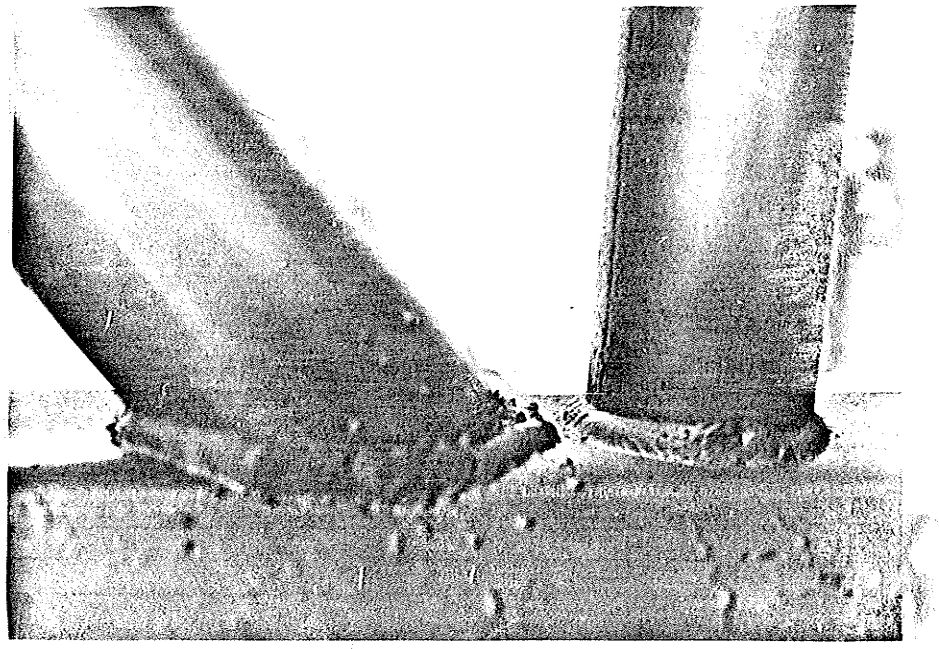

Fig. 1.6 A Sawn N-type Joint

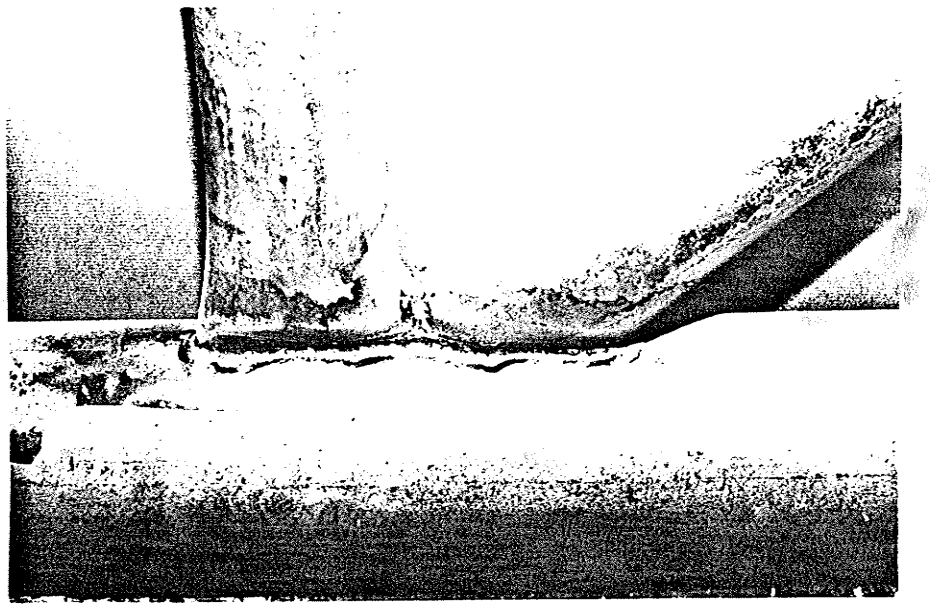

Fig. 1.7 A Cropped N-type Joint

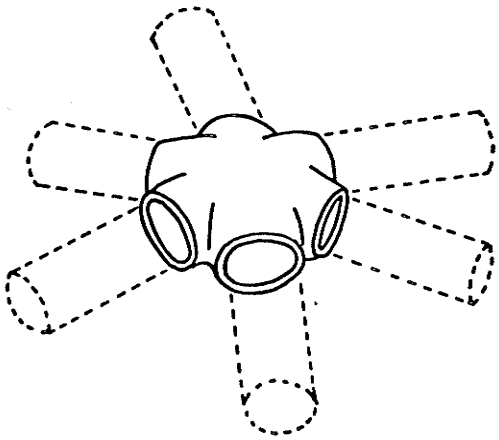

a. Welded Cast Steel Connector

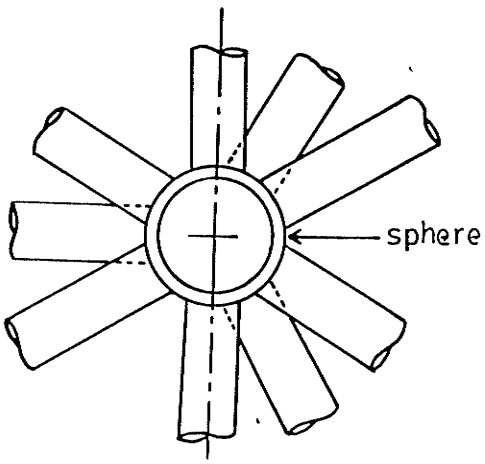

b. Cast Steel Spherical Connector

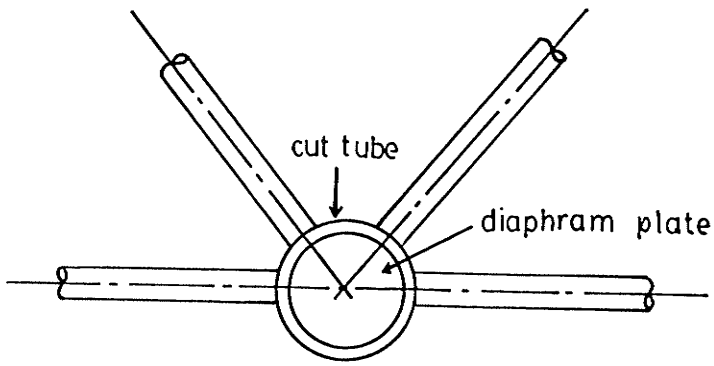

c. Short Tube Stiffened with a Diaphram Plate

Fig. 1.8 Various Types of Connectors

fabricators is necessary. Moreover, the welding of the joint is greatly simplified, since only simple fillet welding along straight lines is required. Thus, a relatively economical tubular joint can be obtained (see Fig. 1.7).

However, the behaviour of cropped-web joints has not been thoroughly investigated. Additional investigation of their behaviour is essential before they can be used safely in important structures.

This study deals with the statical behaviour of tubular truss joints between round end-cropped web members and square chords.

1.2 Performance of H.S.S. Truss Joints

1.2.1 Performance criteria

In general, the performance of H.S.S. joints can be characterized by joint efficiency, joint load factor and joint stiffness.

Jamm (1951), Bouwkamp (1968) and Hlavacek (1973) have defined the joint efficiency as the ratio of the failure load for the joint to the ultimate strength of the tension web member. Cran et al. (1971) and Thiensiripipat et al. (1979) have defined it in terms of the yield load of the tension web member, rather than its ultimate strength.

Eastwood et al. (1970) have defined the joint load factor as the ratio of the failure load for the joint to its design load. Since either the tension web or the compression web may govern the design, the joint strength can be represented in terms of a tension load factor or a compression load factor.

Joint stiffness is represented as the initial slope of the load-deformation curve.

1.2.2 Parameters affecting joint performance

As illustrated in Fig. 1.9, a simple tubular truss joint usually consists of a number of web members welded directly to a larger-diameter chord member. There is either an overlap of the web members or a gap between them. The parameters which affect the load-deformation behaviour of the joint include:

(1) t_o/b_o - ratio of chord wall thickness to its width or outside diameter;

(2) d/b_o - ratio of web diameter or width to chord width or diameter;

(3) e - eccentricity; i.e., the distance from the intersection of the webs to the chord axis;

(4) O_v or O_g - overlap or gap;

(5) θ_1 and θ_2 - angles of intersection;

(6) t/d - ratio of web thickness to its diameter or width; and,

(7) P_o and M_o - preload in chord member.

The parameter t_o/b_o gives a measure of the radial stiffness of the chord wall. The bending strength and punching shear strength of the chord tube are greatly dependent on this factor.

The parameter d/b_o is a measure of how concentrated the web loading is. The load distribution on the loaded chord face and the web member forces transmitted to the side walls of the chord are influenced by the relative magnitude of the chord and web diameters. Moreover, the greater

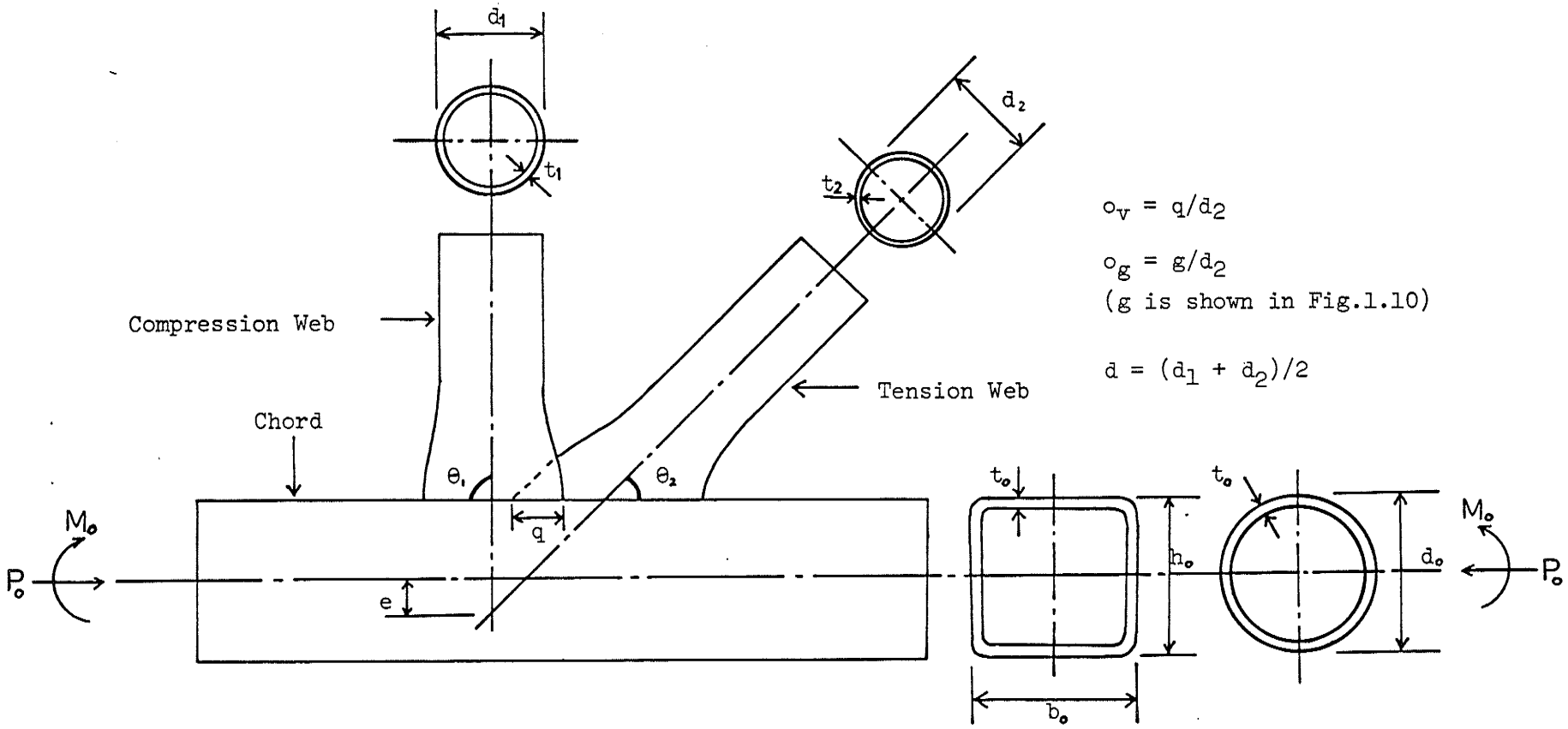

Fig. 1.9 Parameters Affecting Joint Behaviour

this factor, the greater the restraining effects due to the welding of the joint.

The eccentricity e may be negative, zero or positive, as shown in Fig. 1.10. It is negative if the web member axes intersect before meeting the chord axis, and positive if they intersect beyond the chord axis. When the web and chord axes are concurrent, the joint has zero eccentricity. If there is an eccentricity, a bending moment of the magnitude $(P_1 - P_2)e$ is introduced in the joint, where P_1 and P_2 are the axial loads in the chord on either side of the joint.

The overlap is defined as $o_v = q/d_2$. Similarly, the gap is defined as $o_g = g/d$. If there is an overlap, o_v, there is a direct load transfer between the web members. In general, there is an overlap of the web members for joints with negative eccentricity, and a gap for joints with positive eccentricity.

The parameters θ_1 and θ_2 affect the performance of a joint, since the values of the normal and longitudinal components of the web force applied to the chord wall change with a variation in θ_1 and θ_2.

The parameter t/d is a measure of the bending stiffnesses of the web members. The larger this factor, the stiffer the webs and the larger the end restraint on the chord. Moreover, this parameter affects the resistance to both local and overall buckling of the web member.

Finally, the axial stress in the chord due to the axial force P_o and bending moment M_o resulting from overall truss action are additive to those due to the forces in the web members. They therefore influence joint performance.

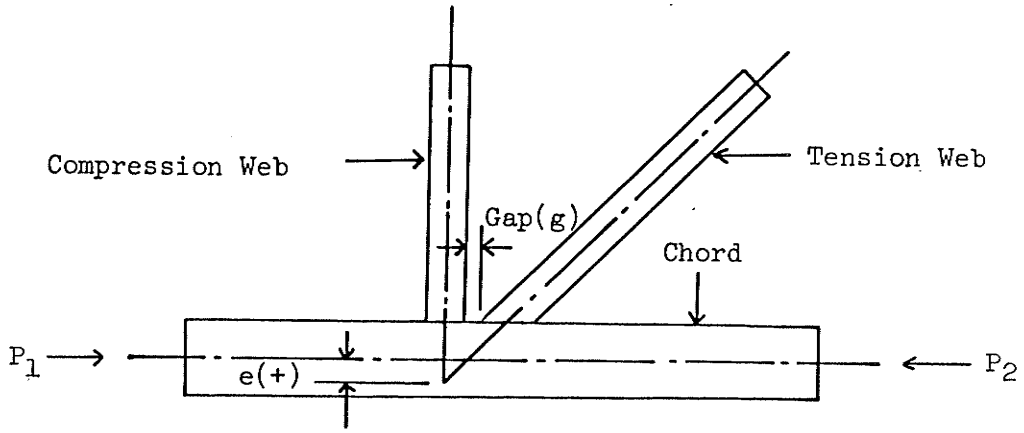

a. Positive Eccentricity

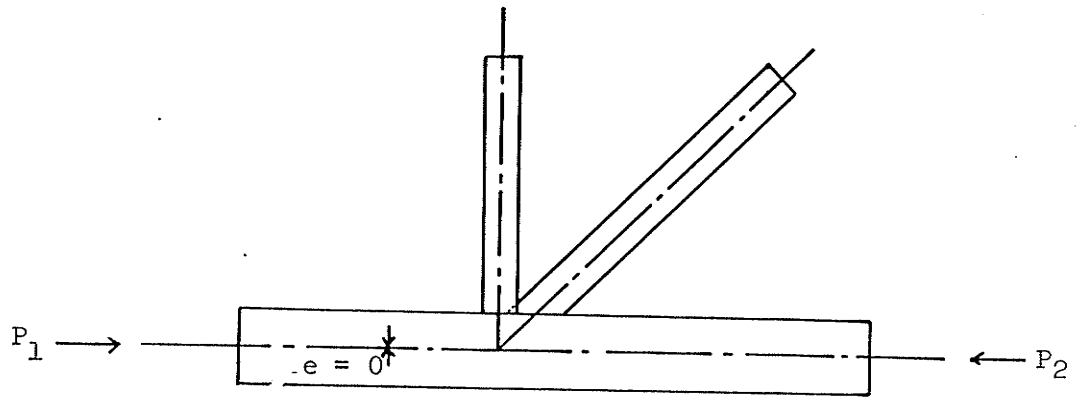

b. Zero Eccentricity

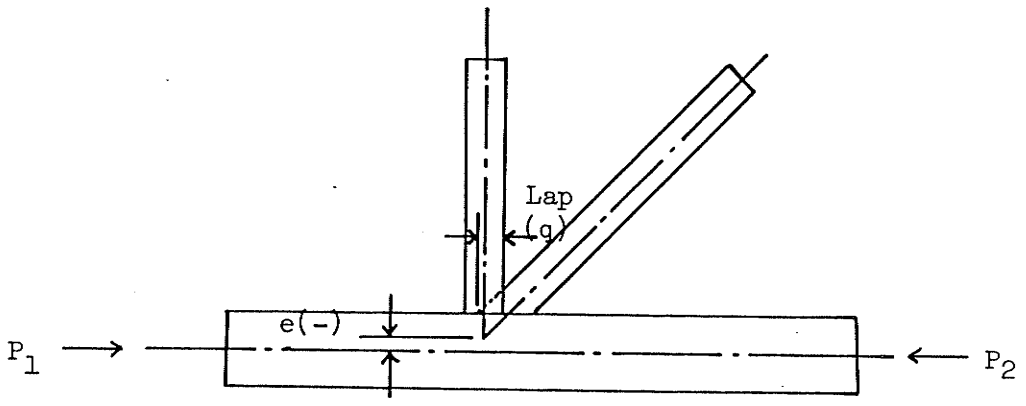

c. Negative Eccentricity

Fig. 1.10 Joint Eccentricity

1.2.3 Modes and criteria of failure

Tests on tubular truss joints by many investigators have shown that there are several different modes of failure. They include the following:

(1) Excessive local deformation of the loaded chord face
(Jamm 1951; Anderson 1961; Washio et al. 1961; Naka et al. 1961; Kaneya 1965; Bouwkamp 1968; Eastwood et al. Dec. 1969; Dasgupta 1970; Hlavacek 1973; Okumura et al. 1973; Morris et al. 1974; Ghosh 1978).

(2) In-plane buckling of compression web member
(Anderson 1961; Eastwood et al. Nov. 1967; Dasgupta 1970; Hlavacek 1973; Morris et al. 1974).

(3) Tearing of tension web member
(Washio et al. 1961; Bouwkamp 1968; Dasgupta 1970; Hlavacek 1973; Morris et al. 1974; Ghosh 1978).

(4) Fracture in welds
(Jamm 1951; Anderson 1961; Eastwood et al. Nov. 1967; Washio et al. Jun 1968; Dasgupta 1970; Hlavacek 1973).

(5) In-plane buckling of chord member
(Anderson 1961; Naka et al. 1961; Eastwood et al. Nov. 1967).

(6) Local buckling of compression web member
(Washio et al. 1961; Eastwood et al. 1969; Hlavacek 1973).

(7) Out-of-plane buckling of compression web member
(Anderson 1961; Ghosh 1978).

(8) Tearing of chord wall
(Bouwkamp 1968; Dasgupta 1970).

(9) Out-of-plane buckling of chord
(Anderson 1961).

(10) Local bending of tension web
(Anderson 1961).

A tubular joint can exhibit any of these modes of failure or a combination of them, depending upon the geometric parameters of the joint, the arrangement of its members and the loading.

For every type of failure listed above, there can be a failure criterion. However, the most commonly observed mode of failure has been excessive local deformation of the chord face, usually accompanied by a rotation of the web members, which induces either a buckling of the compression web member, a tearing of the tension web member or a combination of these. Consequently, chord face deformation has been used by many investigators as the primary failure criterion.

Eastwood et al. (1967) used a loaded chord face deformation of 0.05 inch as a failure criterion. This value was chosen quite arbitrarily, based on the assumption that such a deformation was very clearly visible and would possibly be regarded as the equivalent of a failure in practice.

Anderson (1961), Washio et al. (1961), Bouwkamp (1968), and Akiyama et al. (1974) used buckling, tension failure and weld fracture as ultimate failure criteria.

1.3 Previous Research on H.S. Truss Joints

A comprehensive review of experimental and analytical research on the behaviour of tubular truss joints is contained in Appendix A. The research that relates to the topic of this study is briefly reviewed in this section.

1.3.1 Behaviour of conventional and cropped-web tubular truss joints

Most testing of tubular truss joints has been done on isolated joint specimens (Jamm 1951; Anderson 1961; Washio 1961, 1963, 1968; Eastwood et al. 1967, 1970; Bouwkamp 1964, 1968; Hlavacek 1973; Thiensiripipat et al. 1979). The typical specimen consisted of a joint plus portions of the webs and chord extending half-way to adjacent joints (see Fig. 1.11). This was based on an assumption that secondary moments in trusses produce a point of inflection at mid-length of all members.

Most of the investigations have shown that the strength of either a profiled- or cropped-web tubular joint is increased by an increase in t_o/d_o, the ratio of the thickness to diameter of the chord member, d/d_o, the ratio of the web diameter to chord diameter, q/d_2, the ratio of web member overlap to diameter, or e(-), the negative eccentricity.

Jamm (1951) and Anderson (1961) found that flattened-web joints and cropped-web joints with circular chords had strengths similar to those of conventional profiled joints. Washio et al. (1961) and Hlavacek (1973), however, found that flattened-web joints had lower strengths than did profiled joints.

Thiensiripipat et al. (1979) tested 34 N-type joints with square chords and round end-cropped webs. They found that the strengths of

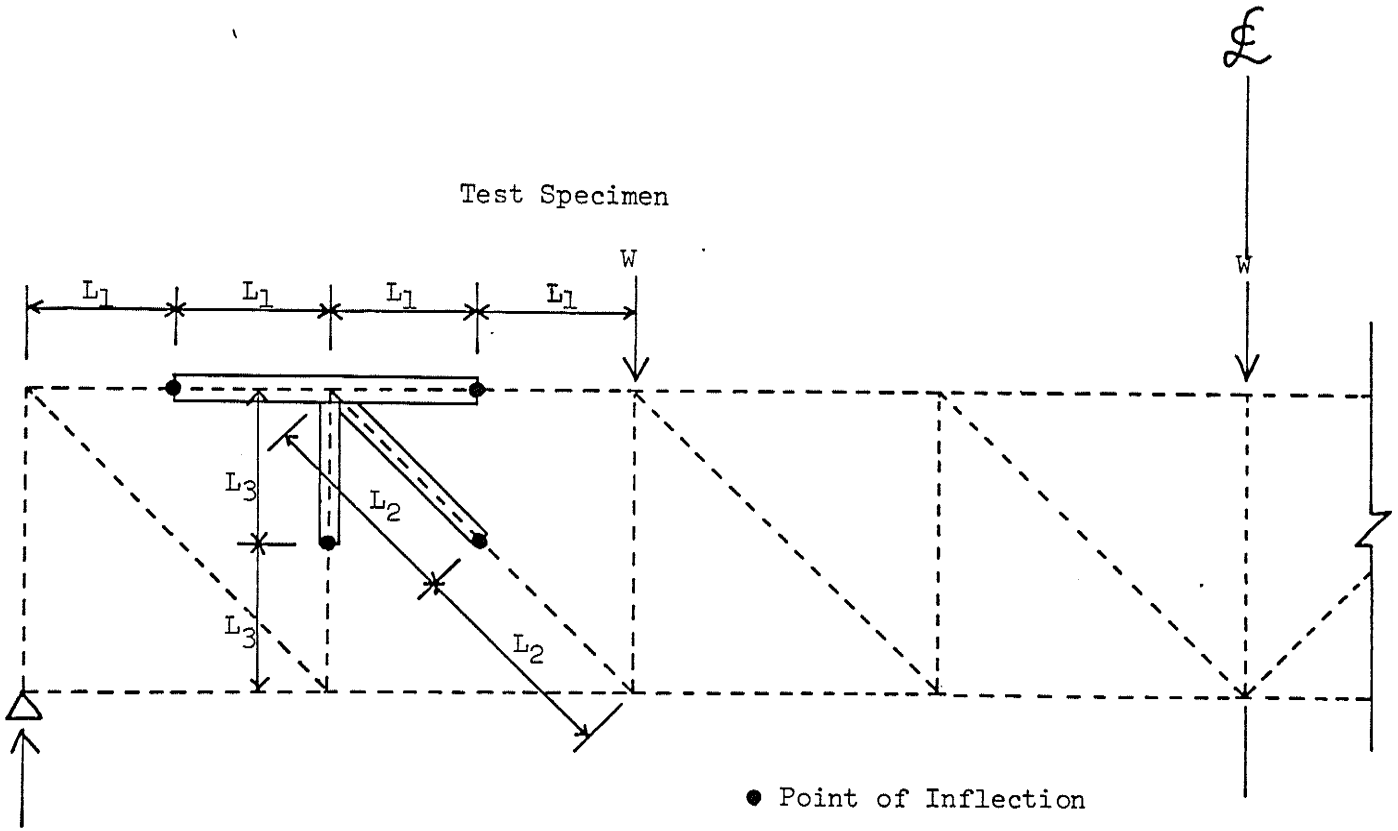

Fig. 1.11 A Typical Test Specimen

cropped-web joints were comparable to those of conventional gap joints.

1.3.2 Effect of chord preload

In practice, as a truss is loaded, large axial forces and secondary moments due to truss deflections occur in the chord members. In order to simulate this condition in isolated joint specimens, some researchers (Eastwood et al. 1961; Bouwkamp 1968; Washio et al. 1968; Mee 1969) have employed a chord preload P_o. This is illustrated in Fig. 1.12.

Eastwood et al. (1961), Bouwkamp (1968) and Mee (1969) found that the compressive loads on the chord had little effect on the strength of a profiled joint. Washio et al. (1968) found that compressive loads in the chord decreased the joint strength considerably, while tensile loads scarcely influenced it.

There is no general agreement among the researchers on the effect of chord preload. Moreover, there is little or no information about the effect of chord preload on the behaviour of cropped-web joints.

1.3.3 Comparison of behaviour of truss joints and isolated joint specimens

Dasgupta (1970) tested 11 full-scale tubular trusses with spans of about 20 feet (6.1m) to examine the behaviour of gap joints with circular, profiled web members and a rectangular chord member. The results were compared with those for isolated joints tested by Eastwood et al. (1967). The failure loads of the joints in the truss tests were approximately 25 to 30 percent lower than those in isolated joint tests. Dasgupta reported that the difference was due to the improper representation of truss conditions in the Sheffield work. The isolated joint tests were based

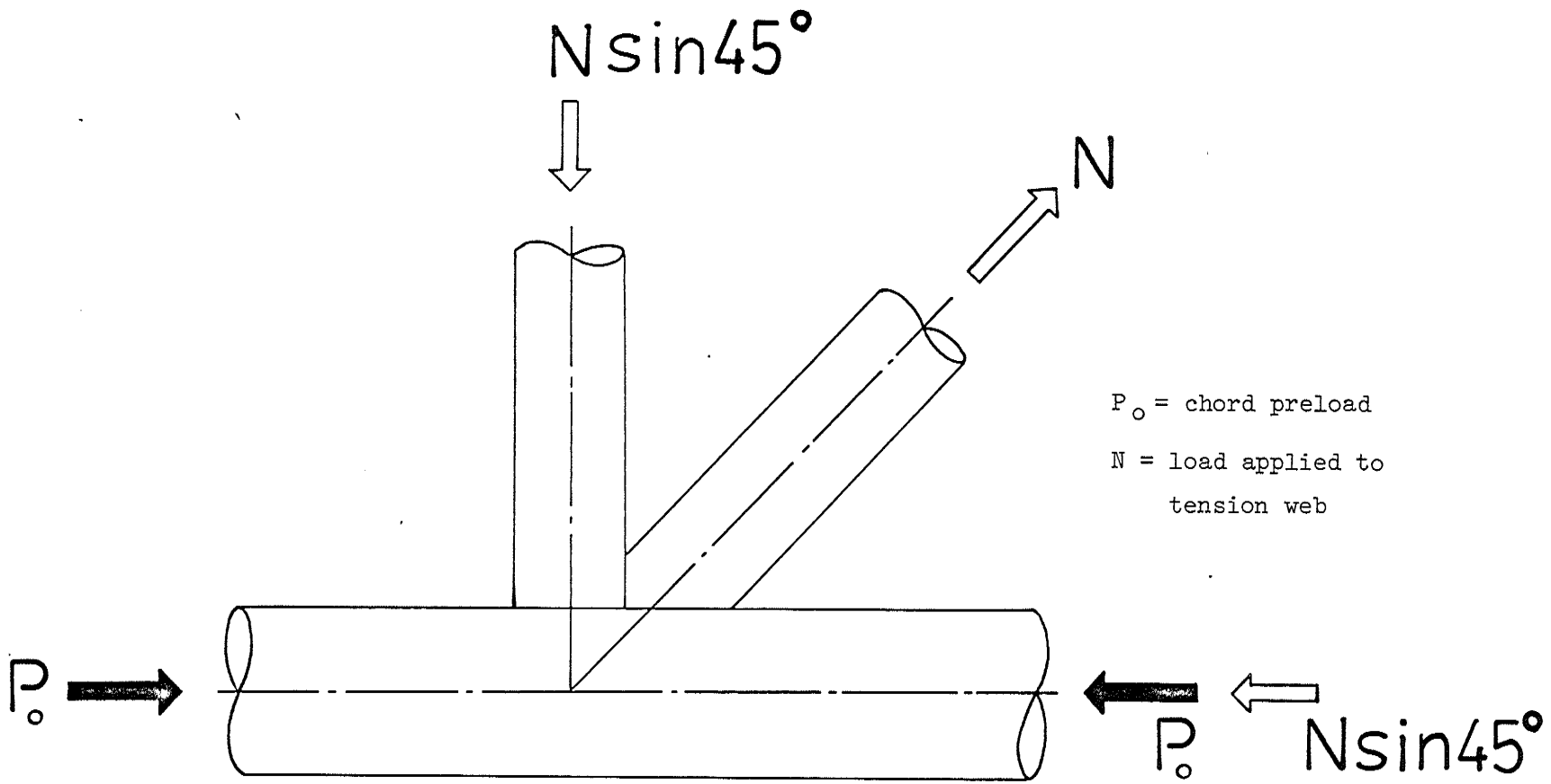

Fig. 1.12 Chord Preload, P_o

upon the assumption that secondary moments produce points of contra-flexure at the mid-points of all members in a truss. Therefore, the isolated joint specimens comprised one joint and the portions of the connected members extending half-way to the adjacent joints. However, this arrangement was not capable of simulating the displacement boundary conditions completely, as these points of contraflexure were not allowed to undergo relative displacements. Therefore, the secondary truss moments were not developed.

Daspugta also found from the full-scale truss tests that although points of contraflexure developed close to the mid-points of web members, the points of contraflexure in the chords, when they existed, were not necessarily at the mid-points. Furthermore, he found that the secondary bending moments generated in the web members of the isolated joints were negligible in comparison to those generated in a full scale truss. He concluded that these secondary truss moments caused high stress concentrations at the truss joints which resulted in failure loads which were lower than those observed in the isolated joint tests. He suggested that the results of isolated joint tests should be reviewed in the light of additional moments imposed on the joints acting as a part of a complete structure.

Ghosh (1978) tested two Pratt trusses with spans of 24 feet (7.3 m) , each involving four joints with circular end-cropped web members and square chord member. The results were compared with those for similar isolated joint specimens, tested by Thiensiripipat et al.(1978). He found that the failure loads of the joints in truss tests

were from 17 to 23 percent lower than those in the isolated joint tests. He considered that the reduction was due to the relative rotation between the web members and the chord in the truss joint. The relative rotation, and hence the reduction in strength, did not occur in the isolated joint tests. He also found that the point of inflection in the compression web connecting the test joints was located at the mid-length of the web member throughout the elastic range.

Both studies suggested that truss joints had lower strengths than isolated specimens, the difference being attributable to chord axial force and bending not simulated in isolated test specimens.

1.4 Scope of Study

The research cited above on full-scale trusses involving tubular joints has indicated that truss joints have lower strengths than do isolated joint specimens. The reduction in the strengths of truss joints has been attributed to the influence of chord axial force and moment, which were not simulated in isolated joint specimens.

Because of the uncertainty regarding this influence, this study of isolated cropped-web joint specimens was undertaken in order to investigate the influence of chord preload on their strengths and load-deformation behaviour.

1.5 Assumptions and Limitations

In this study, longitudinal chord stress due to compressive axial preload was made three times that due to the preload bending moment. In a given truss, this relationship would depend on the configurations of

the joints, the type of truss, the method of support and the loading conditions for the truss.

The scope of the investigation was limited to an experimental study, with no attempt to predict joint behaviour analytically. Statical loading only was considered. Eight test specimens were investigated, each having a Pratt-truss configuration. The two members of each specimen had the same circular cross-section, and had cropped ends welded at angles of 45 degrees and 90 degrees respectively to the face of a square chord. The chord thickness-to-width ratio (t_o/b_o), and the chord preload (P_o) were variables in the tests. The preload P_o was expressed as a percentage of the yield load of the chord. The yield stress at 0.2% strain offset was used.

CHAPTER 2

DESIGN AND FABRICATION OF TEST SPECIMENS

2.1 Choice of Joint

In order to facilitate comparisons, joint configurations similar to ones previously tested by Thiensiripipat et al. (1979) were employed. It was hoped also to use configurations similar to those employed by Ghosh (1978) so that the results for isolated joint tests could be compared with those for joints incorporated into trusses. However, the unavailability of the necessary materials precluded this.

In the tests performed by Thiensiripipat et al. (1979) each test specimen consisted of a chord and two web members, each extending from the test joint half-way to the adjacent joints,as shown in Fig. 2.1. In this study, the same configuration of joints was used.

Because earlier investigators had found a 50 percent web member lap to be optimal, it was used for all joints tested in this study.

2.2 Specimen Designation

The joints chosen were those designated 3B50 and 4B50 by Thiensiripipat et al. The two joint geometries are shown in Fig. 2.2 and Fig. 2.3. The joint configurations are described in Table 2.1.

As indicated in the table, the specimen designation employed by Thiensiripipat et al. was used in this study, except that one more designator was used to represent the magnitudes of preload. The first character, 3 or 4, represented the chord thickness-to-width ratio, t_o/b_o. The next

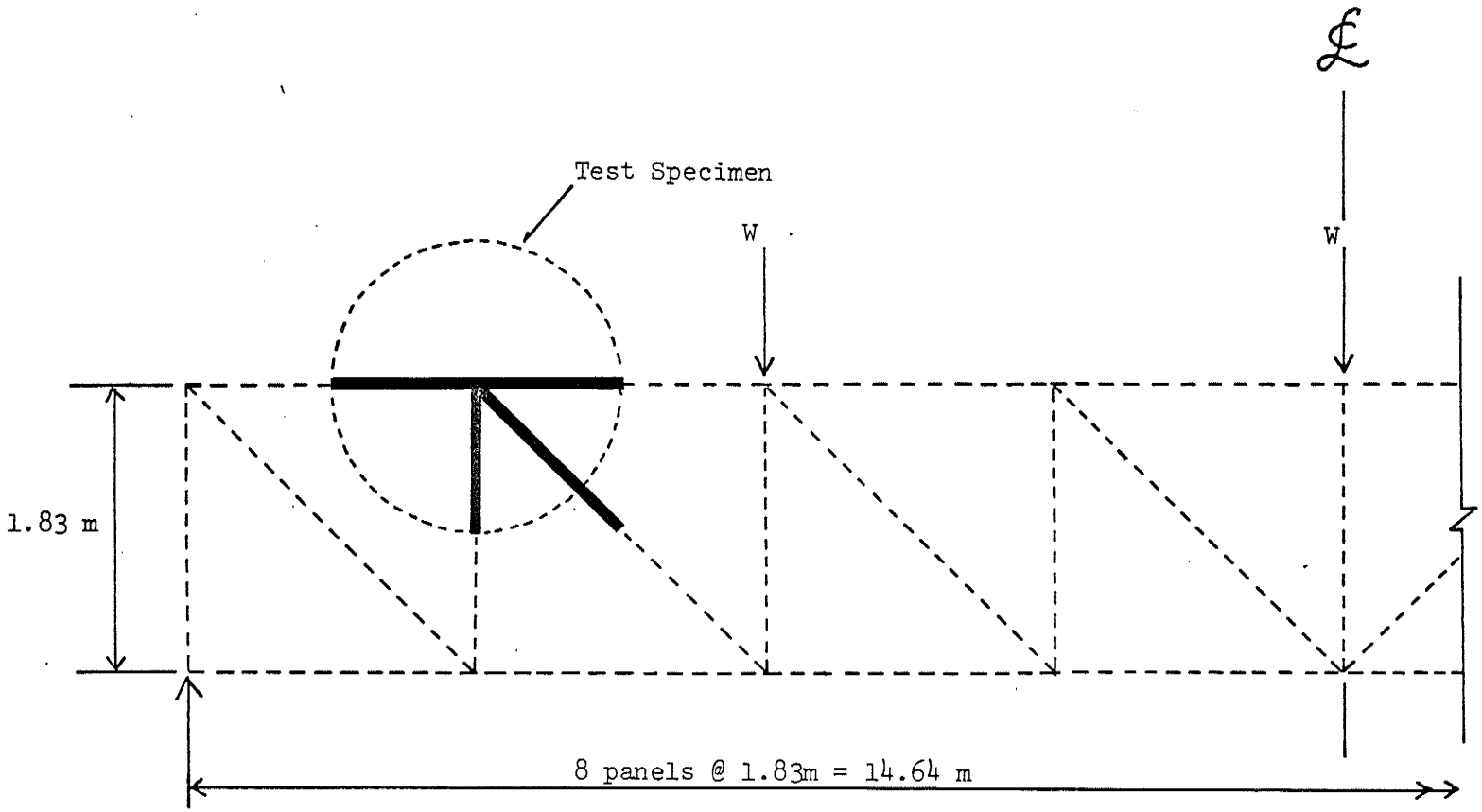

Fig. 2.1 Pratt-truss and Test specimen

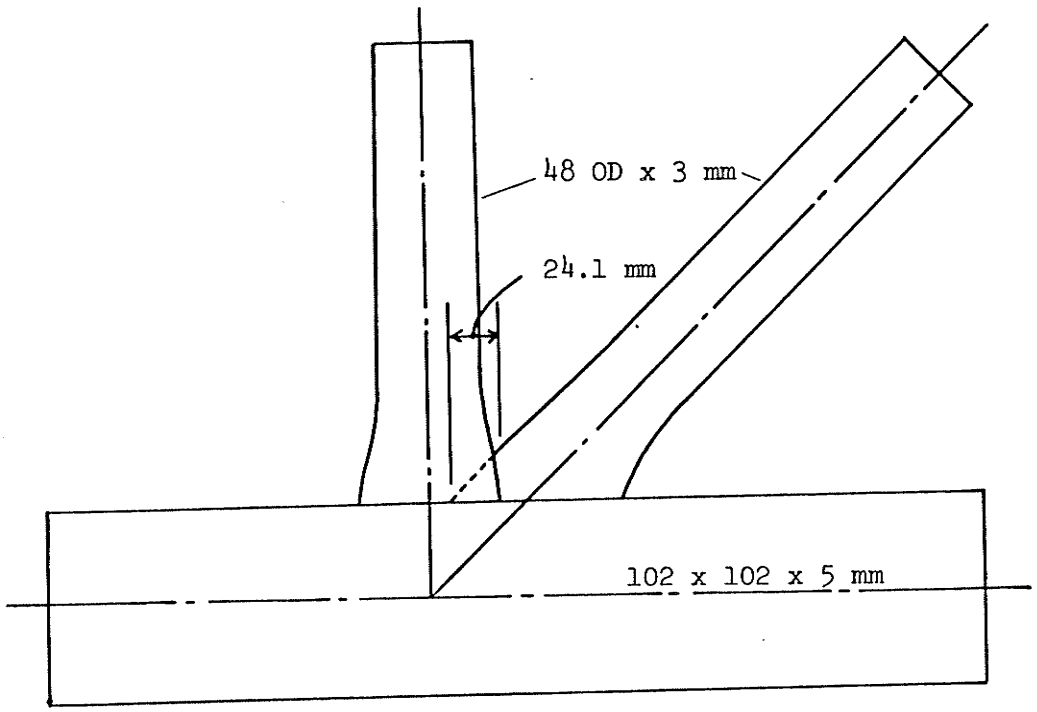

Fig. 2.2 Test Specimen 3B50

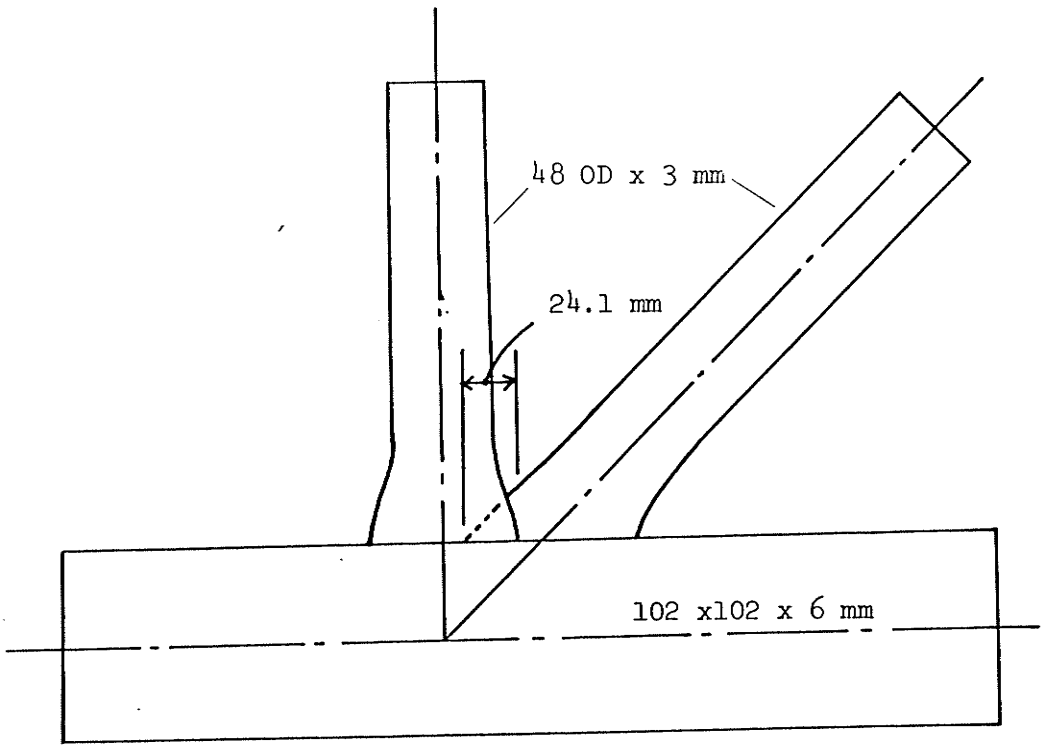

Fig. 2.3 Test Specimen 4B50

TABLE 2.1: Specimen Properties.

Specimen	CHORD				WEBS							d/b_o %	O_v (Lap) %
	b_o mm	h_o mm	t_o mm	t_o/b_o mm	d_1 mm	d_2 mm	d mm	t_1 mm	t_2 mm	t mm	t/d %		
3B50-I	102.36	100.79	4.32	4.22	48.39	48.44	48.41	3.00	3.05	3.02	6.24	47.2	50
3B50-II	101.93	101.12	4.32	4.24	48.46	48.36	48.41	3.05	3.00	3.02	6.24	47.5	50
3B50-III	101.55	100.99	4.34	4.28	48.36	48.51	48.44	3.02	3.00	3.02	6.24	47.7	50
3B50-IV	100.71	101.96	4.29	4.26	48.34	48.49	48.41	3.02	3.05	3.05	6.30	48.1	50
4B50-I	102.57	102.13	5.99	5.84	48.39	48.18	48.29	3.02	3.02	3.02	6.26	47.1	50
4B50-II	102.51	102.16	6.05	5.90	48.44	48.31	48.39	3.00	3.02	3.02	6.25	47.2	50
4B50-III	102.06	102.24	6.07	5.95	48.41	48.49	48.46	3.00	3.02	3.02	6.24	47.5	50
4B50-IV	102.54	102.72	5.97	5.82	48.34	48.46	48.41	3.02	3.02	3.02	6.24	47.2	50

N.B. The average of t_o/b_o is 4.25% for series 3B50, and 5.88% for series 4B50
The average of $t/_d$ is 6.25% for both series.
The average of d/b_o is 47.5% for both series.
Symbols used here are defined in Fig.1.9 (P.10).

TABLE 2.1: (continued) Specimen Properties.

Specimen	CHORD		COMPRESSION WEB		TENSION WEB		Specified Weld Size
	σ_e MPa	σ_{ult} MPa	σ_{e1} MPa	σ_{ult1} MPa	σ_{e2} MPa	σ_{ult2} MPa	mm
3B50-I	347.9	518.8	374.1	565.7	368.6	553.3	4.8
3B50-II	347.9	518.8	374.1	565.7	368.6	553.3	4.8
3B50-III	347.9	518.8	368.6	553.3	399.6	567.7	4.8
3B50-IV	347.9	518.8	374.1	565.7	368.6	553.3	4.8
4B50-I	354.8	525.0	374.1	565.7	399.6	567.7	4.8
4B50-II	354.8	525.0	374.1	565.7	368.6	553.3	4.8
4B50-III	354.8	525.0	374.1	565.7	399.6	567.7	4.8
4B50-IV	354.8	525.0	374.1	565.7	399.6	567.7	4.8

N.B. The modulus of elasticity of all specimens is 207,000 MPa

σ_e, σ_{e1}, σ_{e2}: Yield stresses (at 0.2% offset) of chord, compression web and tension web, respectively.

σ_{ult}, σ_{ult1}, σ_{ult2}: Ultimate stresses of chord, compression web and tension web, respectively.

character, B represented a particular ratio of web diameter to chord width. The next two characters, 50, indicated the overlap percentage of the web members. The final designator I, II, III or IV represented one of the four values of preload, P_o used.

2.3 Materials

The rectangular hollow sections 102 x 102 x 5 mm and 102 x 102 x 6 mm were used for the chord members, while the circular hollow sections 48ØD x 3 mm were used for the web members. All of these sections were hot-formed, and conformed to C.S.A. Specifications G40.21 Grade 50W Class H.

Tension tests conducted according to ASTM A370 at the University of Manitoba indicated that the yield stresses, σ_e , at 0.2% offset, for the rectangular hollow sections were approximately 345 MPa, while those for the circular hollow sections ranged from 369 to 400 MPa, as indicated in Table 2.1. The measured ultimate stresses, σ_{ult}, and moduli of elasticity, E, are also given. Configurations of the tension test specimens and load-deformation curves of the tension tests are given in Appendix C.

2.4 Fabrication

The web tubes were cropped in a specially designed cropping machine in the University of Manitoba Structures Laboratory. As shown in Fig. 2.4, the cropping machine consisted of two V-shaped steel alloy blades. A 2,670-kN capacity Universal Testing Machine was used in the cropping operation.

During the cropping operation, the web tube was placed between the blades, and the welded seam of the H.S.S. was deliberately located close

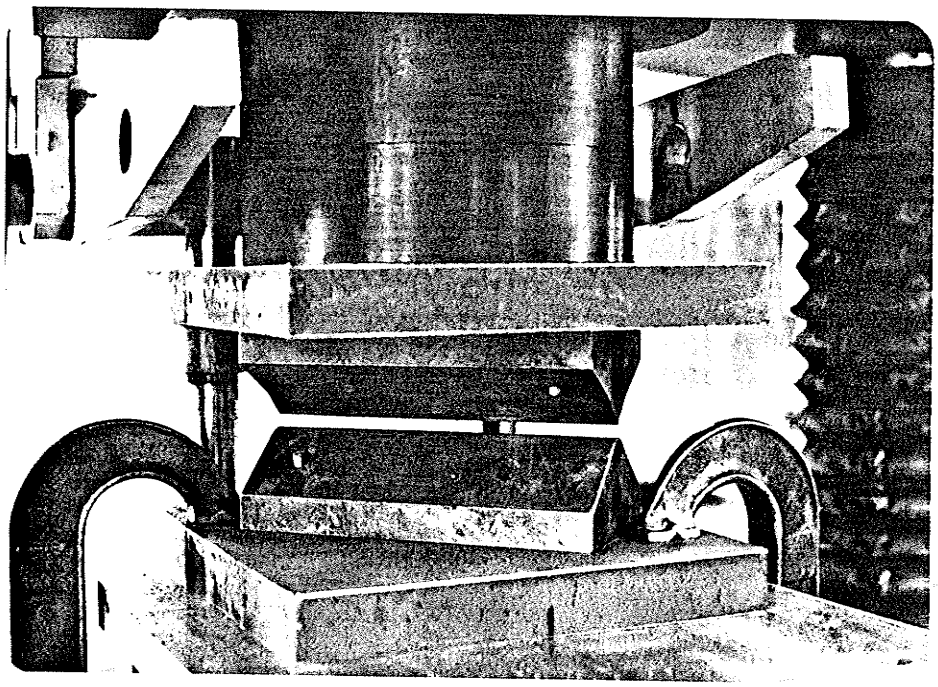

Fig. 2.4 Cropping Machine

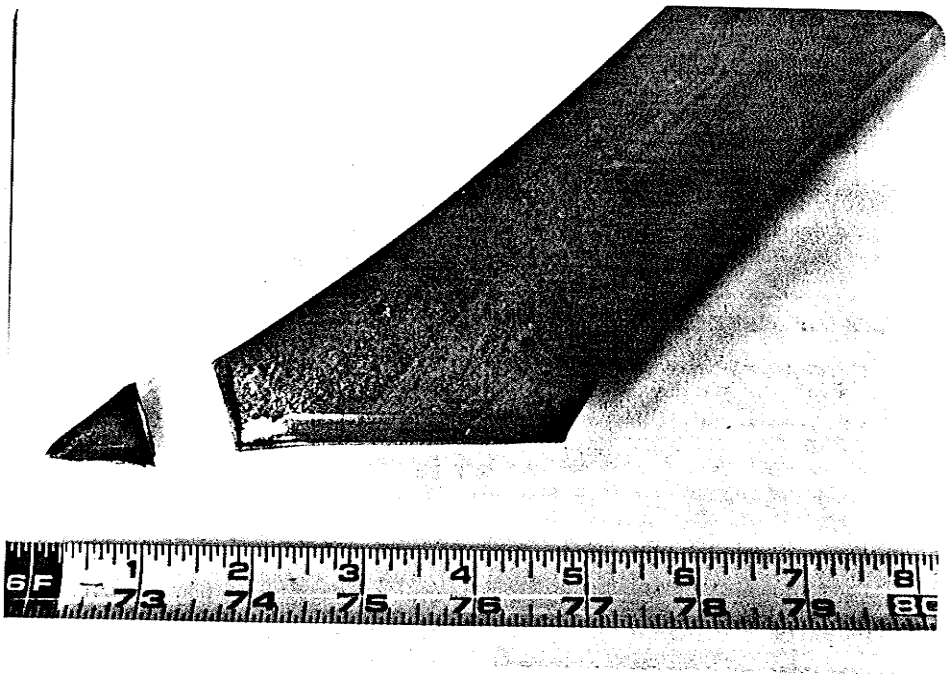

Fig. 2.5 Cropping of Tension Web

to either one of the blades. This was done so as to avoid the formation of longitudinal cracks along the welded seam due to the shearing and bending mechanism associated with the cropping operation. According to Jamm et al. (1952), it is advantageous to have only one of the webs being cut to fit the connection. Therefore, the procedure employed by Thiensiripipat et al. (1979), that of using a double cut on the tension web only for proper fitting,was followed (see Fig. 2.5).

The cropped tubes and a chord tube were then assembled for tack welding in a jig as shown in Fig. 2.6. The final welding was done by a certified welder using E7018 electrode and the welding sequence illustrated in Fig. 2.7. The sequence of welding was chosen such that the highly stressed region at the lap would not be under tension stress due to welding.

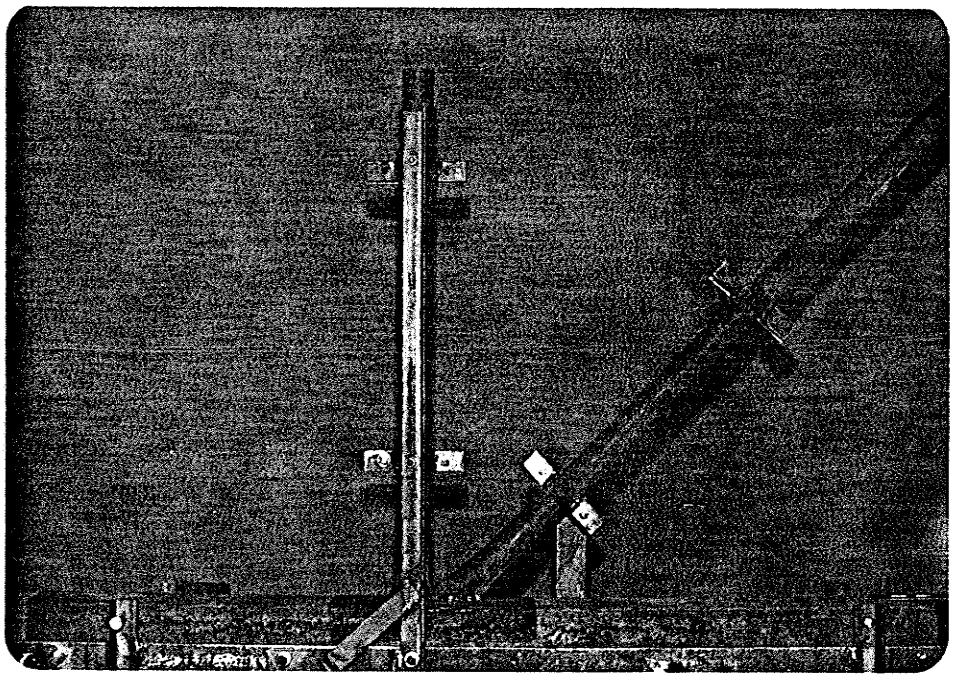

Fig. 2.6a Welding Jig

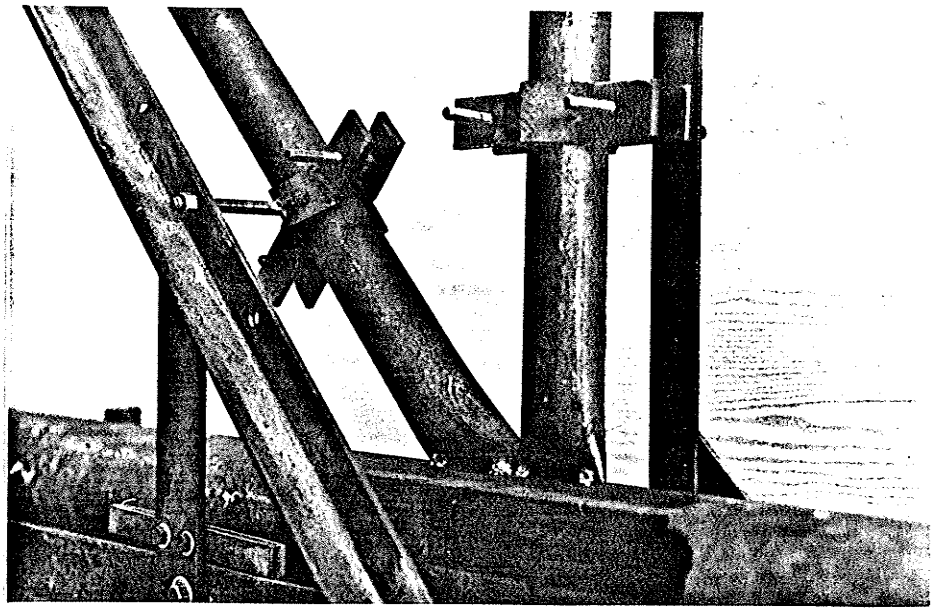

Fig. 2.6b Welding Jig

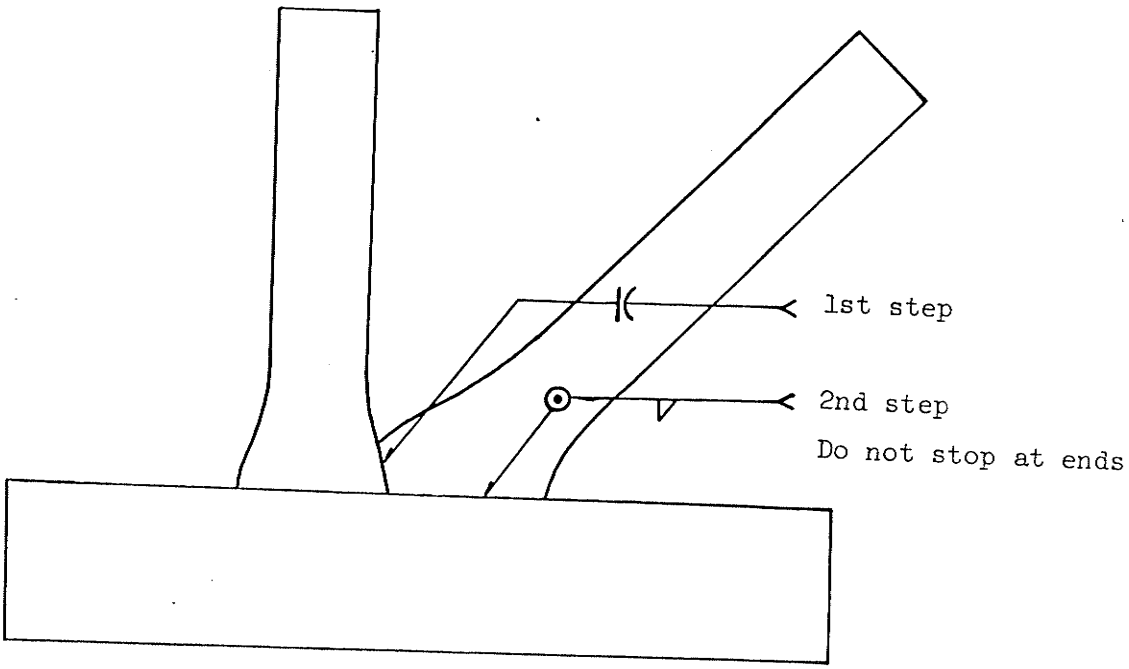

Fig. 2.7 Welding Specification

CHAPTER 3

TEST PROCEDURE

3.1 Test Equipment

3.1.1 Loading frame

The loading frame, as illustrated in Fig. 3.1, consisted of two W21 x 68 beams supporting two reaction assemblies which were inclined at 45 degrees to the horizontal. Each reaction assembly was approximately 305 mm high and 560 mm long. Pin supports about 200 mm long and 25 mm high with a semi-cylindrical bearing surface, located at the middle of the inclined surface of each reaction assembly, were used to support the compression web and the chord of a specimen during each test. The compression web and the chord were pin-supported to simulate points of inflection, assumed to occur at the mid-lengths of the members.

Both of the reaction assemblies could be adjusted horizontally, and the adjustment of the pin supports parallel to the inclined surface was also possible. A built-up jacking beam was bolted to the I-beams and horizontal adjustment of it was possible.

3.1.2 Prestressing system

As illustrated in Fig. 3.2, the chord preload was applied by means of four Enerpac manually operated hollow-core hydraulic jacks and transmitted to the chord by four 29-mm-diameter high-strength prestressing bars.

The yield and ultimate strengths of the bars were checked by a tension test, and the prestressing bars were calibrated. Details of the calibration are given in Appendix D.

Fig. 3.1 Loading Frame

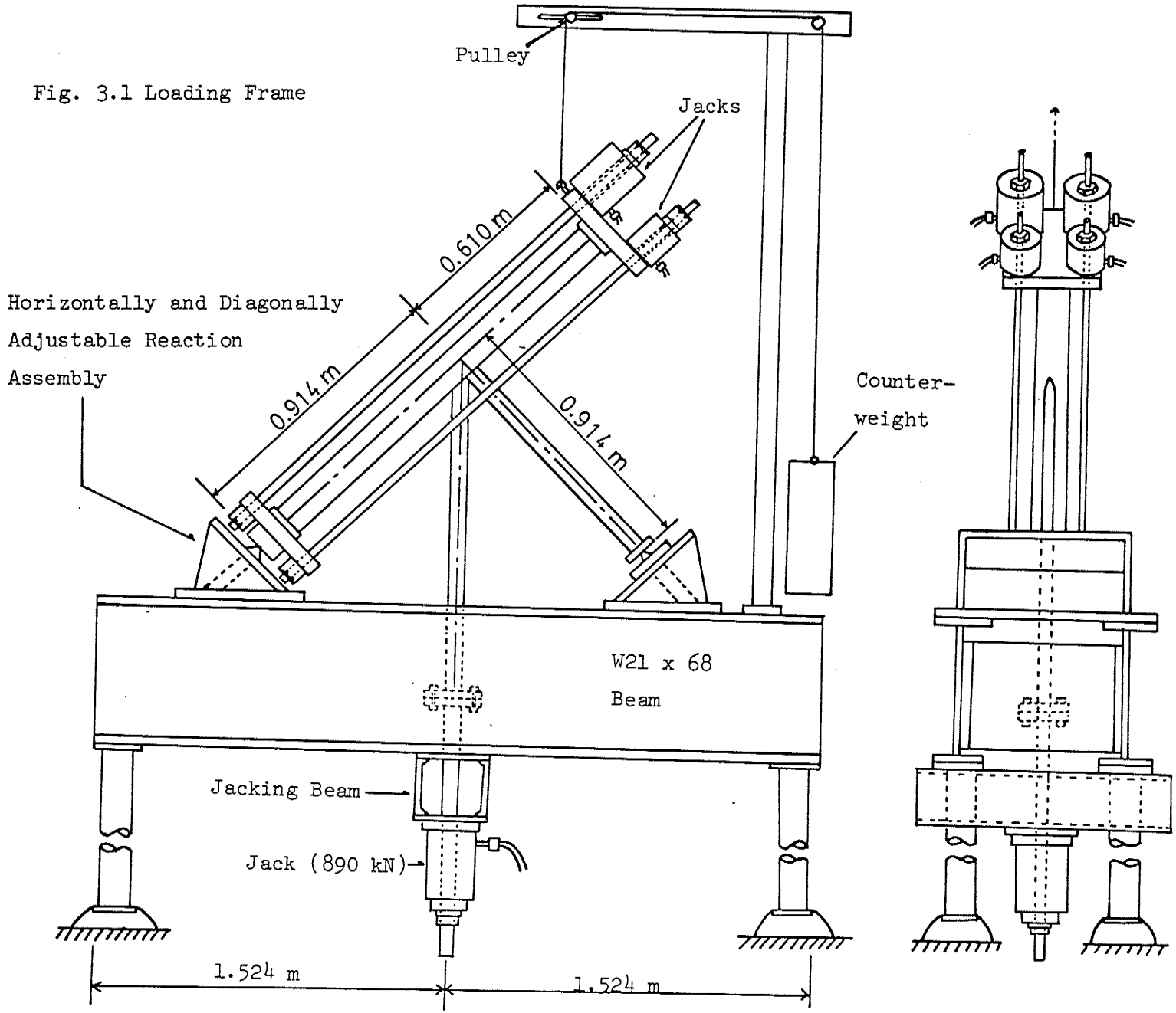

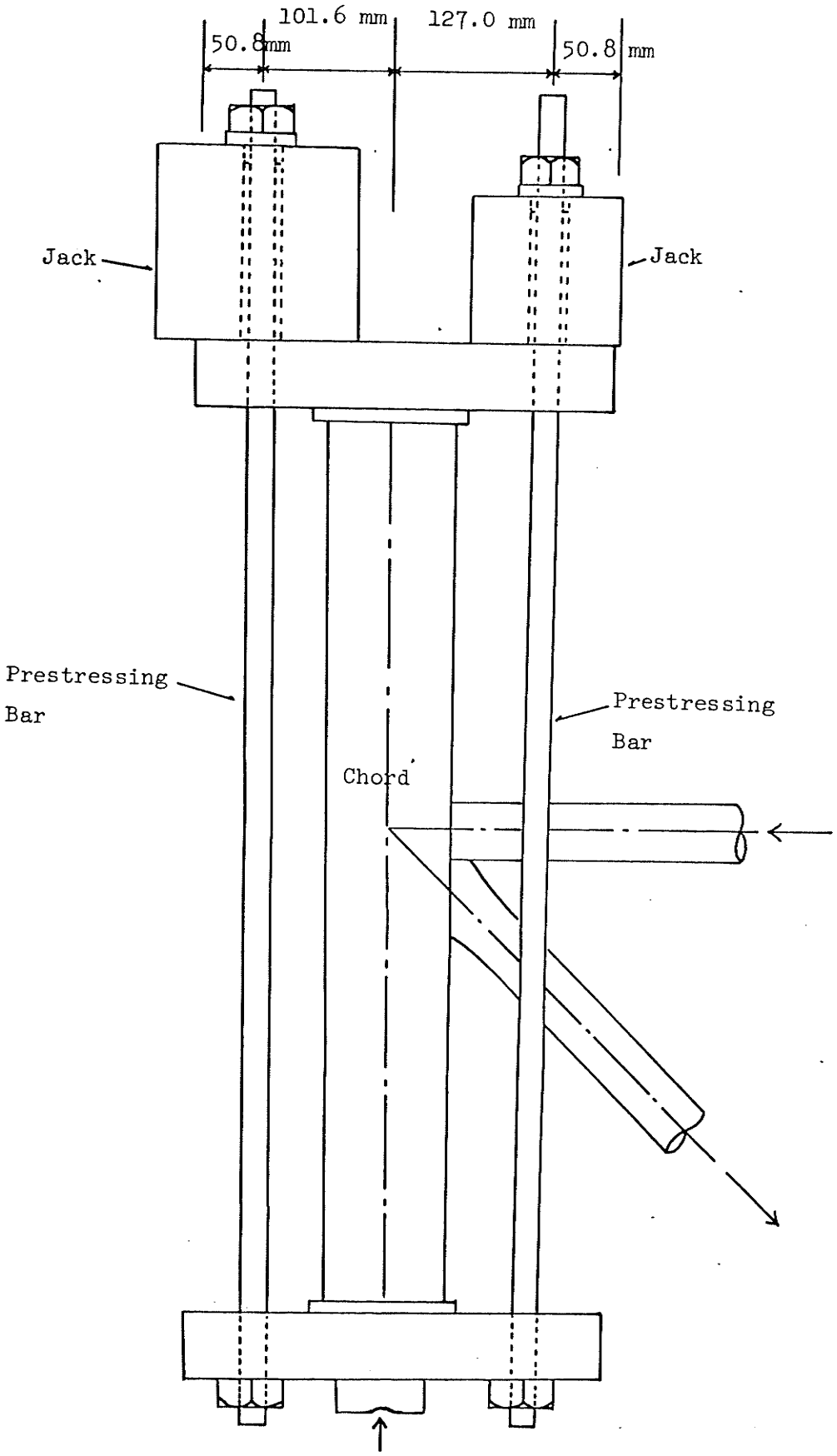

Fig. 3.2 Prestressing System

The system was so arranged that an eccentric axial compressive force could be created during testing.

The axial force in each prestressing bar was measured by means of four strain gauges spaced equally around the circumference of the bar and connected in a half-bridge configuration to nullify temperature and bending effects.

3.2 Instrumentation

3.2.1 Deformation measurements

The deformation along the longitudinal centerline of the loaded chord face was measured using linear voltage displacement transducer assemblies at seven locations, as illustrated in Fig. 3.3. The choice of location was based upon previous test results (Thiensiripipat et al. 1979), which showed that the maximum chord deformation occurred at the extreme edges of the webs.

The transducers had a stroke of $\pm$ 6.35 mm with an accuracy of 0.025 mm and a sensitivity of 0.16 volts per mm. They were mounted on the face opposite to the loaded face, as shown in Fig. 3.5. The ferrite core of the transducers were connected to probes which passed through the chord and maintained contact with the interior of the connected chord face.

The in-plane buckling of the compression web member was measured using three transducers. The locations and numbering of the transducers are shown in Fig. 3.4.

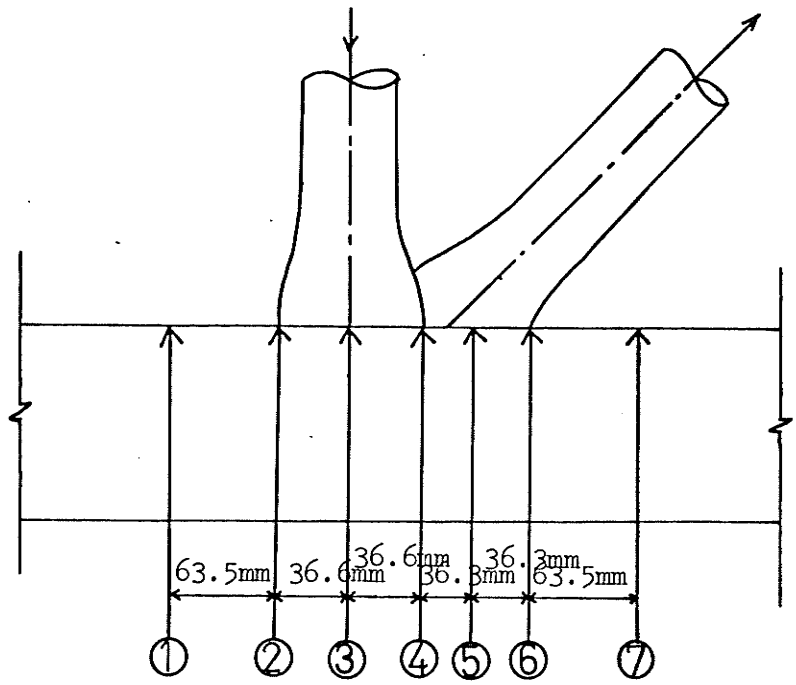

Fig. 3.3 Transducer Locations on Chord Wall

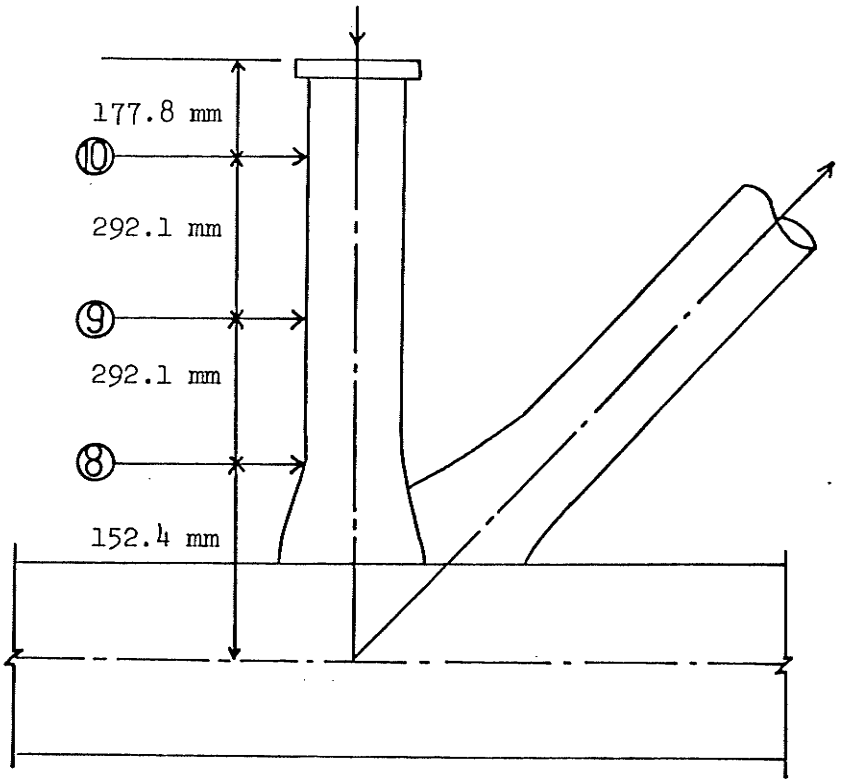

Fig. 3.4 Transducer Locations on Compression Web

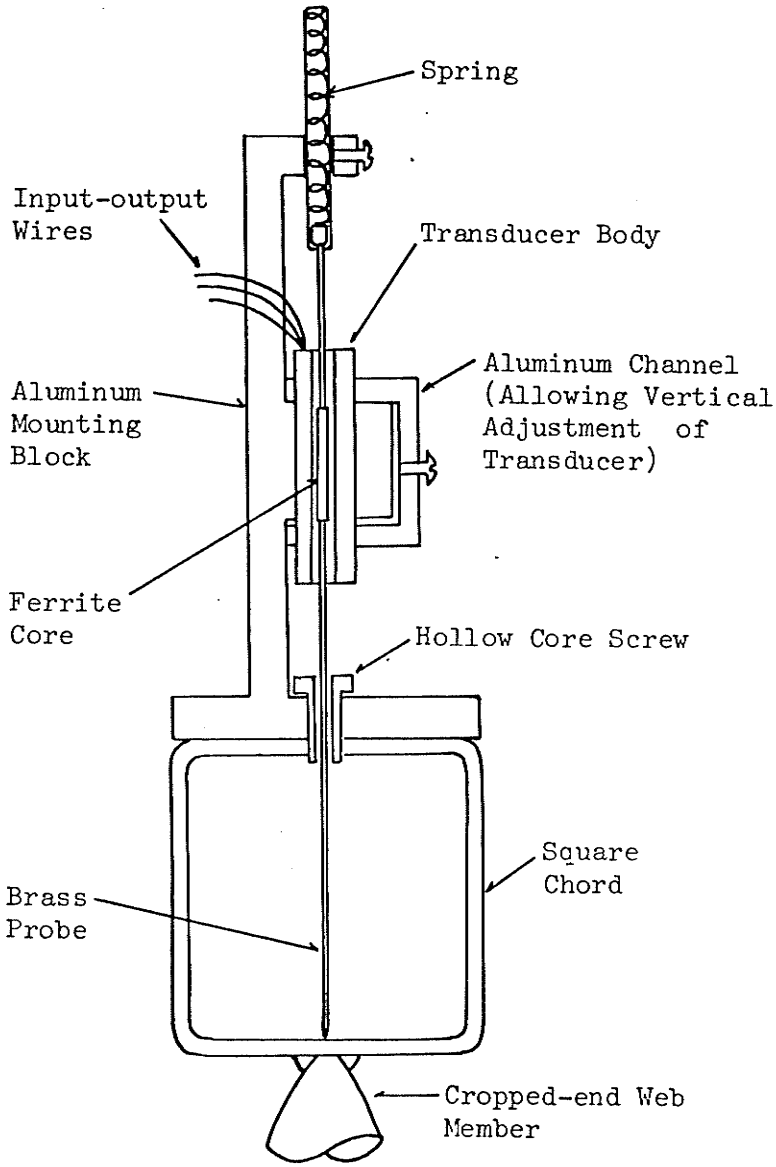

Fig. 3.5 Transducer Assembly

3.2.2 Strain measurements

All joints were instrumented with electric resistance strain gauges in order to determine the strain distribution, and also to check for yielding. The strain gauges were located on the tube walls in presumably highly stressed zones, as shown in Fig. 3.6 to Fig. 3.8. The locations selected were the crotches, the points of intersection of the axes of the web members with the chord face, and the mid-points of the members in the test specimens. Advantage of joint symmetry about the plane of specimen was utilized in order to minimize the use of strain gauges. Six specimens (3B50-I to 3B50-III, 4B50-I to 4B50-III) had 16 gauges, and specimen 3B50-IV had 28 gauges. Only specimen 4B50-IV had a total of 41 gauges.

The strain gauges used were Micro-Measurement precision strain gauges of type EA-06-250BG-120, with a gauge length of 6.35 mm. The gauge resistance in ohms was 120.0 $\pm$ 0.15%, the gauge factor at 24 degrees celsius was 2.03 $\pm$ 0.5% and the strain limit was 5%. The gauges were cemented to the specimens using M-Bond 200.

3.2.3 Data acquisition

A Hewlett-Packard Data Acquisition System (Model 9825A) was used to measure and record all load, strain and displacement data and to print and plot the results. The system is illustrated in Fig. 3.9.

3.3 Testing Procedures

The specimen with the preloading assembly in place, was positioned in the loading frame, as illustrated in Fig. 3.9(b). The

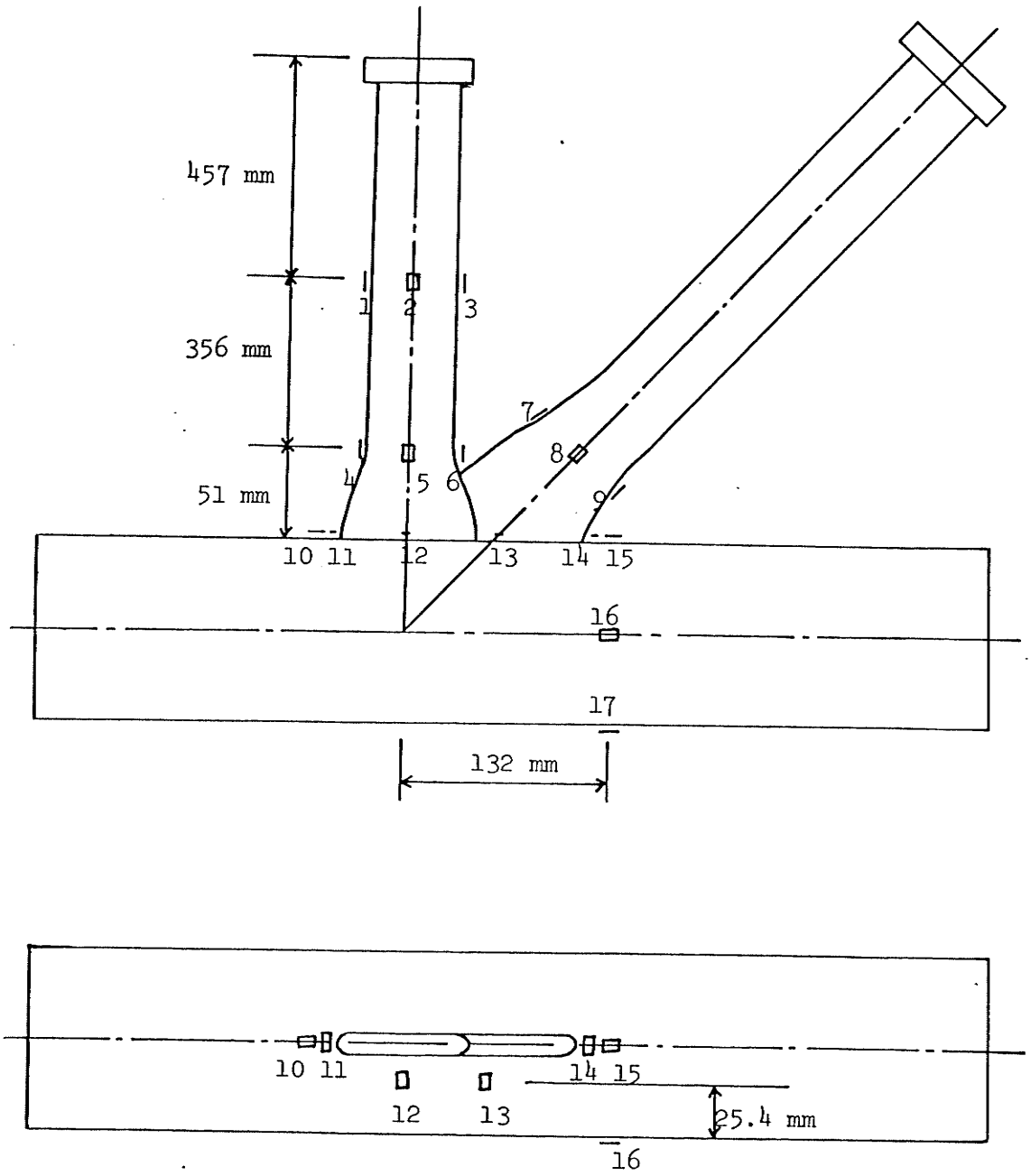

Fig. 3.6 Strain Gauge Locations on Specimens 3B50-I to 3B50-III and Specimens 4B50-I to 4B50-III

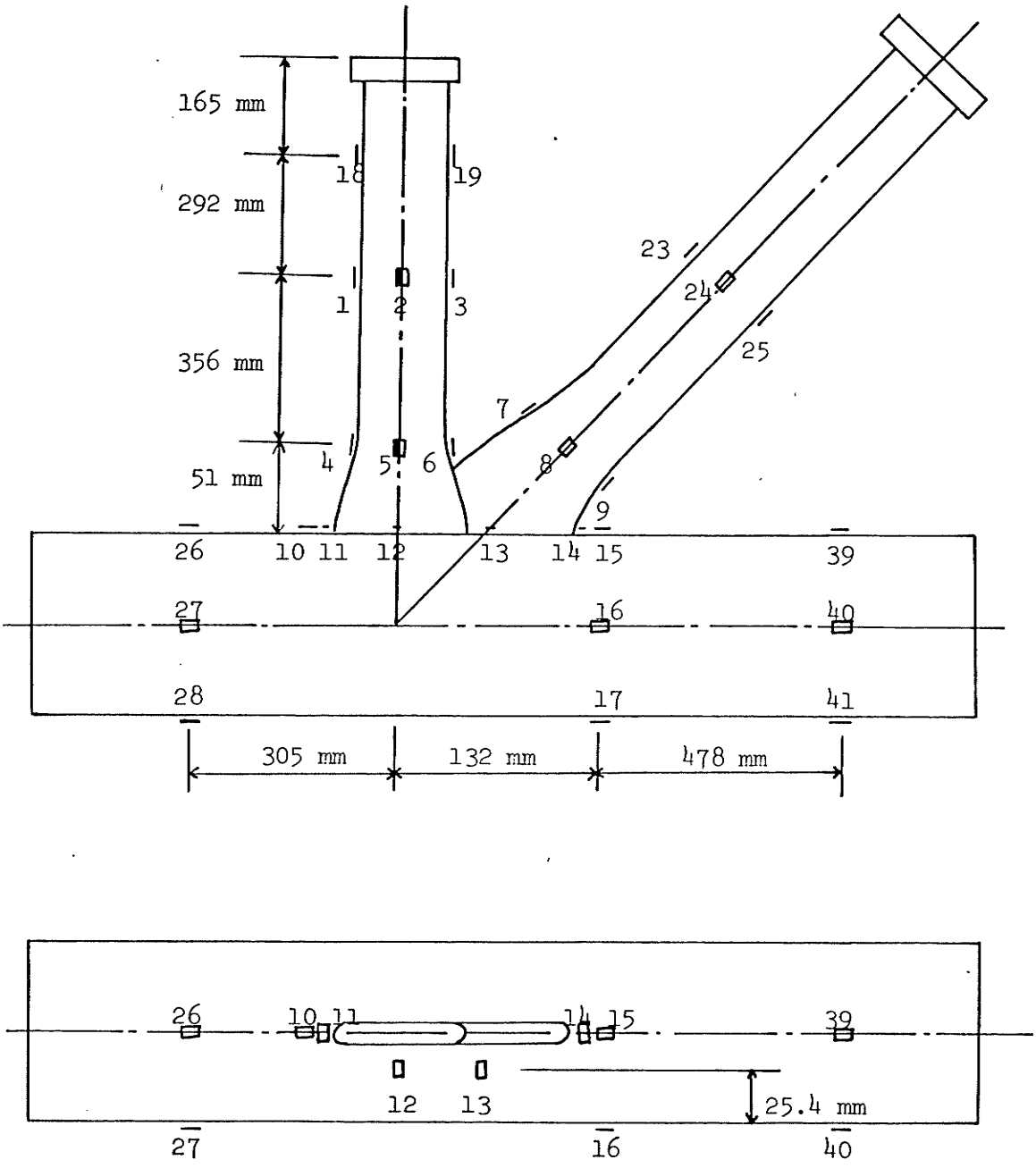

Fig. 3.7 Strain Gauge Locations on Specimen 3B50-IV

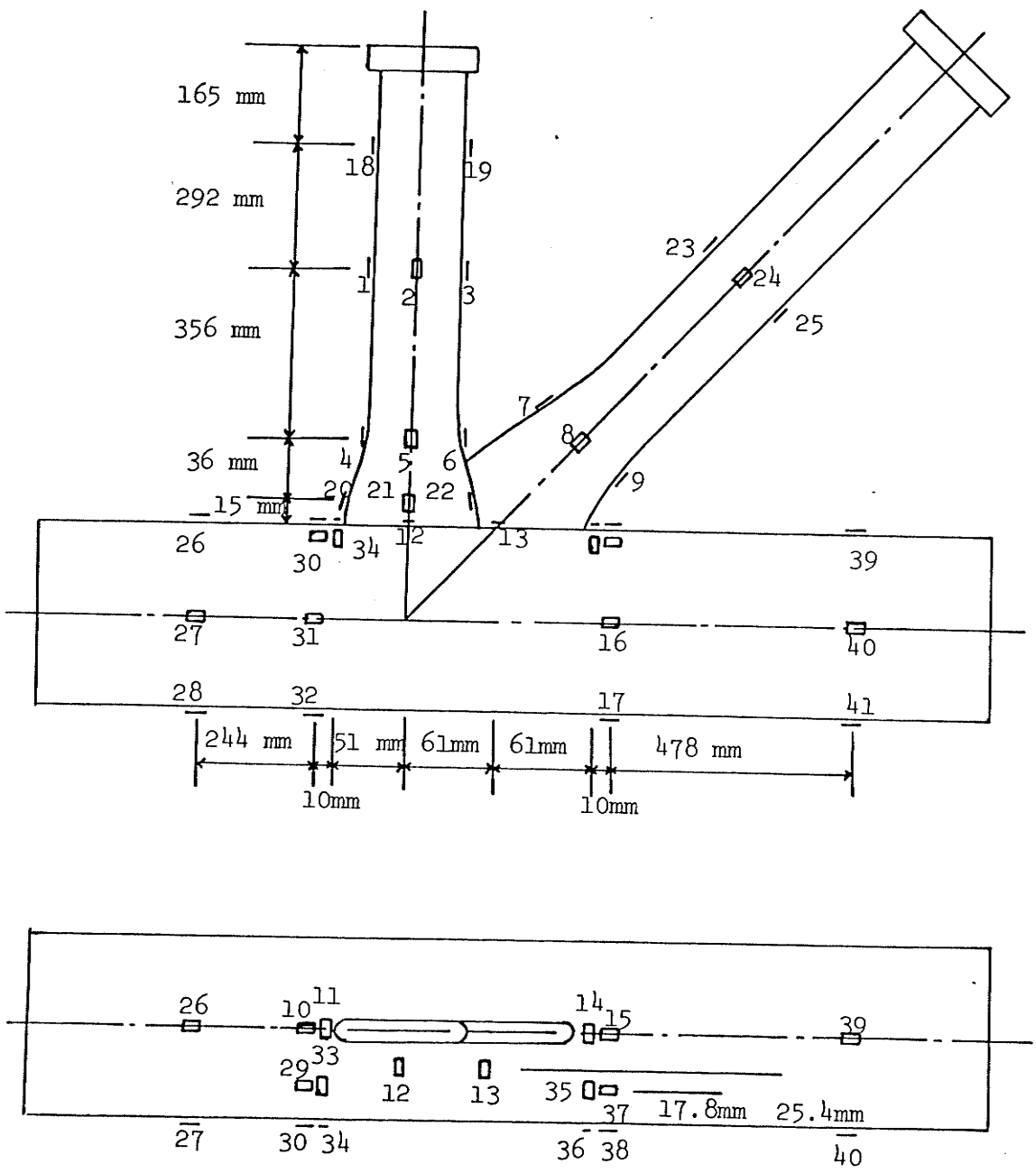

Fig. 3.8 Strain Gauge Locations on Specimen 4B50-IV

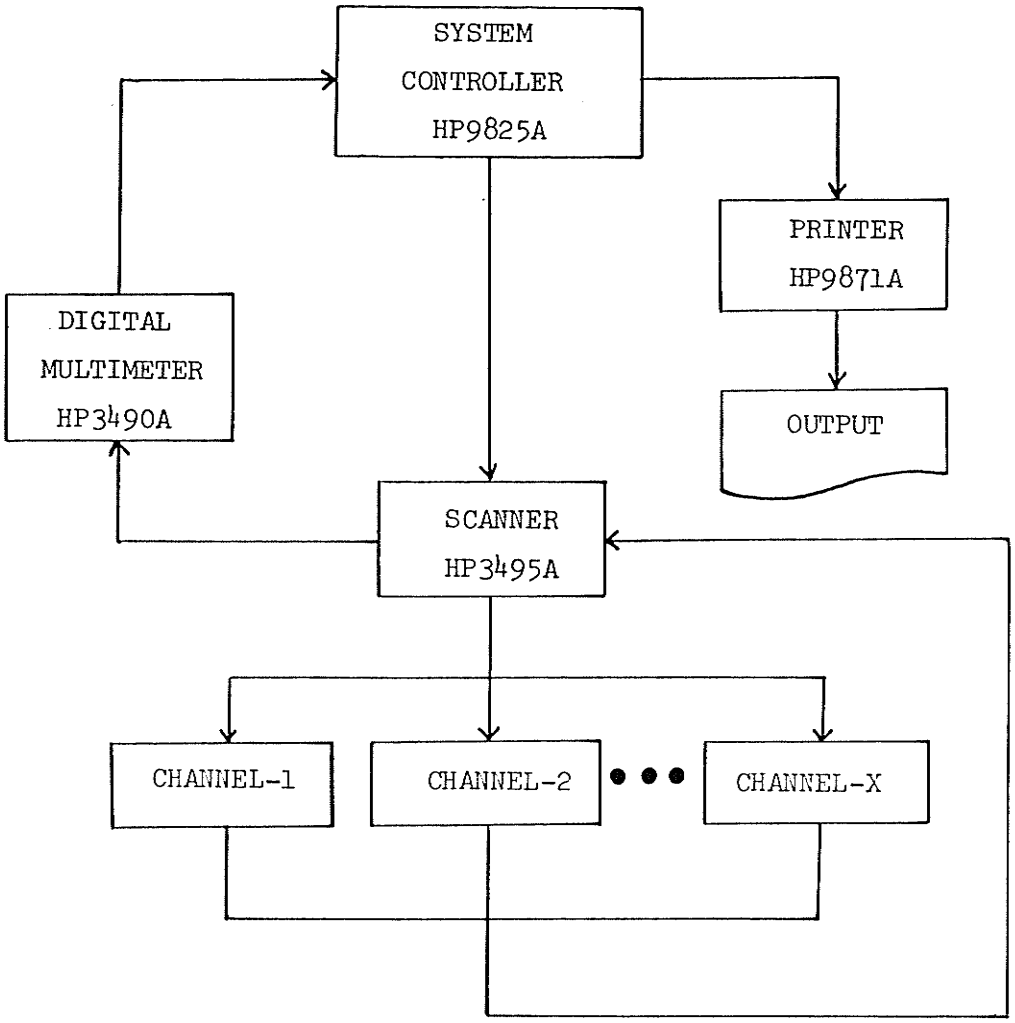

Fig. 3.9a Schematic Diagram of Data Acquisition System

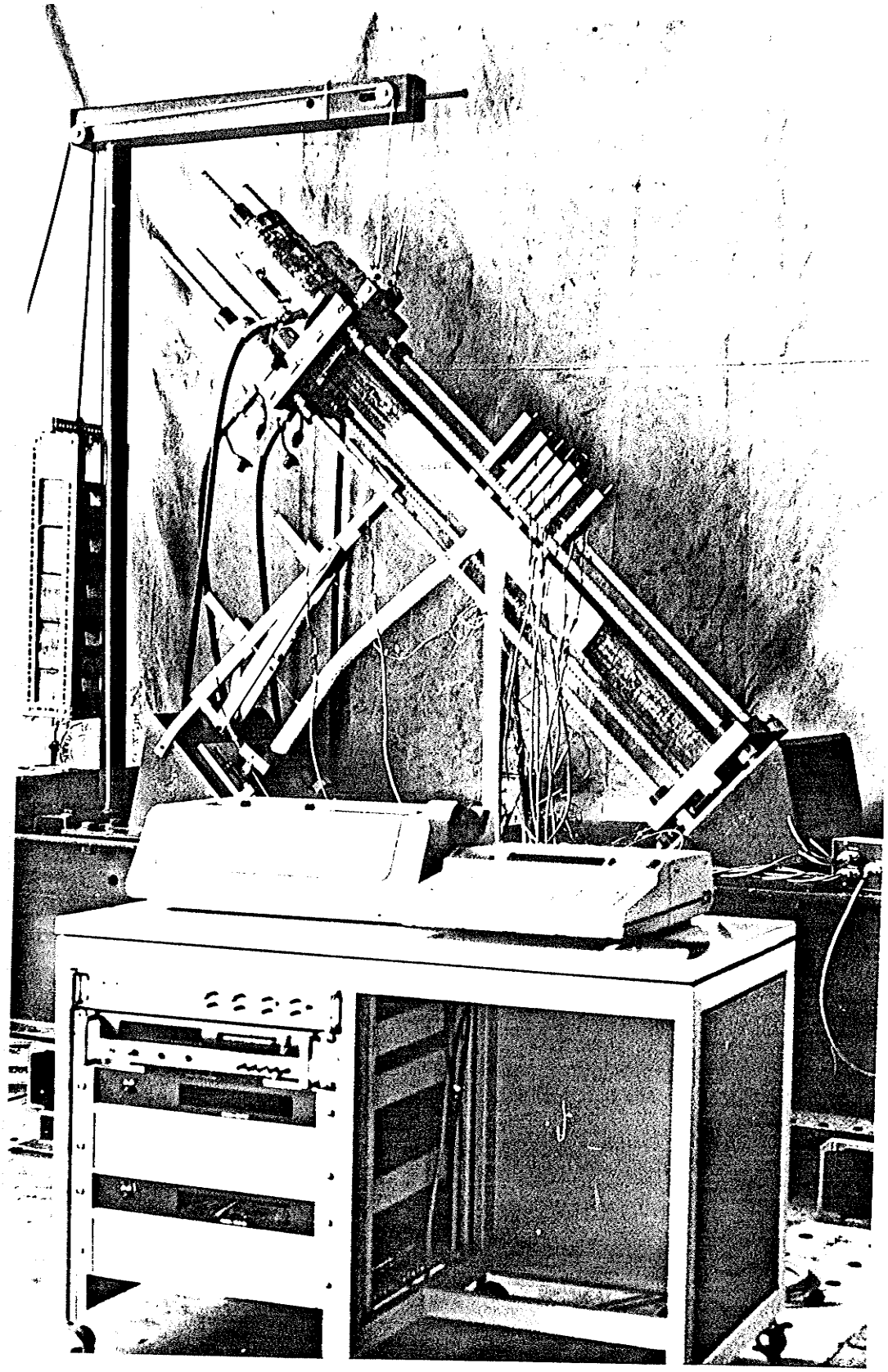

Fig. 3.9b Data Acquisition System

tension web member was attached to an 890-kN hydraulic jack by means of a connecting plate welded to its end. The Hewlett-Packard Data Acquisition System was then connected to the strain gauges and transducers. The gauges and transducers were then checked and adjusted or replaced if necessary. Initial gauge readings were recorded.

The specimen was painted with a brittle coating, which supplemented the use of strain gauges to detect the points of maximum stress.

Preload was then gradually applied to the specimen up to the value specified in Table 3.1. It was then kept constant throughout all loading stages. Load was applied to the tension web by an 890-kN jack and measured by means of a load cell. Initial loading increments of 4.5 kN were reduced to 2.25 kN as yielding was approached.

After each load increment, the forces in the prestressing bars were checked and adjusted to the values specified before the readings were taken. All specimens were tested to failure and the failure mode was observed and recorded.

TABLE 3.1: Magnitudes of Preload in Chord.

Specimen	PRELOAD			AXIAL FORCES IN PRESTRESSING BARS			
	n %	P_o kN	M_o Nm	F_1 kN	F_2 kN	F_3 kN	F_4 kN
3B50-I	0	0	0	0	0	0	0
3B50-II	20	85.26	843	20.92	20.92	21.81	21.81
3B50-III	50	213.60	2110	52.07	52.07	54.74	54.74
3B50-IV	80	338.33	3366	82.77	82.77	86.78	86.78
4B50-I	0	0	0	0	0	0	0
4B50-II	50	297.62	2788	72.09	72.09	76.54	76.54
4B50-III	80	477.00	4460	115.70	115.70	122.82	122.82
4B50-IV	90	531.37	5018	129.05	129.05	136.62	136.62

N.B. n is the percentage of preload, equal to σ_0/σ_e. σ_0 is the stress in chord due to preload and σ_e the yield stress (at 0.2% strain offset) of the chord.

CHAPTER 4

TEST RESULTS AND DISCUSSION

The results presented and discussed in this chapter are divided into two parts under eight separate items. The first part consists of the results of test series 3B50-I to 3B50-IV. The second involves those of test series 4B50-I to 4B50-IV.

4.1 Test Series 3B50-I to 3B50-IV

4.1.1 Local chord face deformation

As illustrated for specimen 3B50-I in Fig. 4.1, the local chord deformation under the web-members was non-uniform. The deformations fell from the maximum value at the web extremities to approximately zero at the overlap of the webs. The chord face and the web ends appeared to rotate as a unit about a pivotal point adjacent to the toe of the tension web.

The chord-wall rotation was initiated by a force couple resulting from axial forces in the web members, as illustrated in Fig. 4.2. The rotation then induced bending in the compression web, which gave rise to further bending in the chord wall. The bending of the web and the deformation of the chord continued to help each other until the joint failed by excessive chord wall deformation, accompanied by the buckling of the compression web or the fracture of welds at the toe of tension web.

Fig. 4.1 illustrates that the deflections under the compression web were greater than those under the corresponding tension web. This

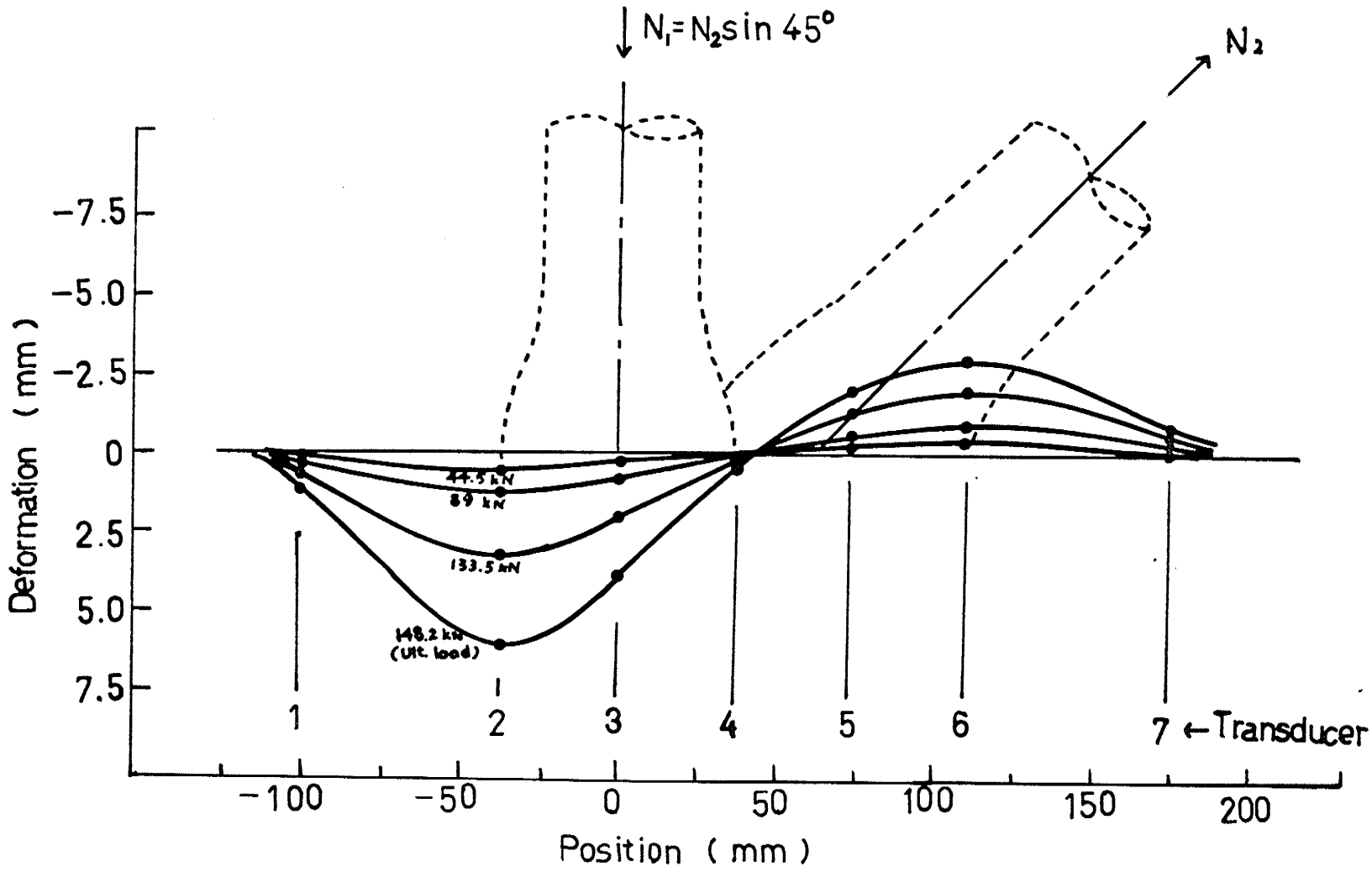

Fig. 4.1 DEFLECTION PROFILES OF LOADED CHORD FACE OF SPECIMEN 3B50-I

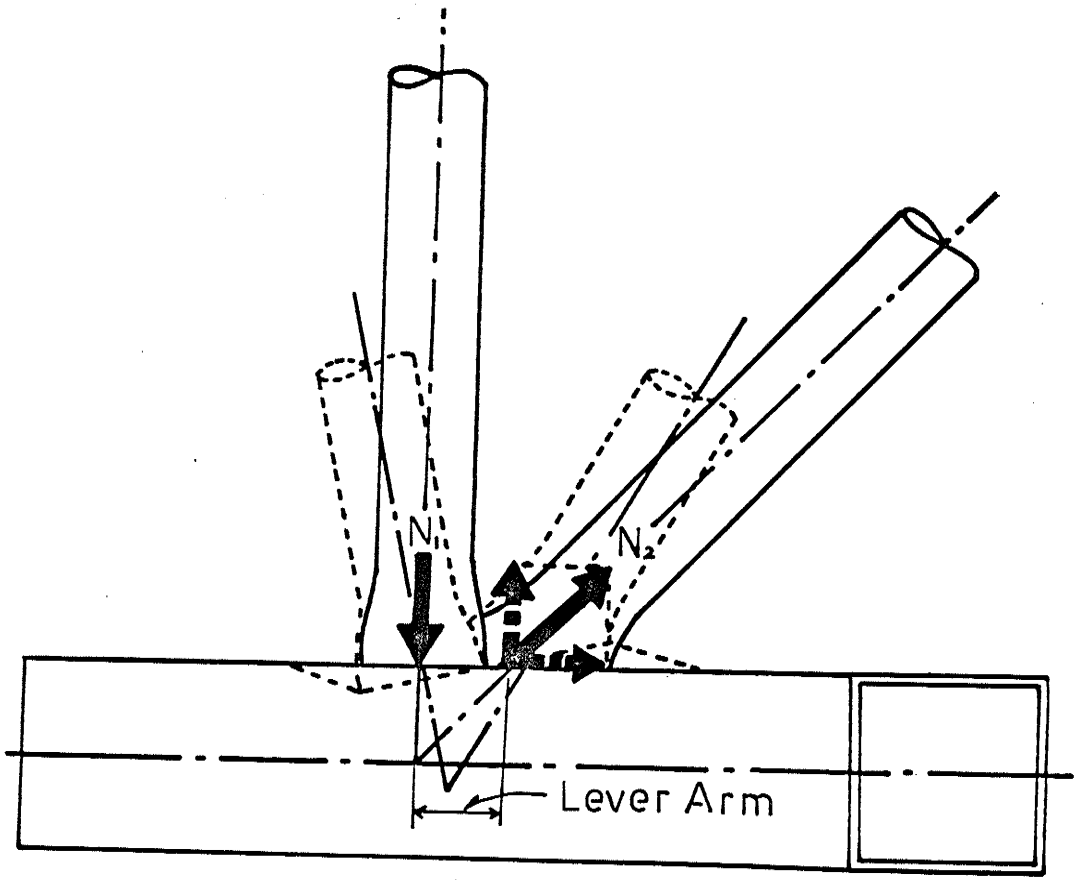

Fig. 4.2 MECHANISM OF CHORD-WALL ROTATION

occurred despite the fact that the bending stress in the chord was highest adjacent to the tension web, as the longitudinal contact length between it and the chord was smaller than that for the compression web. The maximum deflection under the compression web was about twice that under the tension web. This indicates that much of the normal component of the tension web load was transferred through the overlap to the compression web, before it could reach the chord face. As a result, the force per unit length along the chord was smaller under the tension web than under the compression web. As loading was increased, apparent yielding of the chord face took place under the compression web while the chord face under the tension web was still in the elastic range.

As illustrated in Fig. 4.3, the chord face deformation patterns for specimens 3B50-II, 3B50-III and 3B50-IV were similar to those for specimen 3B50-I. The maximum deflections under the compression webs were approximately the same for all specimens. On the other hand, the maximum deflections under the tension webs were almost identical for all specimens except specimen 3B50-IV. The latter had a maximum deflection about twice as large as those of other specimens. The pivotal points of chord-wall rotation for specimens 3B50-I, 3B50-II and 3B50-III remained at about the same position. That of specimen 3B50-IV started right below the overlap, remained stationary for loading up to 89 kN in tension web, and then shifted towards the extremity of the compression web base, for loading up to 126.8 kN. In the local chord deformation profiles for cropped joints in tubular trusses tested by Ghosh (1978), the privotal points in truss joints were always

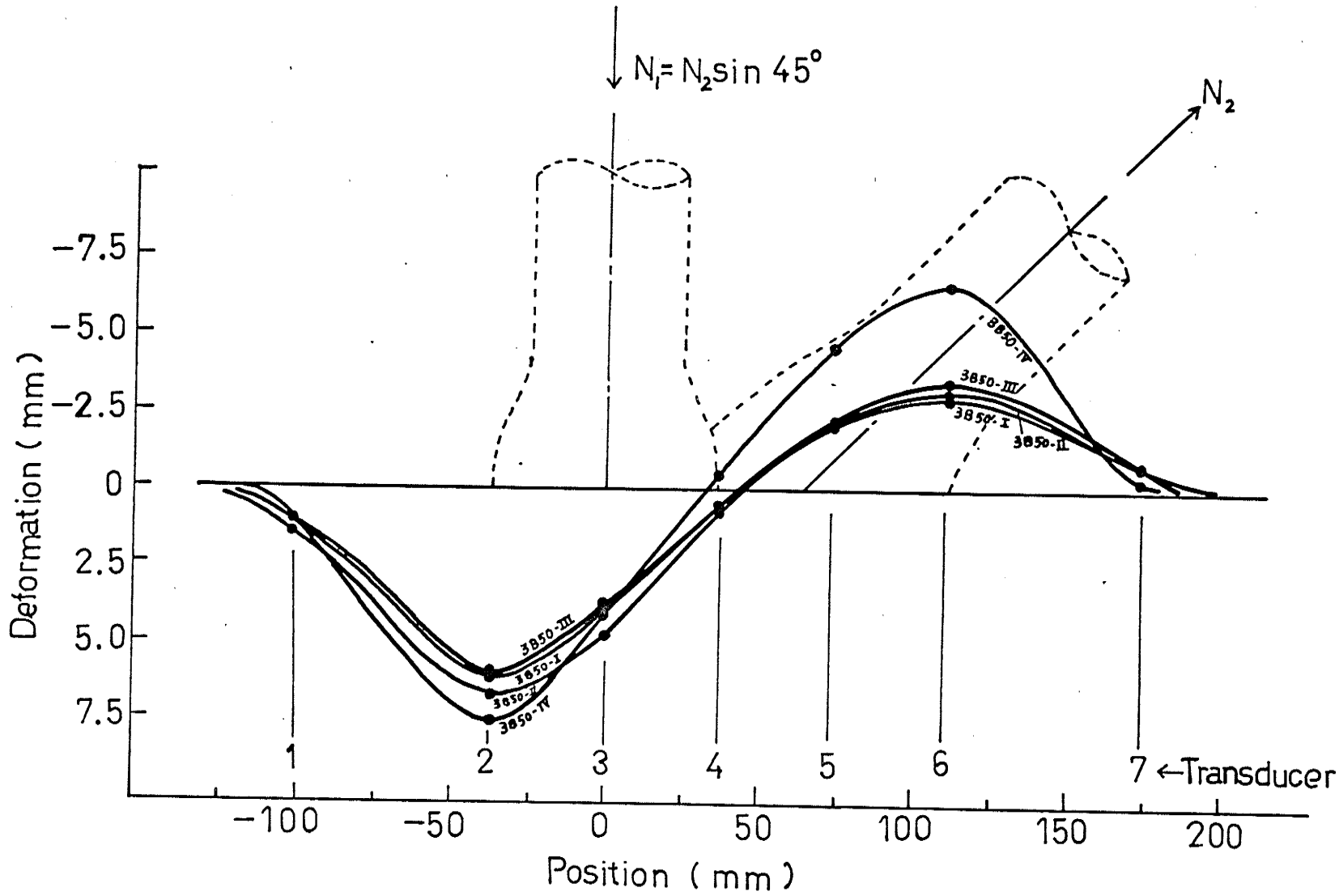

Fig. 4.3 COMPARISON OF CHORD FACE DEFORMATION OF SPECIMENS 3B50-I TO 3B50-IV AT ULTIMATE LOAD

located closer to the extremity of the compression web than were those for similar isolated joints. This indicated that the use of a preload of about 80 percent of the yield load of chord in isolated joint tests best simulated actual truss conditions.

The deflection under the tension web of specimen 3B50-IV was comparable to that under the compression web, despite a lower load per unit length under the tension web, as previously explained. The reason was that the cumulative effect of the preload in the chord and the tension web load transferred to the chord resulted in a compressive yield of the chord wall immediately adjacent to the tension web, at a very early stage of loading. This can be seen in Fig. 4.4, which shows the load-deformation behaviour (gauge 15) of the chord face near the extremity of the tension web. The strains for specimens 3B50-I, 3B50-II and 3B50-III remained linear up to a higher load and then increased non-linearly, but gradually, with an increase in load up to the ultimate load. On the other hand, the strains for specimen 3B50-IV became non-linear at an early stage of loading, indicating the effect due to the preload was not significant until it was increased up to about 80 percent of the yield load of the chord.

The local chord deformations for all specimens were not significant beyond a distance of about b_o (chord width) from the web extremities.

4.1.2 Buckling of compression web members

The yielding in the chord wall at the base of the compression web introduced a large eccentricity and therefore a bending moment into the web. The combined effect of this moment and the compressive axial force

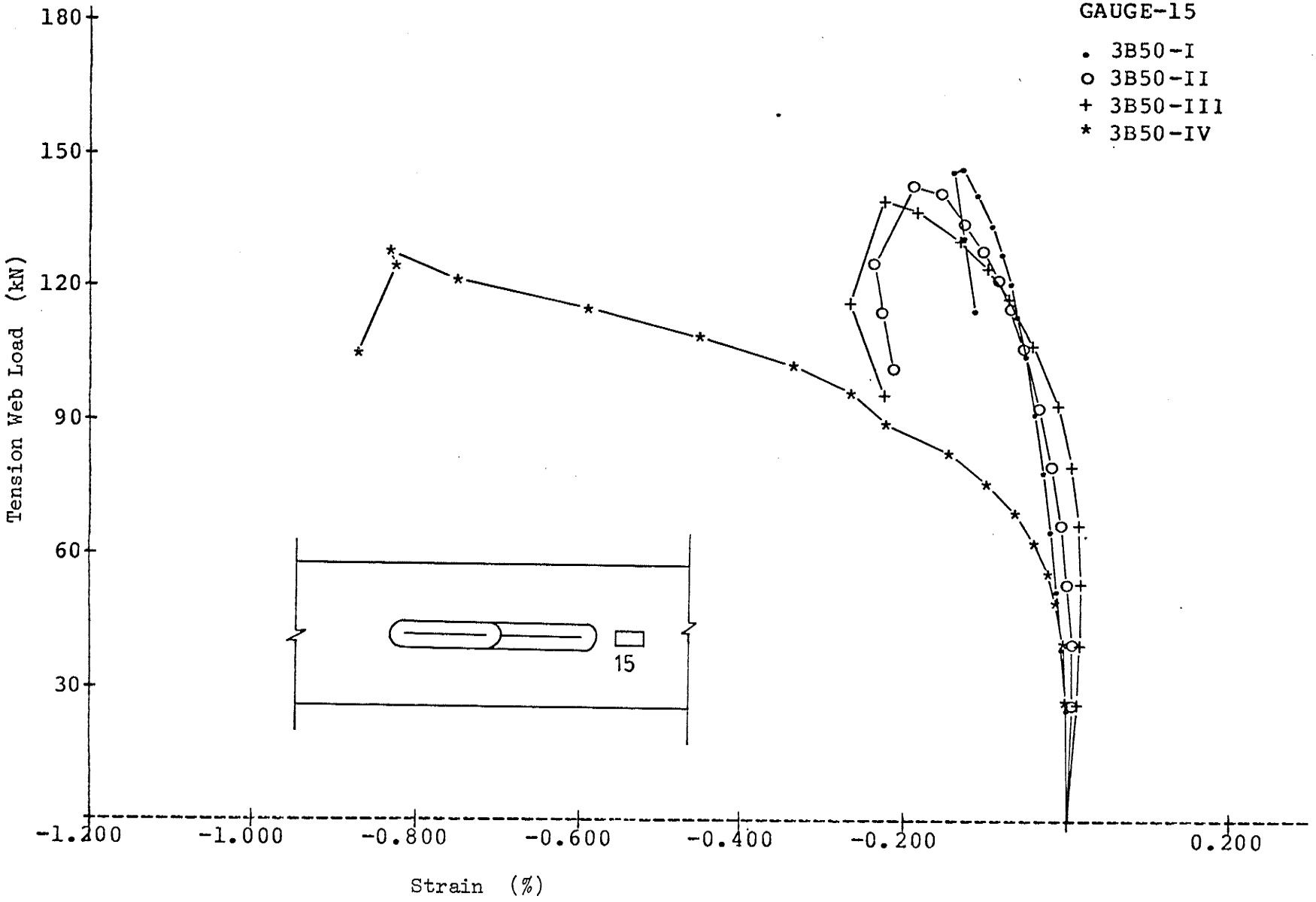

Fig 4.4 LOAD-DEFORMATION BEHAVIOR NEAR THE EXTREMITIES OF TENSION WEBS OF SPECIMENS 3B50-I TO 3B50-IV

in the web led immediately to an instability failure of the compression web. This is illustrated in Fig. 4.5, which shows the deflection profile of the compression web of specimen 3B50-I. When the load was small, the deflection in the web was small. As the ultimate load of the joint was attained, the web experienced large deflection and then buckled in the plane of the specimen. After this, the bending of the web increased with decreasing load.

The compression webs of specimens 3B50-I to 3B50-IV buckled at 148.2 kN, 144.2 kN, 140.2 kN and 126.8 kN,respectively. This indicated that as chord preload was increased, the compression webs buckled at lower and lower loads.

Because of the in-plane moment induced by the eccentricity at the joint, the compression webs always buckled in the plane of the specimen. Moreover, the support conditions permitted rotation only in the plane of the specimen.

4.1.3 Strains of chord face

Fig. 4.6 illustrates strains in the transverse direction of the chord face for specimen 3B50-I. The transverse strains were relatively large near the extremities and small at the flanks near the intersection of the loaded chord face and the web axes. This was consistent with the observed changes in chord deflections.

The transverse strains on the chord faces of all specimens are illustrated in Fig. 4.7 for comparison. It can be seen that the strains

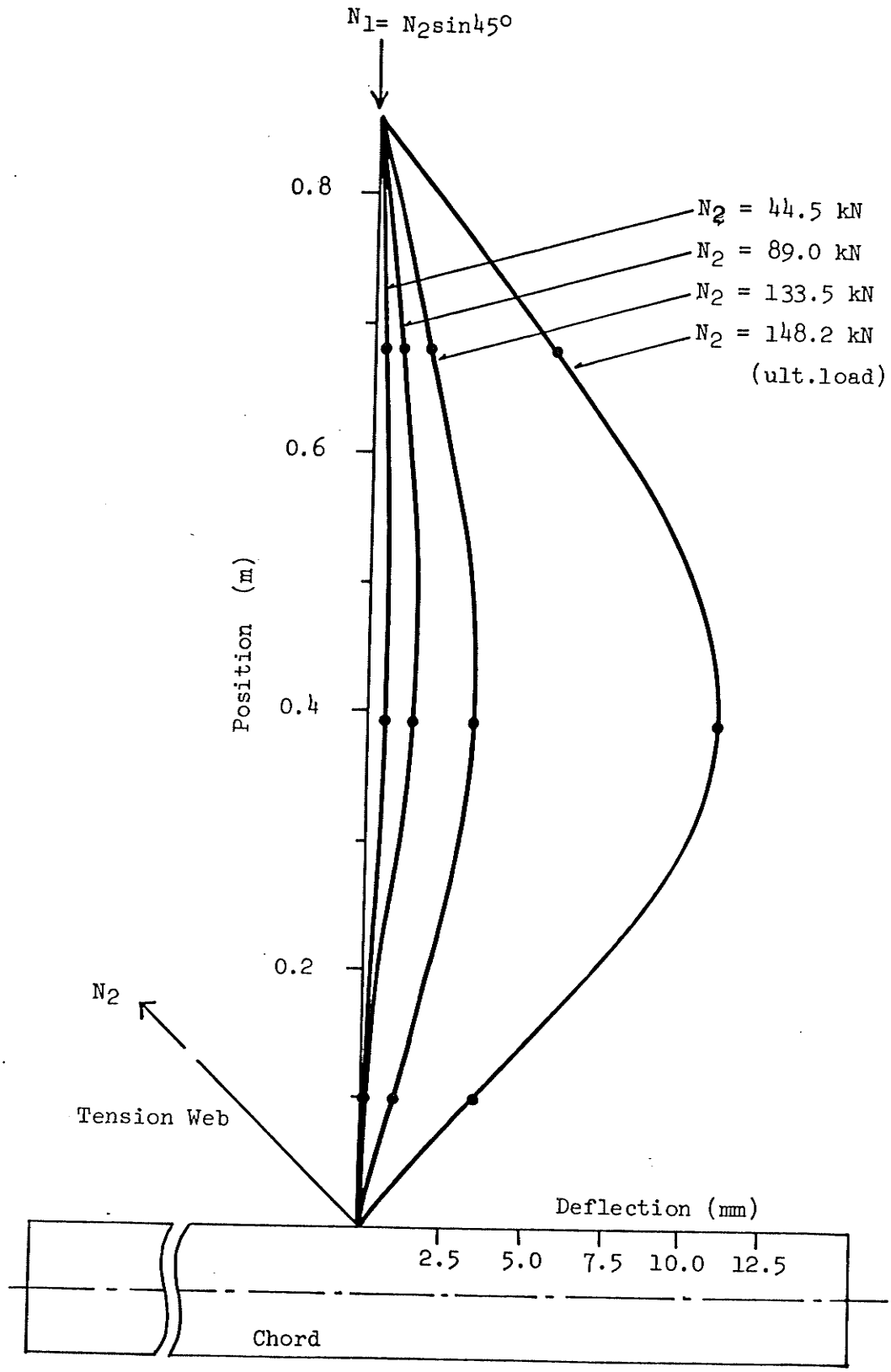

Fig. 4.5 DEFLECTION PROFILES OF COMPRESSION WEB OF SPECIMEN 3B50-I

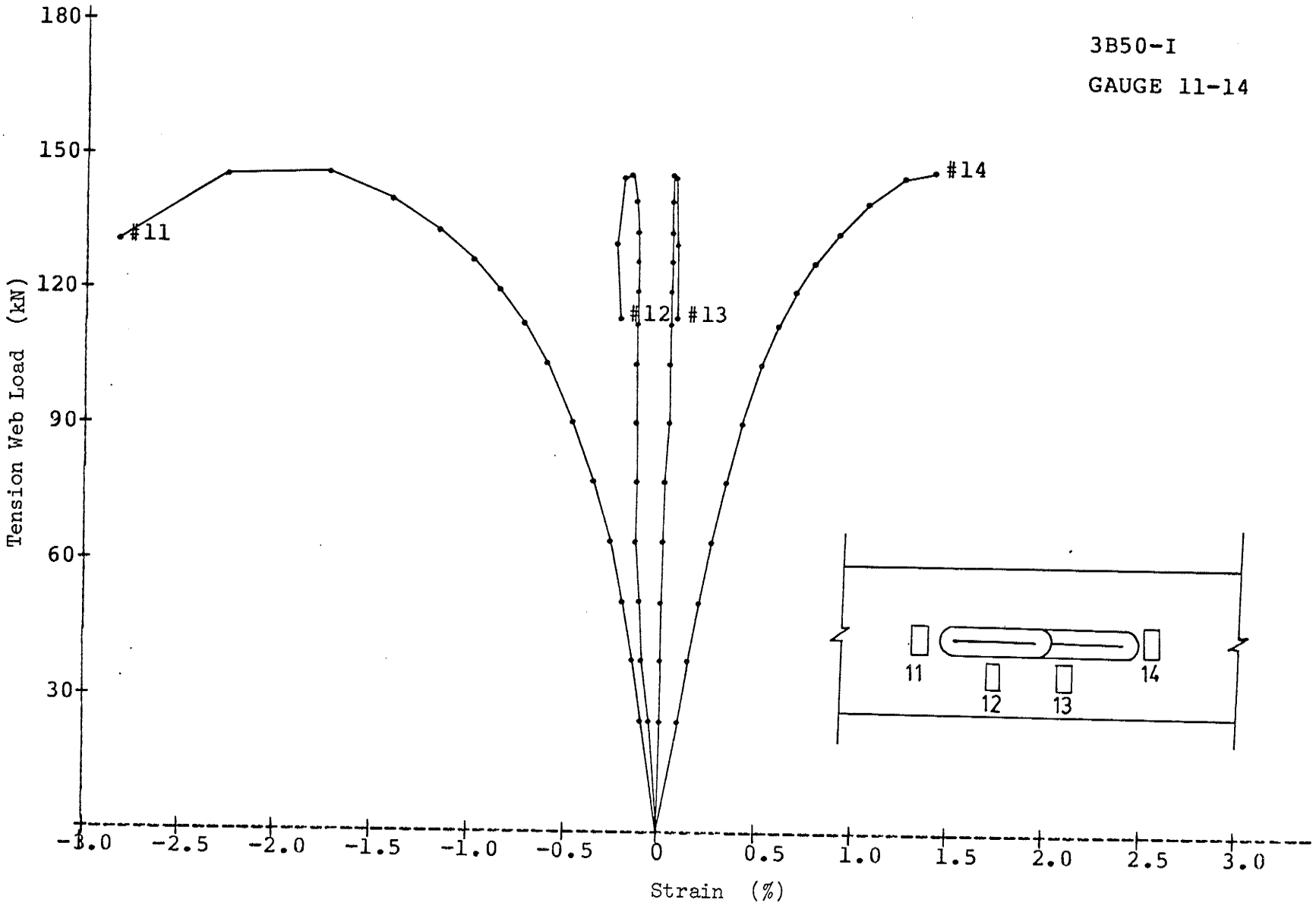

Fig. 4.6 TRANSVERSE STRAINS ON LOADED CHORD FACE OF SPECIMEN 3B50-I

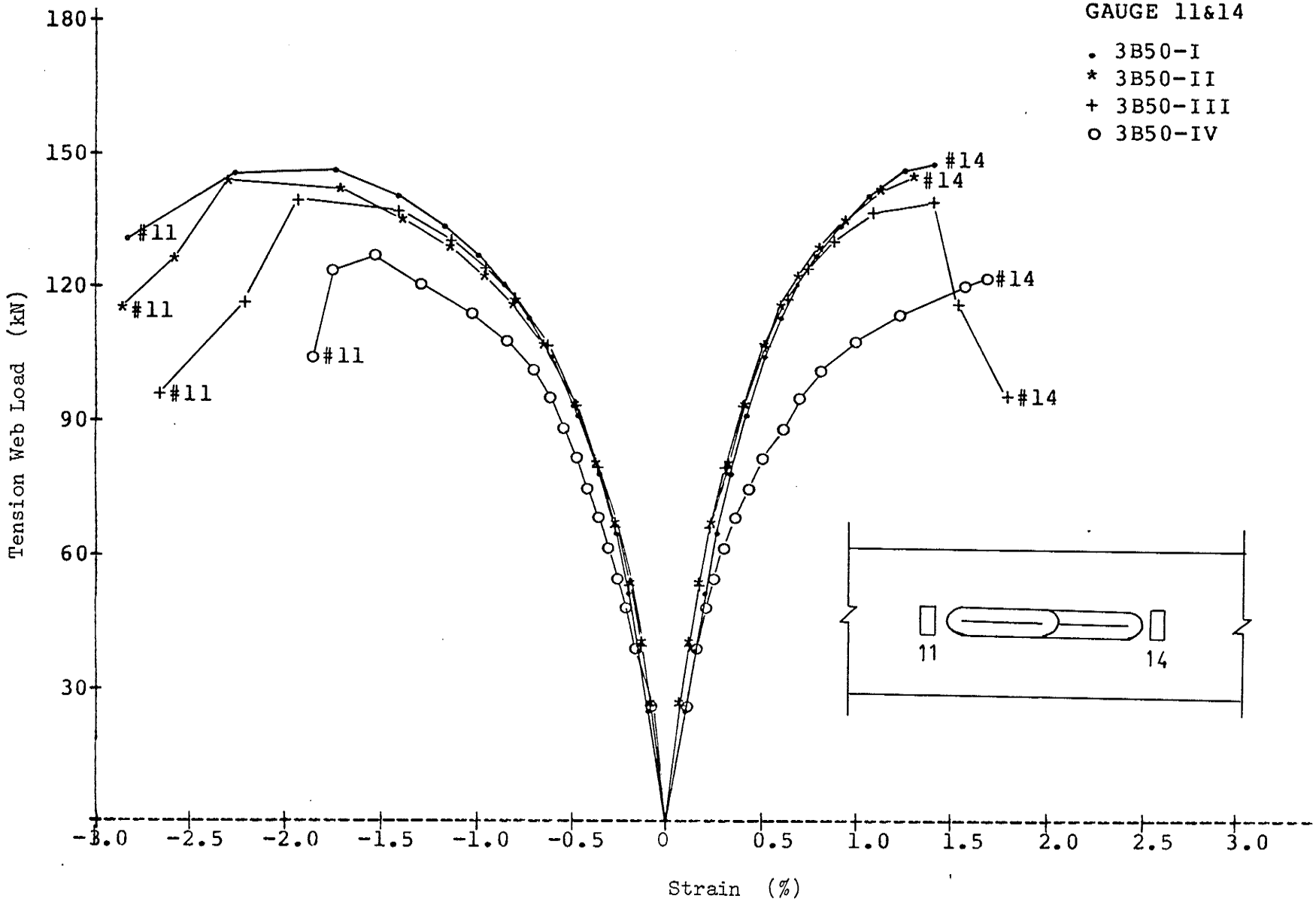

Fig. 4.7 TRANSVERSE STRAINS ON LOADED CHORD FACES OF SPECIMENS 3B50-I TO 3B50-IV

were almost identical for all specimens except specimen 3B50-IV. The strains of the latter became non-linear at an early stage of loading.The effect of preload in increasing the rate of change of local chord strains with load was significant as the preload was increased up to 80 percent.

Fig. 4.8 illustrates the strains in the longitudinal direction of specimens 3B50-I to 3B50-IV. The longitudinal strains were relatively large near the extremities of the compression webs, and small near the extremities of the tension webs. The deformation patterns were fairly similar. However, for specimen 3B50-IV only the longitudinal strains near the tension web extremity became non-linear at an early stage of loading, and increased rapidly with little increase in load. This indicated that the effect of preload was more serious at the extremity of the tension web than at the extremity of the compression web.

4.1.4 Strains in compression web members

The longitudinal strains of the compression web of specimen 3B50-IV at loads of 44.5 kN and 89.4 kN (the working load in tension web) are shown in Fig. 4.9. Even at a low load of 44.5 kN, the strains were non-uniform. They were large at the side near the lap and small on the opposite side. At the working load of 89.4 kN, the average of the strains at section C, about 0.7 m away from the loaded chord face, was 0.073%. This agreed well with the calculated average strain, 0.072%, which was obtained by dividing the axial stress (89.4 x 1000 sin 45°/427.1 MPa).

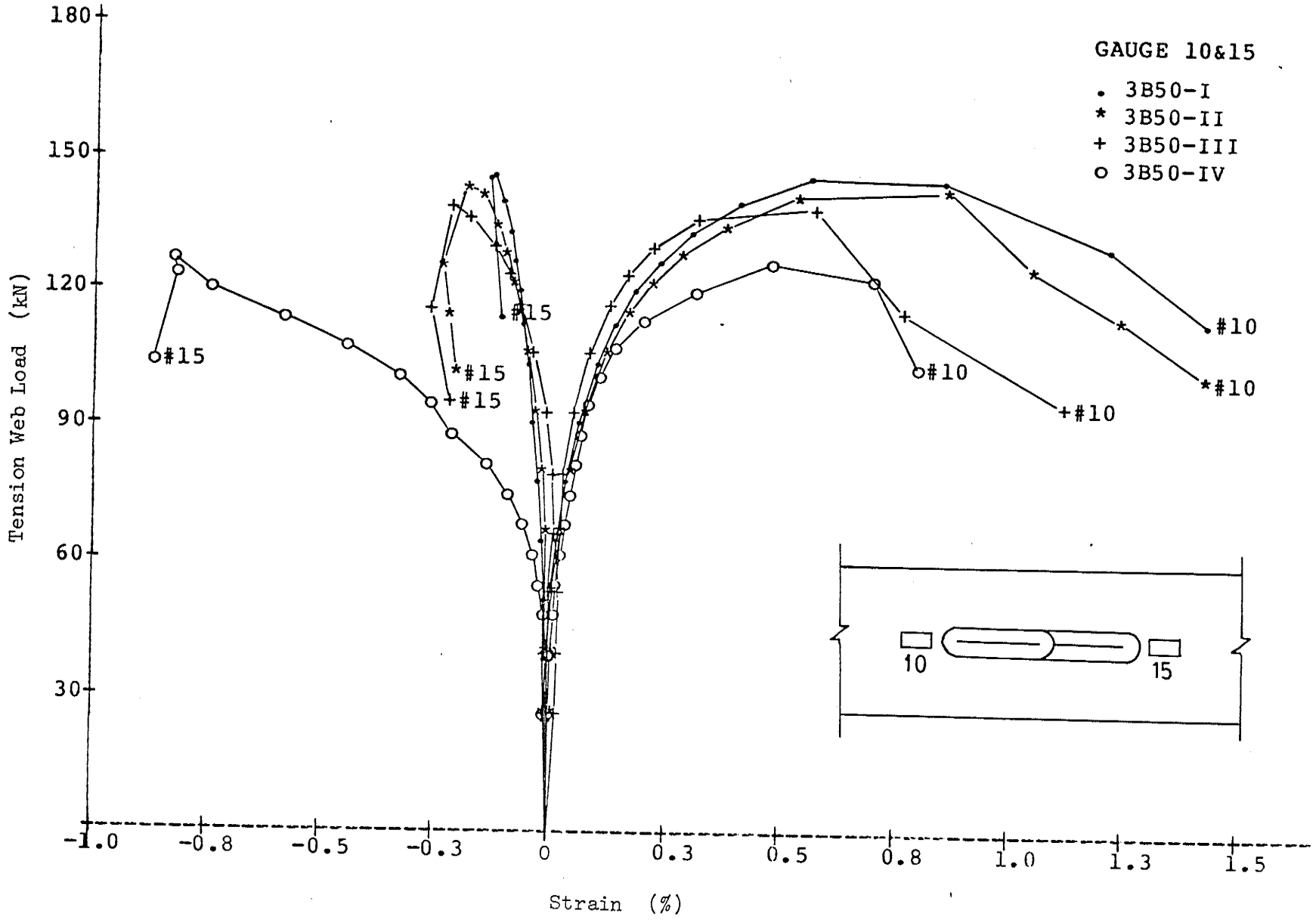

Fig. 4.8 LONGITUDINAL STRAINS ON LOADED CHORD FACES OF SPECIMENS 3B50-I TO 3B50-IV

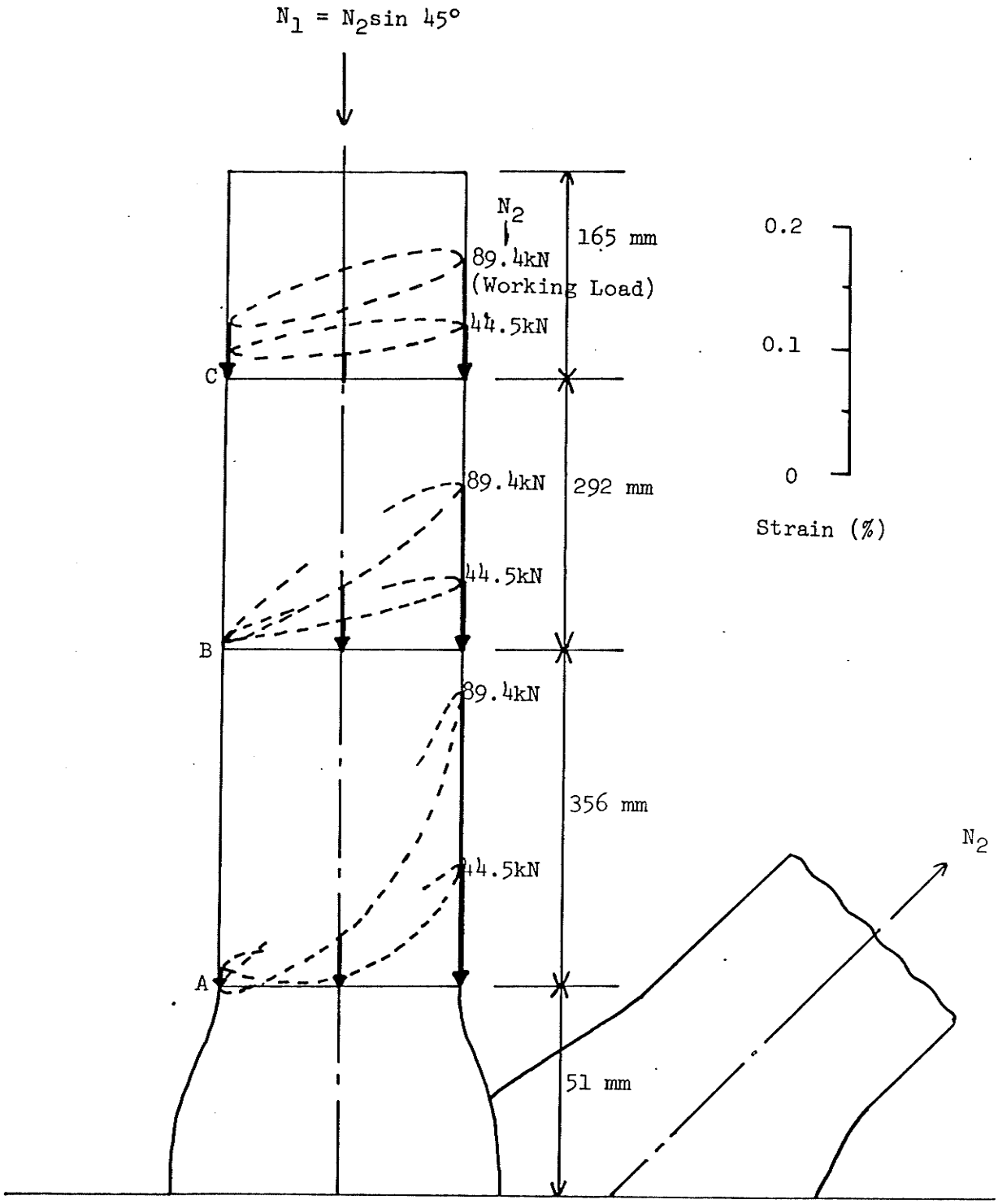

Fig. 4.9 LONGITUDINAL STRAINS ON COMPRESSION WEB MEMBER OF SPECIMEN 3B50-IV

by the modulus of elasticity (207,000 MPa). At section A, the strain near the lap was much larger than that on the opposite side. Moreover, the strain near the lap was 0.25% at 89.4 kN, which already exceeded the nominal yield strain of 0.17% for the member material.

In specimens which had chord preloads, the longitudinal strains in the compression webs were highly non-uniform, indicating bending and stress concentration in the webs.

4.1.5 Strains in tension web members

The plots of longitudinal tension-web strain versus load are presented in Fig. 4.10 for specimen 3B50-IV. The curves were used to plot the deformation profiles at different sections of the web, as shown in Fig. 4.11.

In Fig. 4.10, the strains (gauges 23, 24 and 25) at a section near the mid-length of the web were linear almost up to the ultimate load, while the strains at a section near the lap (gauges 7, 8 and 9) became non-linear at relatively low loads.

In Fig. 4.11, the strain distributions were non-uniform, especially at section A. When the working load was reached, the maximum strain at section A was 0.23%. This was already 1.35 times the nominal yield strain, while the other strains at the same section were still well below the nominal yield strain. Consequently, tearing of the tension web occurred near the lap.

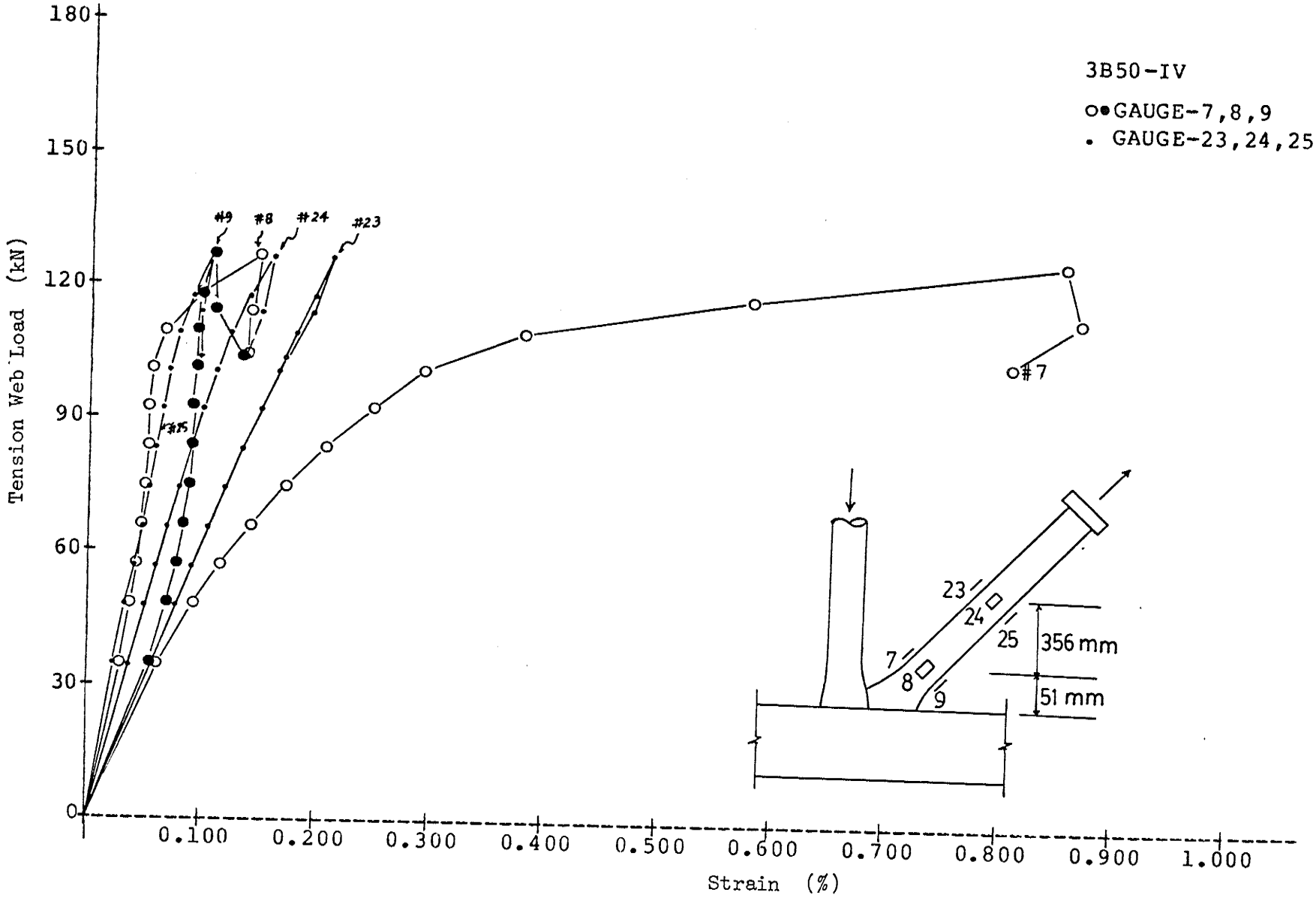

Fig. 4.10 LONGITUDINAL STRAINS ON TENSION WEB MEMBER OF SPECIMEN 3B50-IV

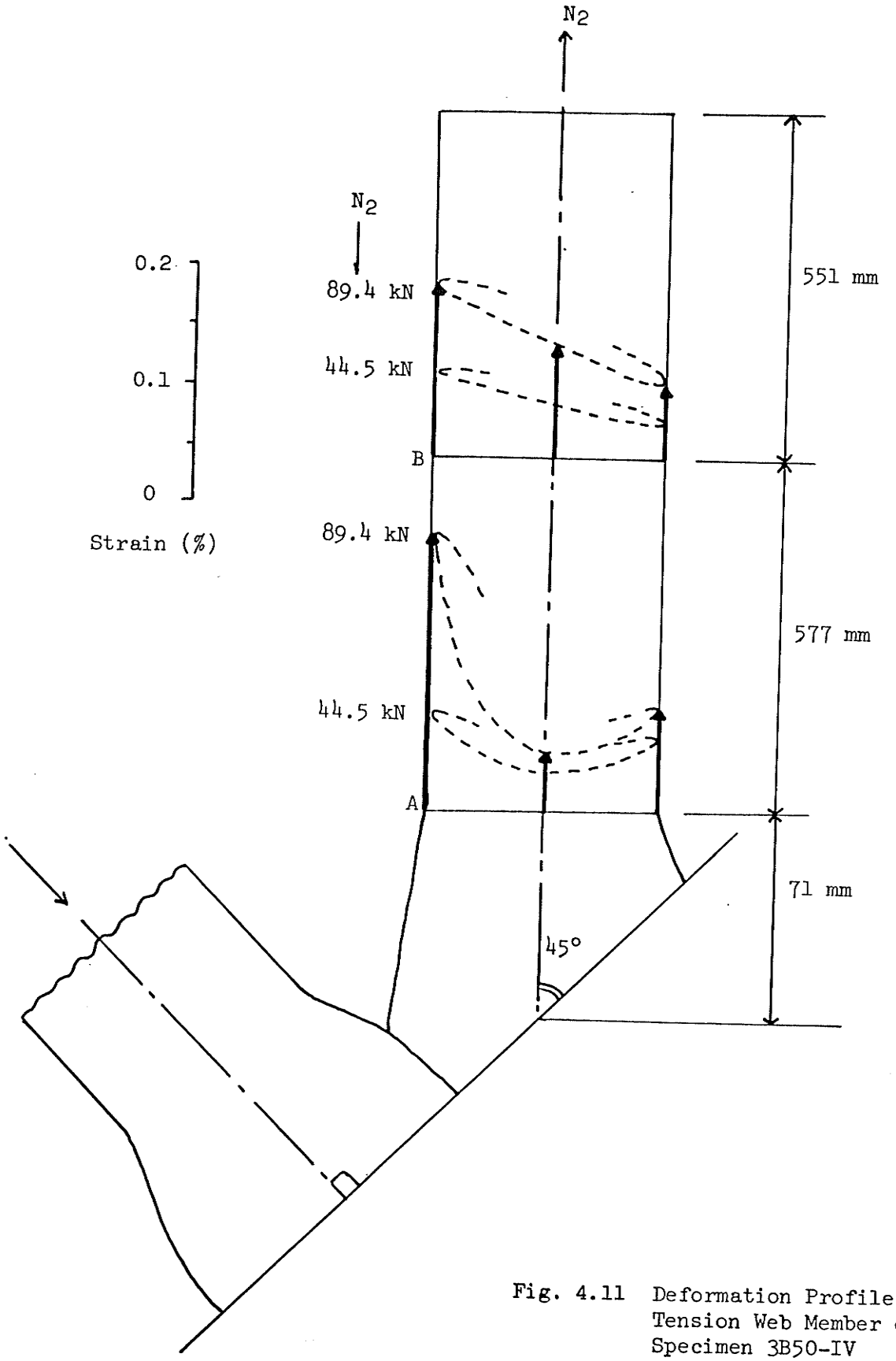

Fig. 4.11 Deformation Profiles of Tension Web Member of Specimen 3B50-IV

At the working load of 89.4 kN, the average of the strains at the mid-length of the web was 0.101%, in very good agreement with the average strain of 0.099%, which was calculated from the measured load.

4.1.6 Failure modes

Failure of the joint in all cases was considered to have occurred when the ultimate load carrying capacity of the joint was reached under test. There were four typical modes of failure: excessive local deformation of the chord, buckling of the compression web, fracture of the weld at the toe of the tension web or tearing of the tension web, and buckling of the chord. A joint usually failed in a combination of two or more of these modes.

Joint failure by excessive local deformation of the chord is illustrated in Fig. 4.12 and Fig. 4.13. It occurred in all specimens. It was caused by the cumulative effect of the web member force couple and the axial and bending loads in the chord. The local overstressing in the chord wall near the intersection increased with an increase in preload. As a result, the bending or buckling pattern of the loaded chord wall was changed. The higher the preload, the larger was the deflection of the chord wall under the tension web. According to thin-plate theory, the deflection is inversely proportional to the cube of the chord thickness for a given load. Therefore, it would be expected that this mode of failure could be prevented by using a thicker chord wall.

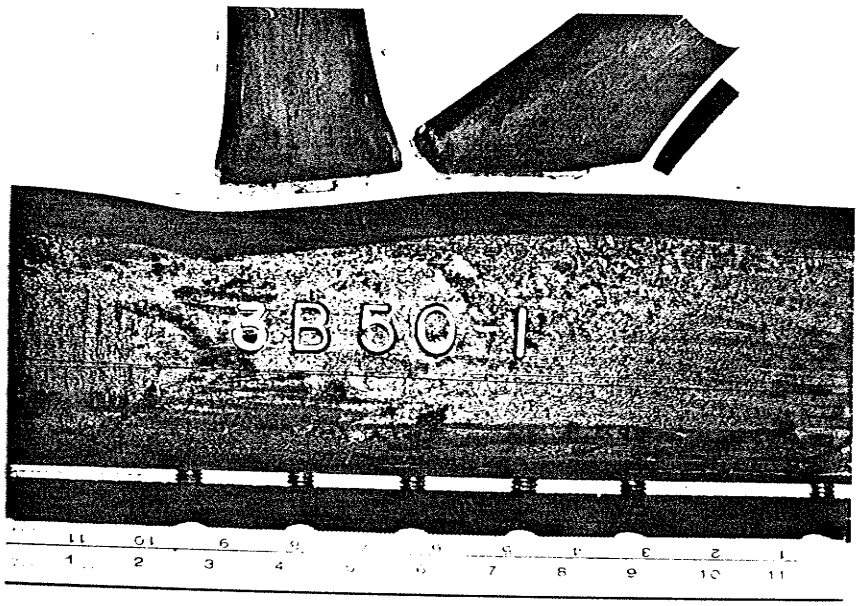

Fig.4.12 FAILURE MODE A -- LOCAL DEFORMATION OF LOADED CHORD FACE OF SPECIMEN 3B50-I

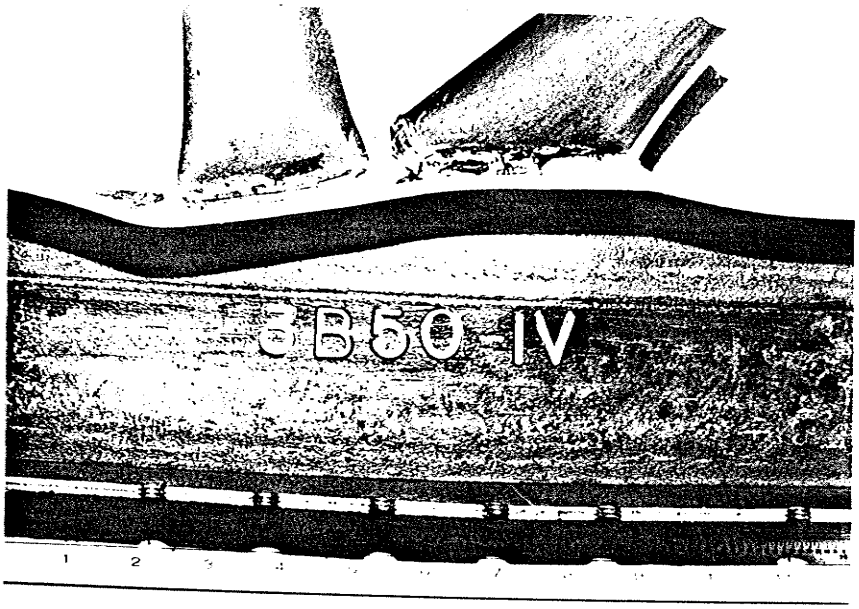

Fig. 4.13 FAILURE MODE A -- LOCAL DEFORMATION OF LOADED CHORD FACE OF SPECIMEN 3B50-IV

Failure by buckling of the compression web is illustrated in Fig. 4.14 and Fig. 4.15. This type of failure occurred in all specimens. Only overall buckling took place, and no local buckling occurred. The compression web always buckled away from the tension web in the plane of the specimen. This was caused by a moment being induced at the joint due to the bending of the chord face. As the preload was increased, the buckling of the compression web occurred at a lower joint load. The effect of preload in increasing the moment induced by chord face deformation was obvious.

Because a large load transfer took place at the lap, the toe of the tension web was usually highly stressed. Moreover, it was considered that high welding residual stresses might exist at the toe. Therefore fracture of welds or tearing of the tension web was expected at the toe of the tension web. This is consistent with the test results in which failure by fracture of weld or tearing of tension web always occurred at the toe near the lap. Examples of this mode of failure are shown in Fig. 4.16 and Fig. 4.17. It is notable that this occurred in all specimens except the one with zero chord preload. This indicated that stress concentration occurred at the toe of tension web with an addition of a preload.

Failure by buckling of the chord is illustrated in Fig. 4.18. This occurred only in specimen 3B50-IV, which had the largest preload in its chord. The local overstressing in the chord wall due to preload and load transfer between members reduced the overall buckling

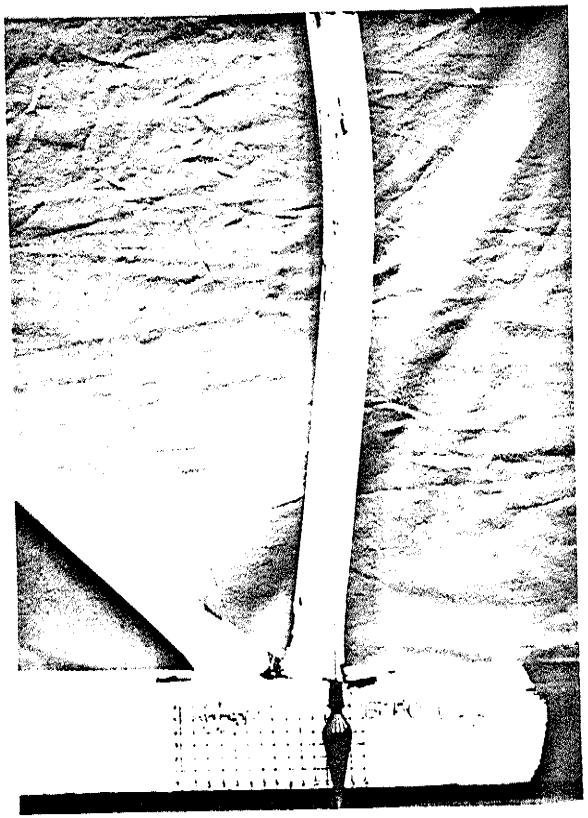

Fig. 4.14 FAILURE MODE B -- BUCKLING OF COMPRESSION WEB MEMBER OF SPECIMEN 3B50-I

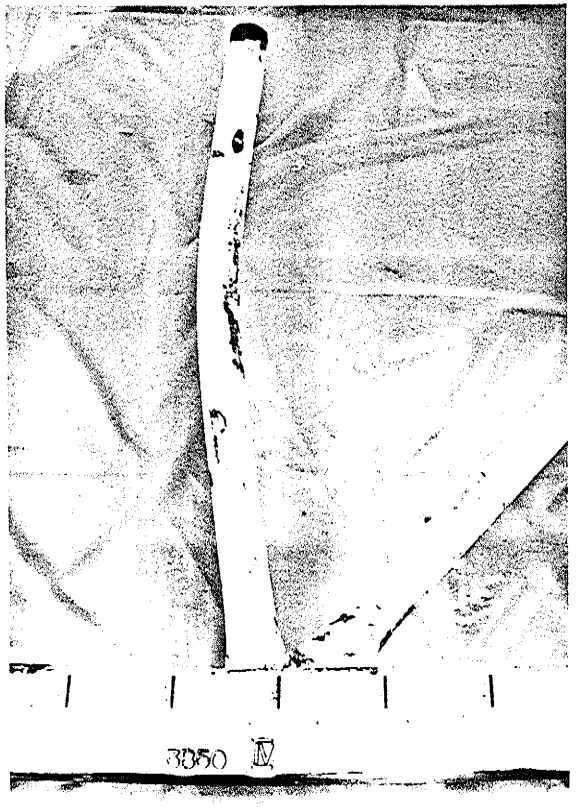

Fig. 4.15 FAILURE MODE B -- BUCKLING OF COMPRESSION WEB MEMBER OF SPECIMEN 3B50-IV

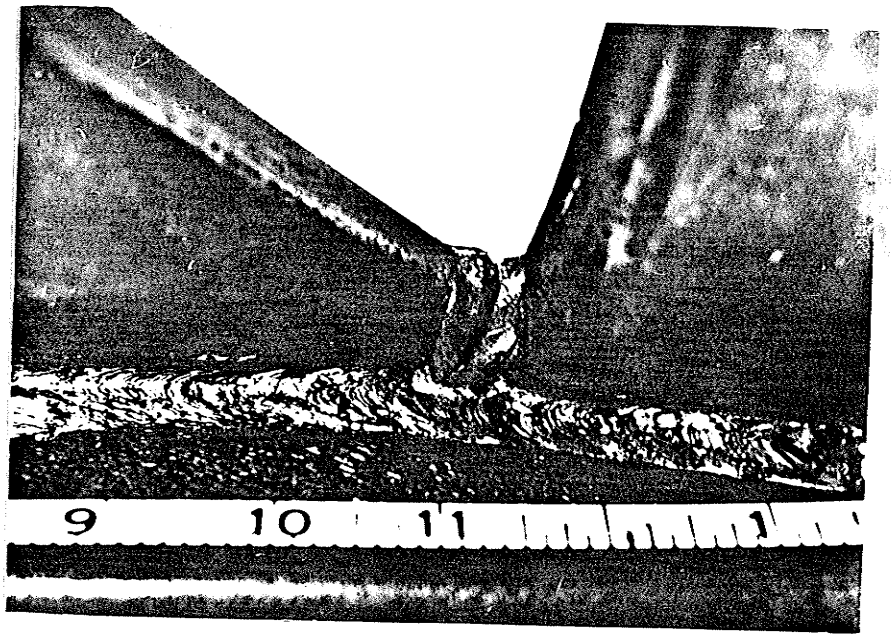

Fig. 4.16 FAILURE MODE C -- FRACTURE OF WELD AT THE TOE OF TENSION WEB MEMBER OR TEARING OF TENSION WEB MEMBER OF SPECIMEN 3B50-III

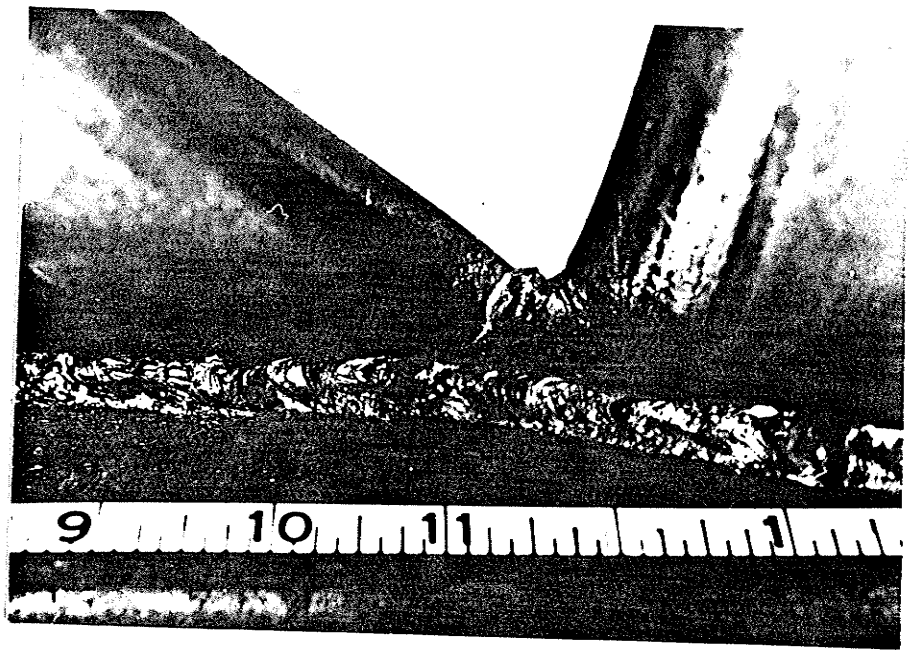

Fig. 4.17 FAILURE MODE C -- FRACTURE OF WELD AT THE TOE OF TENSION WEB MEMBER OR TEARING OF TENSION WEB MEMBER OF SPECIMEN 3B50-IV

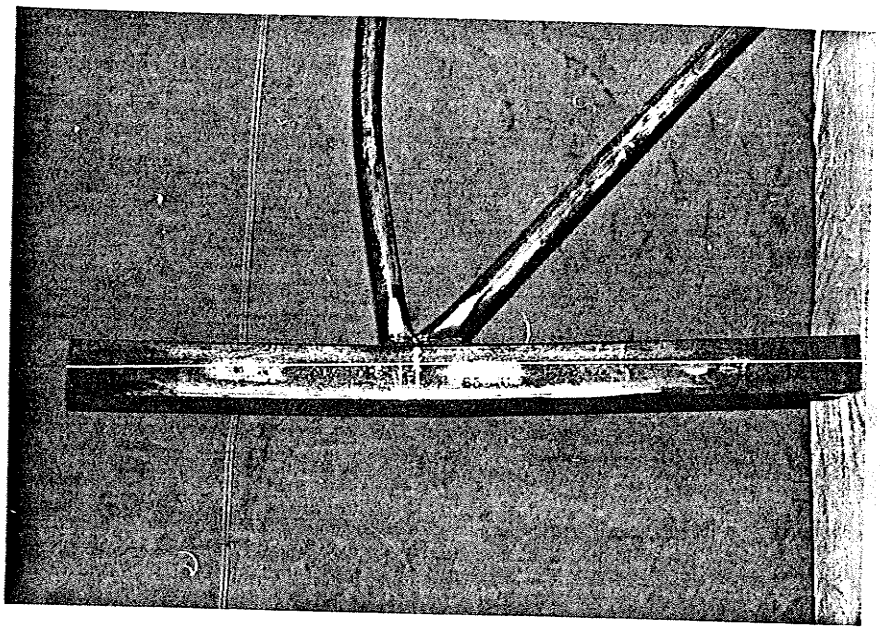

Fig. 4.18 FAILURE MODE D -- BUCKLING OF CHORD OF SPECIMEN 3B50-IV

load of the chord.

4.1.7 Joint strength

The yield load is defined as the load at which the rate of deformation per unit load begins to increase significantly. The yield loads for the joint specimens were found using a method developed by the author. In the author's method, the value of the yield load of a joint may be found by first plotting a load-deformation curve from test data as shown in Fig. 4.19. Then two tangents A and B to the initial and final slopes of the curve are drawn. They intersect at point C, at which point a bisector of /ACB is constructed. The bisector from C interesects the load-deformation curve at point D. The ordinate corresponding to point D is defined as the yield load or yield strength of the joint.

This method was used because there is no distinct yield point for the joint, as the change between the elastic and the plastic response is gradual. Ghosh (1978) defined the yield load as the web force normal to the chord axis when the load-deformation plot begins to deviate from the initial straight line. In Ghosh's method, the deviation is expressed in terms of an arbitrarily chosen value of chord deformation. The method is thus not practical, since the initial straight-line portion of a joint load-deformation curve is usually relatively small. Consequently the yield load so obtained might be well below the elastic limit. Moreover, the values of yield loads depend markedly on judgement

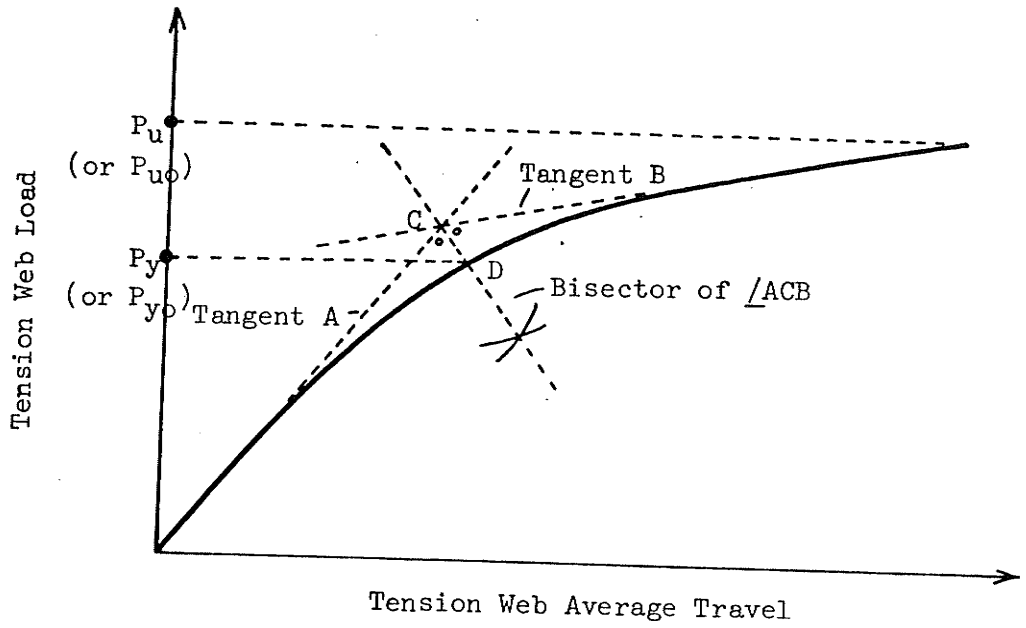

Fig. 4.19 THE AUTHOR'S METHOD OF FINDING JOINT YIELD STRENGTH

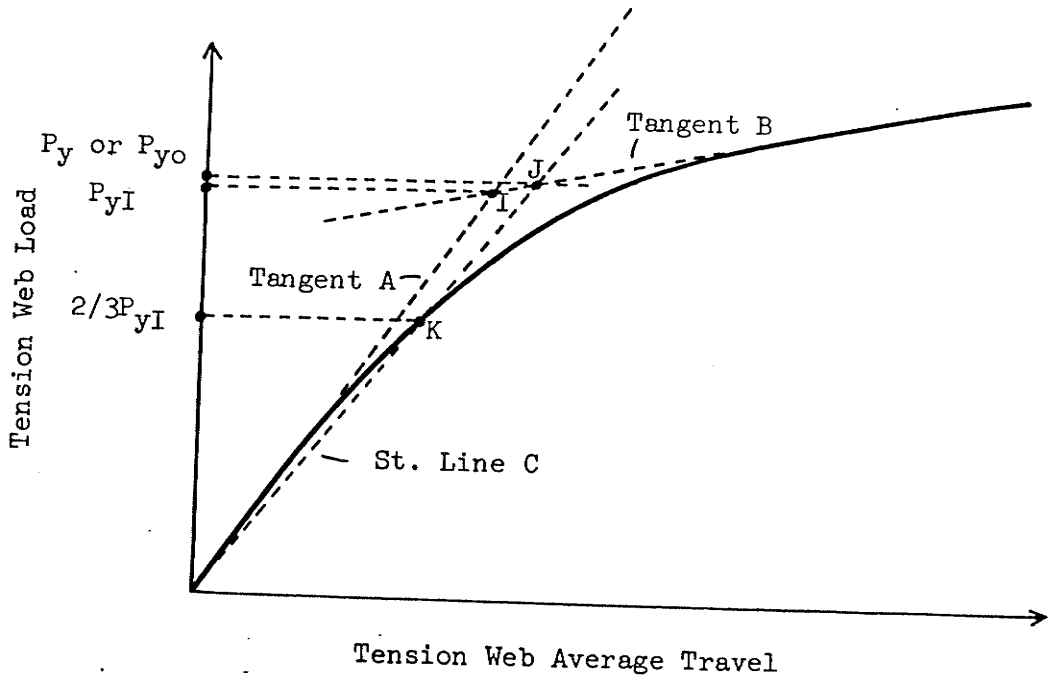

Fig. 4.20 AKIYAMA'S METHOD OF FINDING JOINT YIELD STRENGTH

and the uniqueness of the values is questionable.

For comparison, the yield loads of joints were also found by using Akiyama's method (Akiyama et al. 1974) which can be described as follows:

a. Draw a load-deformation curve as illustrated in Fig. 4.20;

b. draw tangents A and B, which intersect at I as similar to the author's method;

c. find the ordinate P_{yI} of point I and locate point K with an ordinate equal to 2/3 P_{yI} on the curve;

d. connect point K to the origin with a straight line C and let line C intersect the tangent B at J; then

e. find the load corresponding to point J. It is defined as the yield load, P_y of the joint.

The yield loads found by using the author's method are always smaller than those found using Akiyama's method.

In this test series, the plots of load applied to the tension web versus its movement relative to the chord axis are shown in Fig. 4.21. The movement of the tension web was measured as the average of the readings of the three transducers located on the chord wall under the tension web. From those plots, the yield strength of each joint was found using both the author's method and Akiyama's method. The results obtained together with ultimate loads, joint efficiencies, load factors and stiffnesses are given Table 4.1.

In Table 4.1, it can be seen that the joint yield loads decreased as the chord preload increased. This suggests that an increase in preload

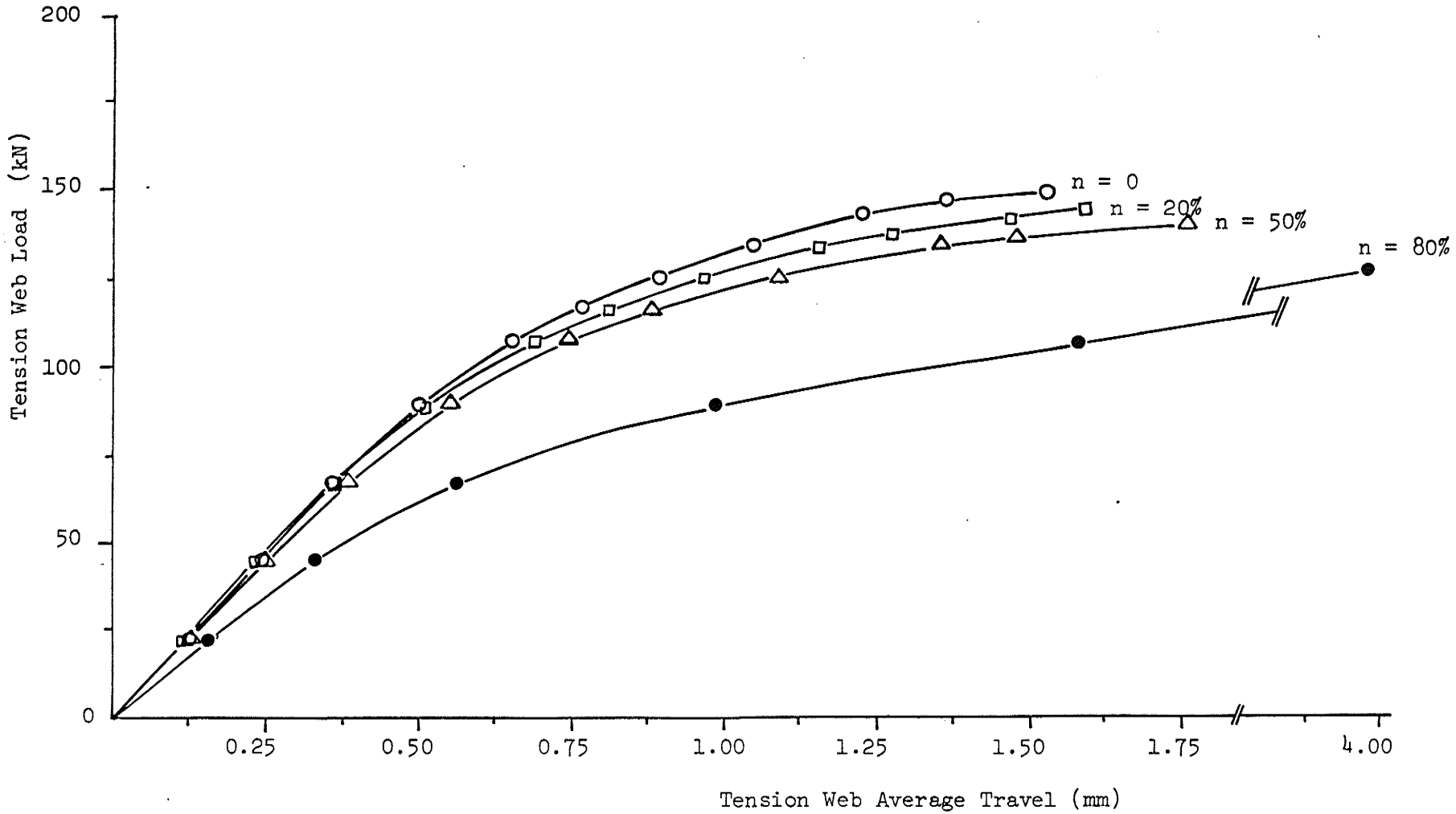

Fig.4.21 LOAD-DEFORMATION BEHAVIOUR OF SPECIMENS 3B50-I TO 3B50-IV

TABLE 4.1: Test Results - Test Series 3B50

Specimen	Preload n %	Yield Load (The Author's Method) kN	Yield Load (Akiyama's Method) kN	Ultimate Load kN	Load Factor	Joint Efficiency	Compression Stiffness $\frac{k_1}{Ed_1}$	Tension Stiffness $\frac{k_2}{Ed_2}$	Failure Mode
3B50-I	0	117.48	138.84	148.36	1.66	99.7	0.0092	0.0987	A,B
3B50-II	20	109.03	128.61	144.14	1.61	96.8	0.0086	0.0617	A,B,C
3B50-III	50	104.58	123.71	140.22	1.57	94.2	0.0092	0.0494	A,B,C
3B50-IV	80	86.78	106.36	126.87	1.42	85.2	0.0077	0.0392	A,B,C, D

Failure Modes:

A = Excessive local deformation of chord

B = Buckling of compression web

C = Fracture of weld at the toe of tension web or tearing of tension web

D = Buckling of chord

The joint load factor is defined as the ratio of the ultimate load to the working load of the tension web member.

TABLE 4.1: (Continued) Test Results - Test Series 3B50

Specimen	Preload n %	Reduction Coefficient of Joint Yield Strength, α (The Author's Method)	Reduction Coefficient of Joint Yield Strength, α (Akiyama's Method)	Reduction Coefficient of Joint Ultimate Strength, β
3B50-I	0	1	1	1
3B50-II	20	0.93	0.93	0.97
3B50-III	50	0.89	0.89	0.94
3B50-IV	80	0.74	0.77	0.85

caused stress concentration and local yielding at the joint, thus diminishing the yield strength of the joint. This phenomenon was particularly significant when the preload was increased up to 80 percent. At this preload, the yield strength was reduced by about 25%, in comparison with that of the joint with zero preload.

The ultimate loads of the joints also reflected this phenomenon, although the ultimate loads were not affected as much as the yield loads. When the chord preload was 50 percent of the yield load of the chord, the ultimate load dropped by about 6 percent. As the preload was increased to 80 precent, the ultimate load was reduced by as much as 15 percent. The joints in the trusses tested by Ghosh (1978) had configurations slightly different from those tested in this study. Ghosh found that the ultimate loads for joints in the trusses were 17 to 23 percent lower than those of similar isolated joint specimens in which no chord preload was used. This indicated that addition of chord preload would simulate more closely the actual truss conditions.

In the following, equations were obtained from the test results by means of the least square method. Here a yield strength reduction coefficient, α, is defined as the ratio of the yield strength of a joing with a chord preload to that of a similar joint with no chord preload. The reduction coefficient corresponding to preload can be estimated using the following empirical equation:

$$\alpha = 1 - 0.18n\ (1 + 0.94n) \quad (0 \leq n \leq 80\%) \tag{4.1}$$

where n is the percentage of preload, equal to σ_o/σ_e, σ_o the stress in chord due to preload and σ_e the yield stress at 0.2% offset, of chord material.

The mean error of the equation is 0.02. The yield strengths used in deriving this equation were found using the author's method. Using Akiyama's method, the following formula was obtained:

$$\alpha = 1 - 0.22\ n\ (1 + 0.32\ n) \qquad (0 \leq n \leq 80\%) \qquad (4.2)$$

The mean error of this equation is 0.017. The experimental values of α were plotted against n in Fig. 4.22. Also shown in the figure are plots of equations (4.1) and (4.2). The curves show that α decreases rapidly as n increases.

It is interesting to notice that the curves obtained by Akiyama's method and by the author's method are quite similar, giving similar rates of change in yield strength with respect to chord preload.

An ultimate strength reduction coefficient, β, is defined as the ratio of the ultimate strength of a joint with a chord preload to that of a similar joint with no chord preload. The reduction coefficient can be estimated using the following equation:

$$\beta = 1 - 0.07\ n\ (1 + 2\ n) \qquad (0 \leq n \leq 80\%) \qquad (4.3)$$

The mean error is 0.007 for this equation. The experimental values of β were plotted against n in Fig. 4.23. The figure also includes a plot of equation (4.3).

The strength of a tubular joint in terms of joint load factor and joint efficiency is also given in Table 4.1. The joint efficiency, E_{ff}, defined as the ratio of the ultimate load to the yield load in the

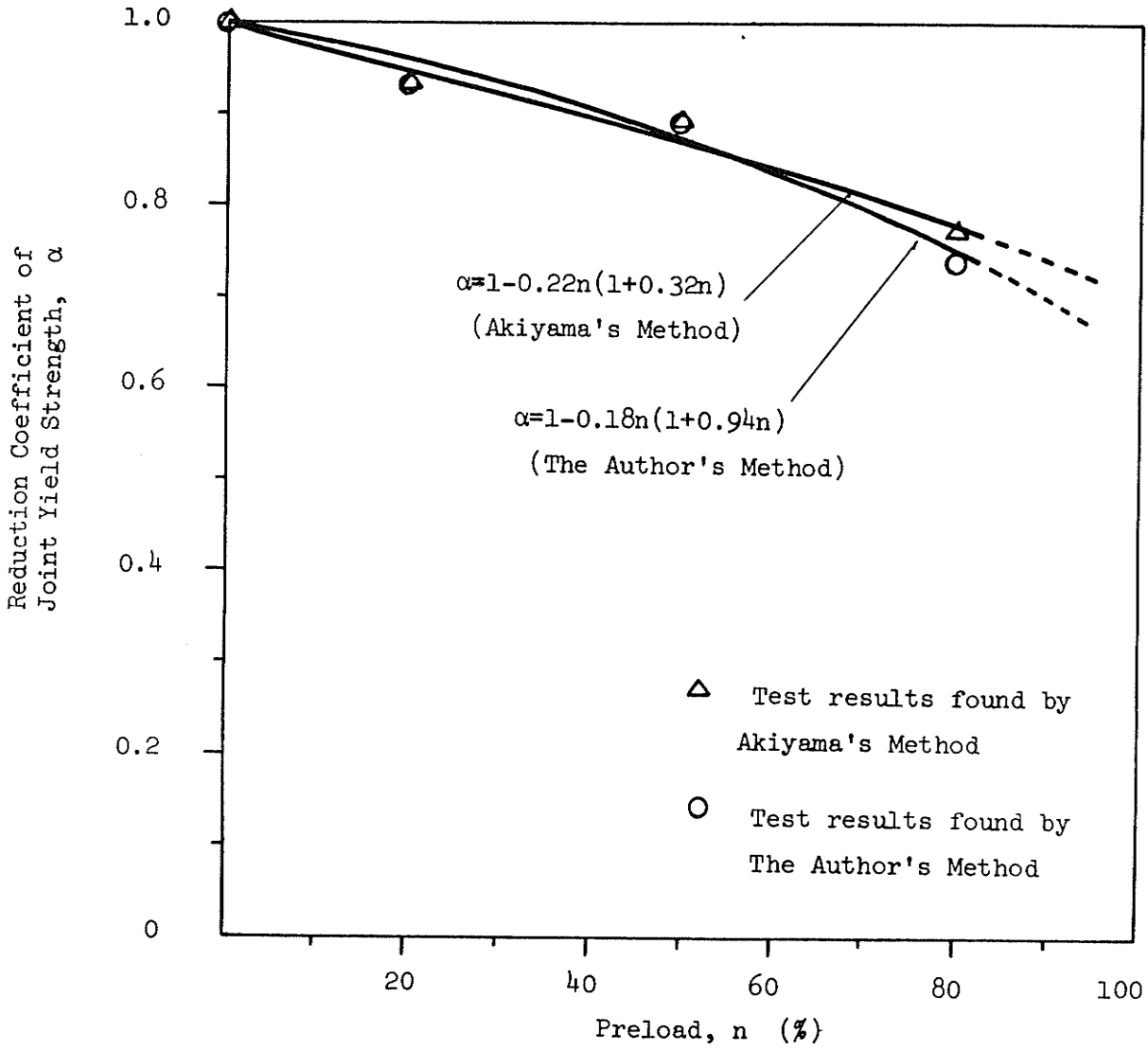

Fig. 4.22 REDUCTION COEFFICIENT OF JOINT YIELD STRENGTH

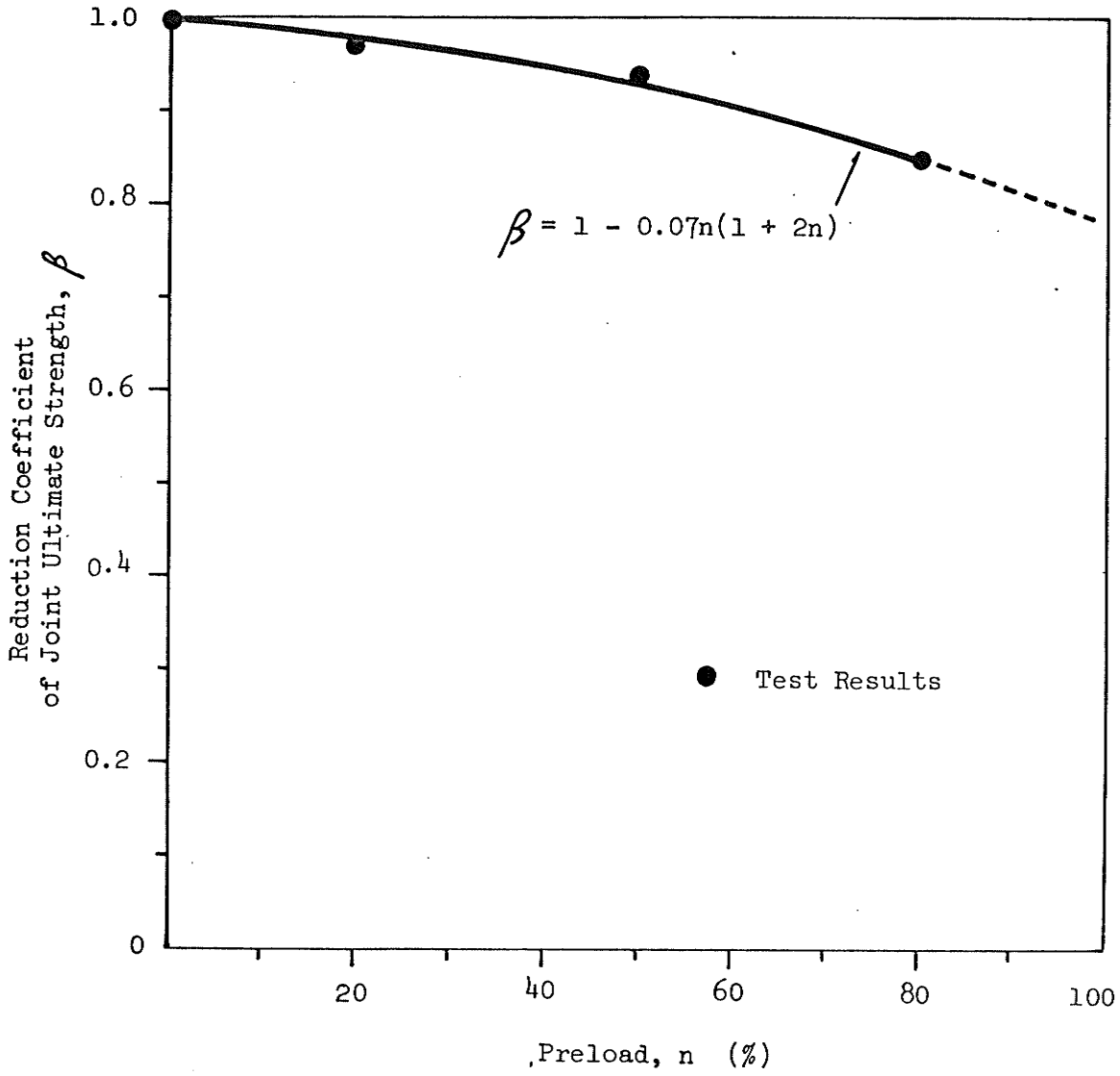

Fig. 4.23 REDUCTION COEFFICIENT OF JOINT ULTIMATE STRENGTH

tension web, can be estimated using the following equation:

$$E_{ff} = 99.7 - 3.52\ n\ (1 + 5.13\ n) \qquad (0 \leq n \leq 80\%) \qquad (4.4)$$

A plot of experimental values of E_{ff} is presented in Fig. 4.24, together with a plot of equation (4.4). It can be seen that the joint efficiency decreased as preload increased.

4.1.8 Joint stiffness

Joint stiffness is a measure of the ability of a joint to resist deformation in the linear range. The deformation of a tubular joint is usually significant at the chord face under the web members. Hence, the joint stiffness is defined as the ratio of the force and displacement in the linear range, along the web axes. The stiffness may be represented as either a tension stiffness or a compression stiffness, depending on which web member is considered. As illustrated in Fig. 4.25, the stiffness along the compression web axis is defined as compression stiffness, $k_1 = N_1/\delta_1$, where N_1 and δ_1 are respectively the force and displacement in the linear range along the compression web axis at the loaded chord face. Likewise, the stiffness along the tension web axis is defined as tension stiffness, $k_2 = N_2/\delta_2$, where N_2 and δ_2 are respectively the force and displacement in the linear range along the tension web axis at the loaded chord face.

The values of $\frac{k_1}{Ed_1}$ and $\frac{k_2}{Ed_2}$ are given in Table 4.1. E is the

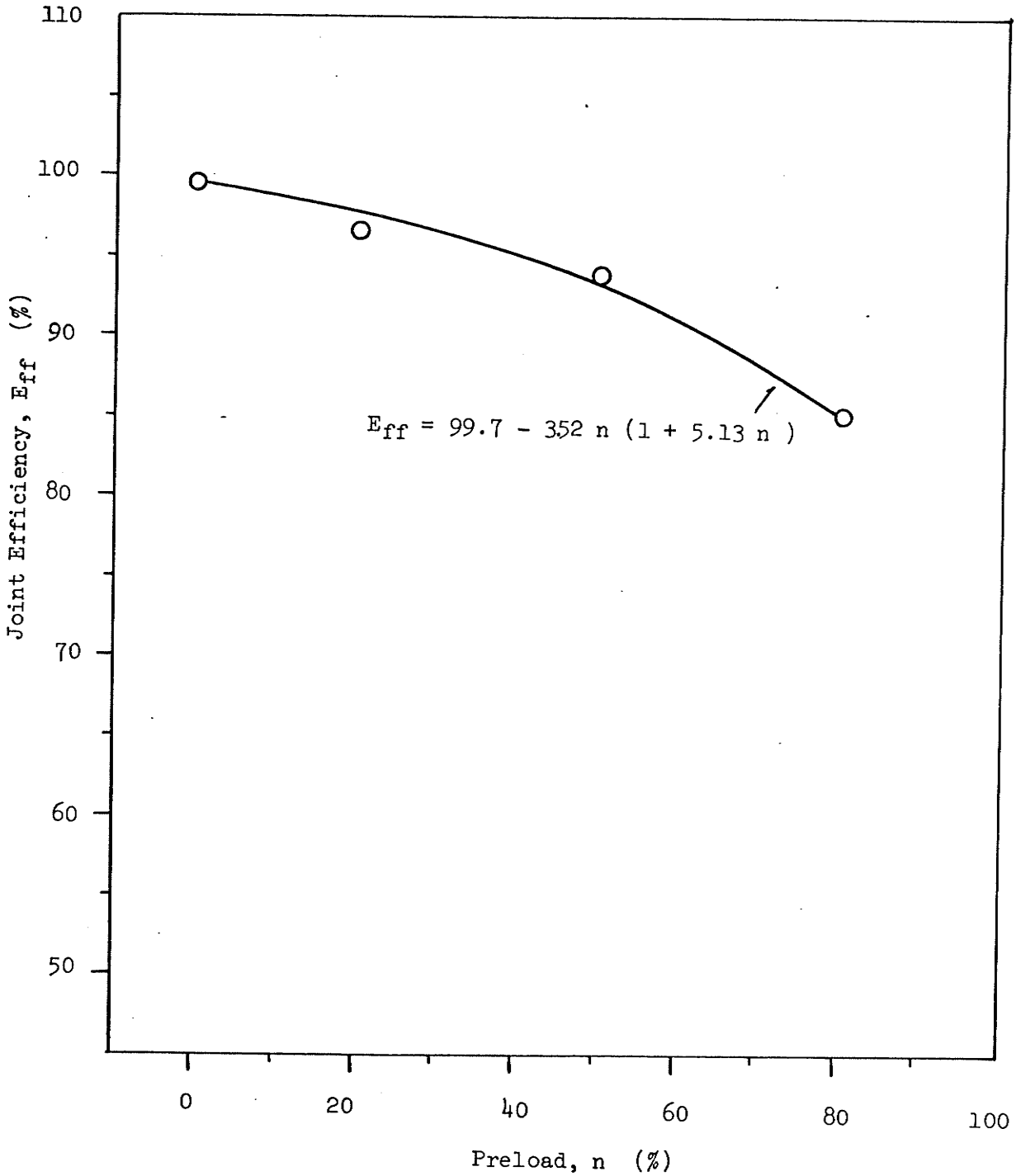

Fig. 4.24 Joint Efficiency

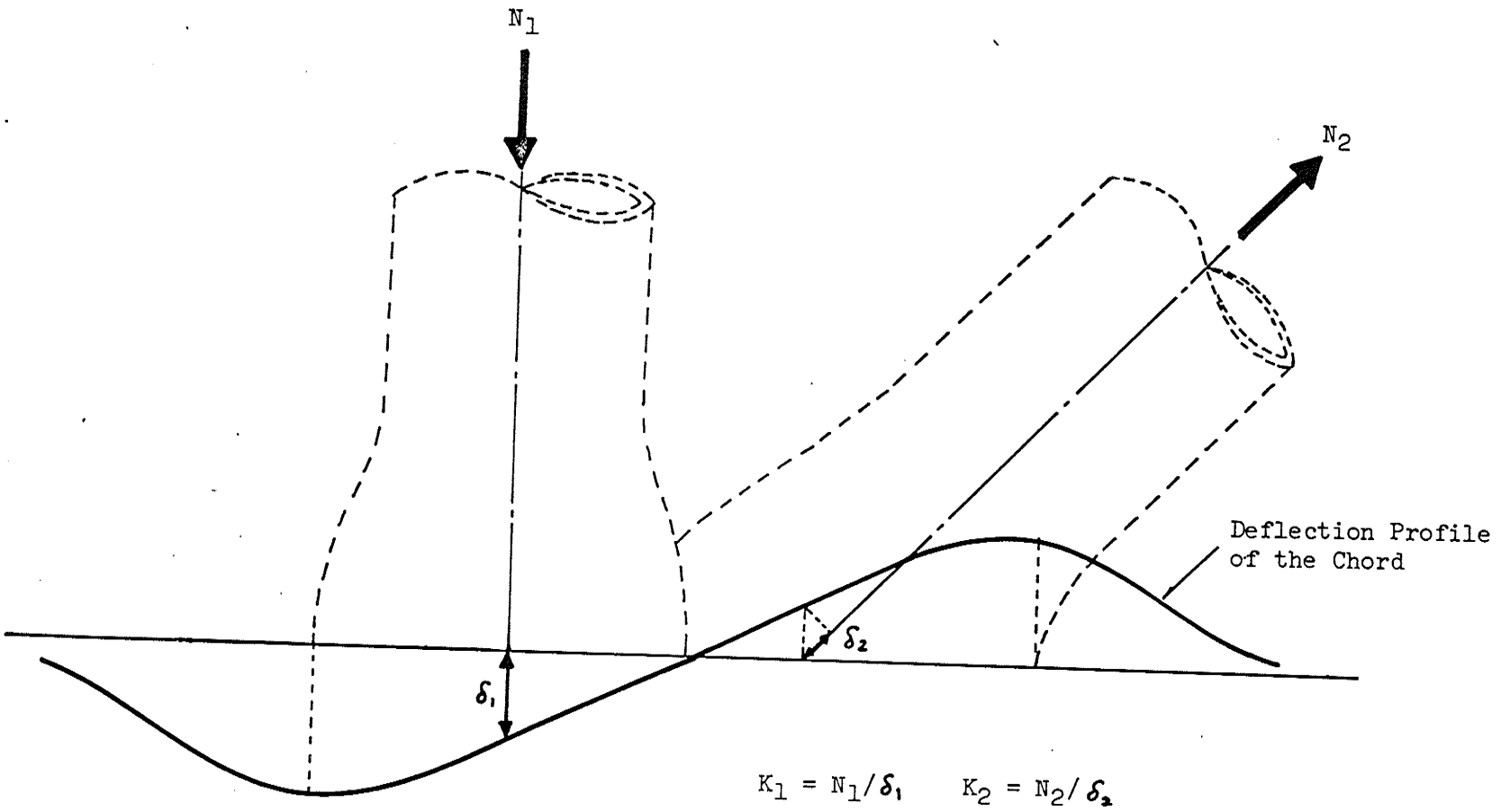

Fig. 4.25 DEFINITION OF JOINT STIFFNESS

modulus of elasticity and d_1 and d_2 are the diameters of the compression and tension webs respectively. The values of k_1/Ed_1 and k_2/Ed_2 vs. n are plotted in Fig. 4.26. It can be seen that the chord preload had little effect on the compression stiffness, which was approximately constant and equal to 0.009. The tension stiffness, on the other hand, decreased with an increase in chord preload. The tension stiffness decreased rapidly with an initial increase of 20 percent in chord preload, and then more gradually as the preload was increased to 80 percent. The tension stiffness can be estimated using the following equation:

$$\frac{k_2}{Ed_2} = 0.099 - 0.277n + 0.530n^2 - 0.346n^3 \qquad (0 \leq n \leq 80\%) \qquad (4.5)$$

4.2 Test Series 4B50-I to 4B50-IV

4.2.1 Local chord face deformation

The local chord deformations under the web members, like those of test series 3B50, were non-uniform, being maximum at the web extremities and approximately zero at the overlap. This is indicated in Fig. 4.27, which shows the deformation profiles of the chord of specimen 4B50-I.

The deflections under the webs at ultimate load were compared in Fig. 4.28. It can be seen that the deformation increased with an increase in preload. Moreover, unlike the results of test series 3B50, the deformations under both the compression and tension webs were significantly affected by the chord preload. This indicated that the

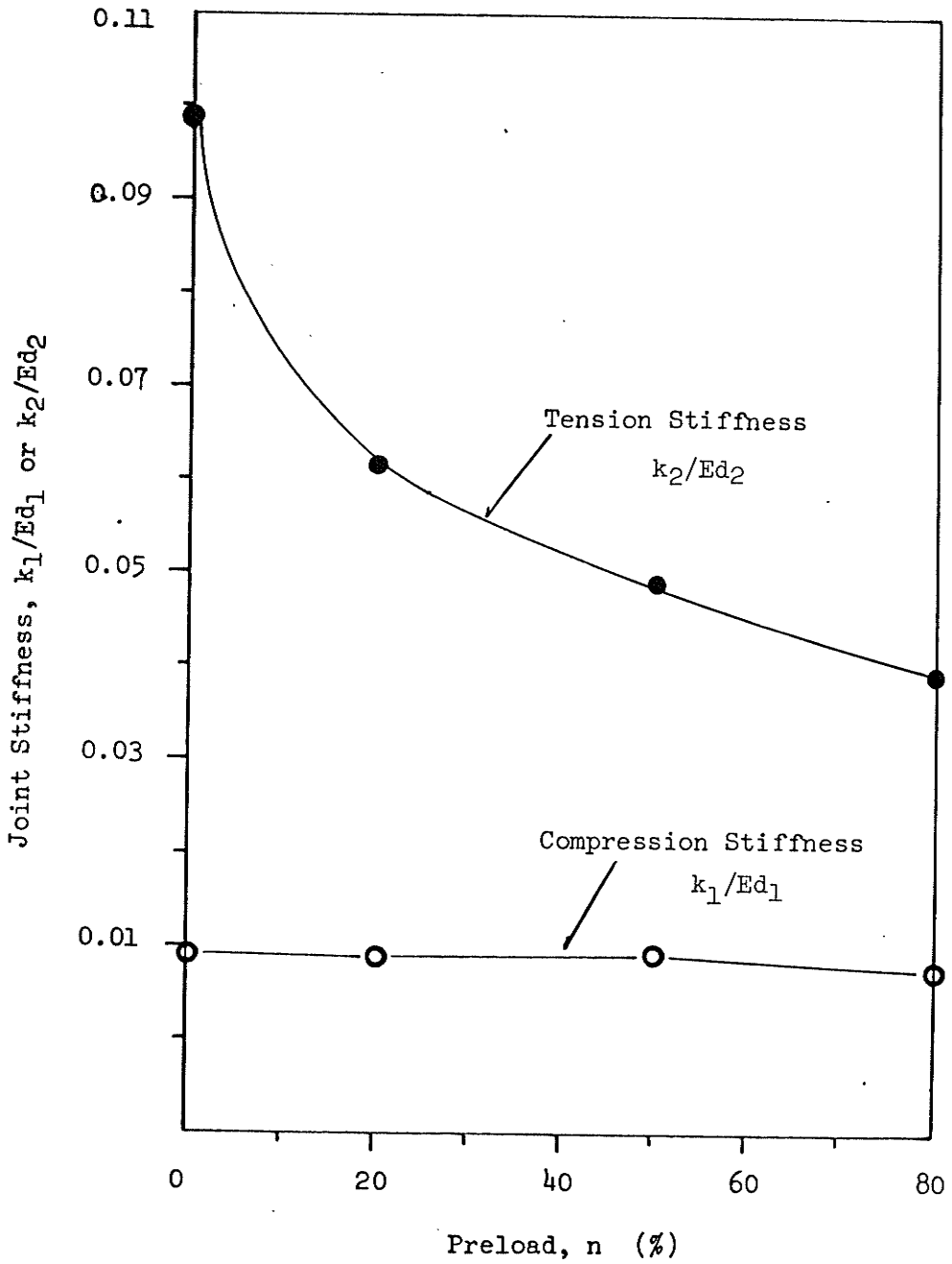

Fig.4.26 JOINT STIFFNESS

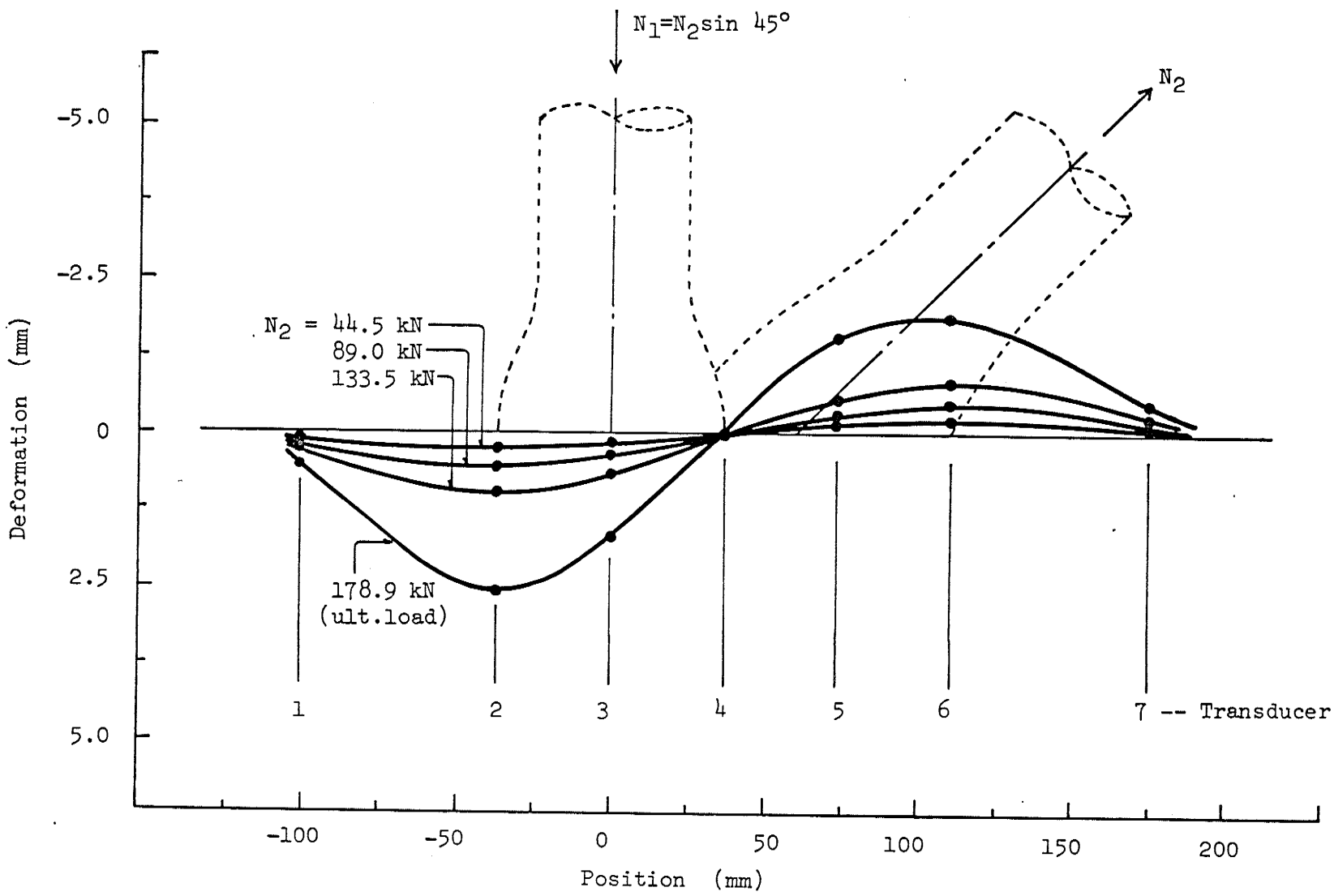

Fig. 4.27 DEFLECTION PROFILES OF LOADED CHORD FACE OF SPECIMEN 4B50-I

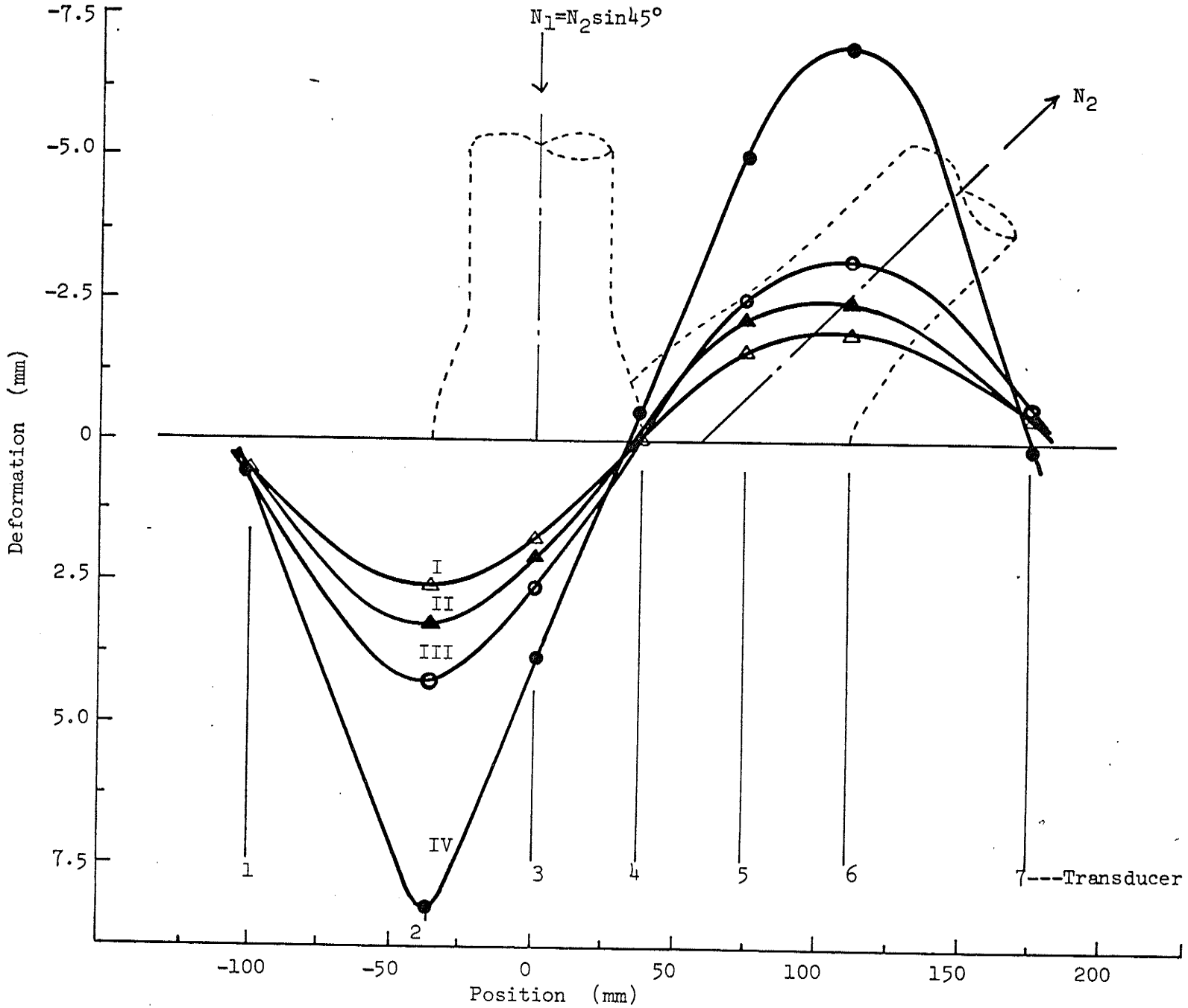

Fig. 4.28 COMPARISON OF CHORD FACE DEFORMATION OF SPECIMENS 4B50-I TO 4B50-IV AT ULTIMATE LOAD

thickness of chord had a significant effect on the stress distribution and hence the deformation at the joint.

The local chord deformation was not significant beyond a distance of about b_0 from the extremities of the webs.

4.2.2 Buckling of compression web member

The deflection profiles of the compression webs of specimens 4B50-I and 4B50-IV are illustrated in Fig. 4.29 and Fig. 4.30. It can be seen that the buckling patterns were quite different. The deflection at the mid-length of compression web of specimen 4B50-IV was approximately 100 percent more than that of 4B50-I as the load in the tension web was increased to 133.5 kN. Moreover, the final deflection was 250 percent as much as that of specimen 4B50-I, even though the axial load in the compression web of specimen 4B50-IV was about 15 percent smaller than that of specimen 4B50-I. This indicated that a relatively large moment was induced at the compression web base of specimen 4B50-IV. This moment caused the compression web to bend excessively and buckle at a lower load.

4.2.3 Strains of chord faces

Fig. 4.31 illustrates the longitudinal strains of the chord face of specimen 4B50-IV at the working load of 89.4 kN in the tension web. The longitudinal strains were highly non-uniform near the joint. At the extremity of the tension web the strain was about three times as large as the nominal yield strain, while at the extremity of the compression

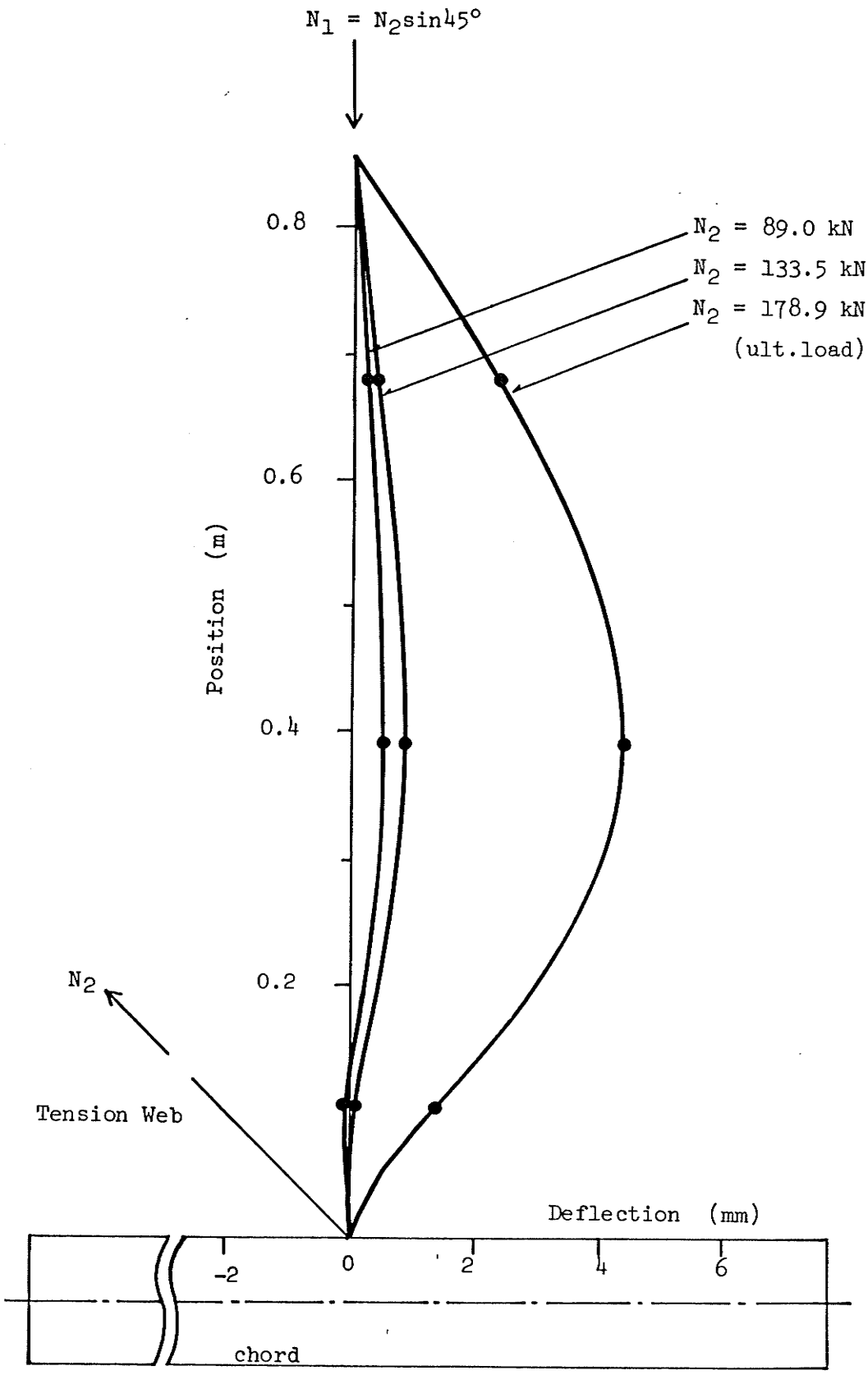

Fig. 4.29 DEFLECTION PROFILES OF COMPRESSION WEB OF SPECIMEN 4B50-I

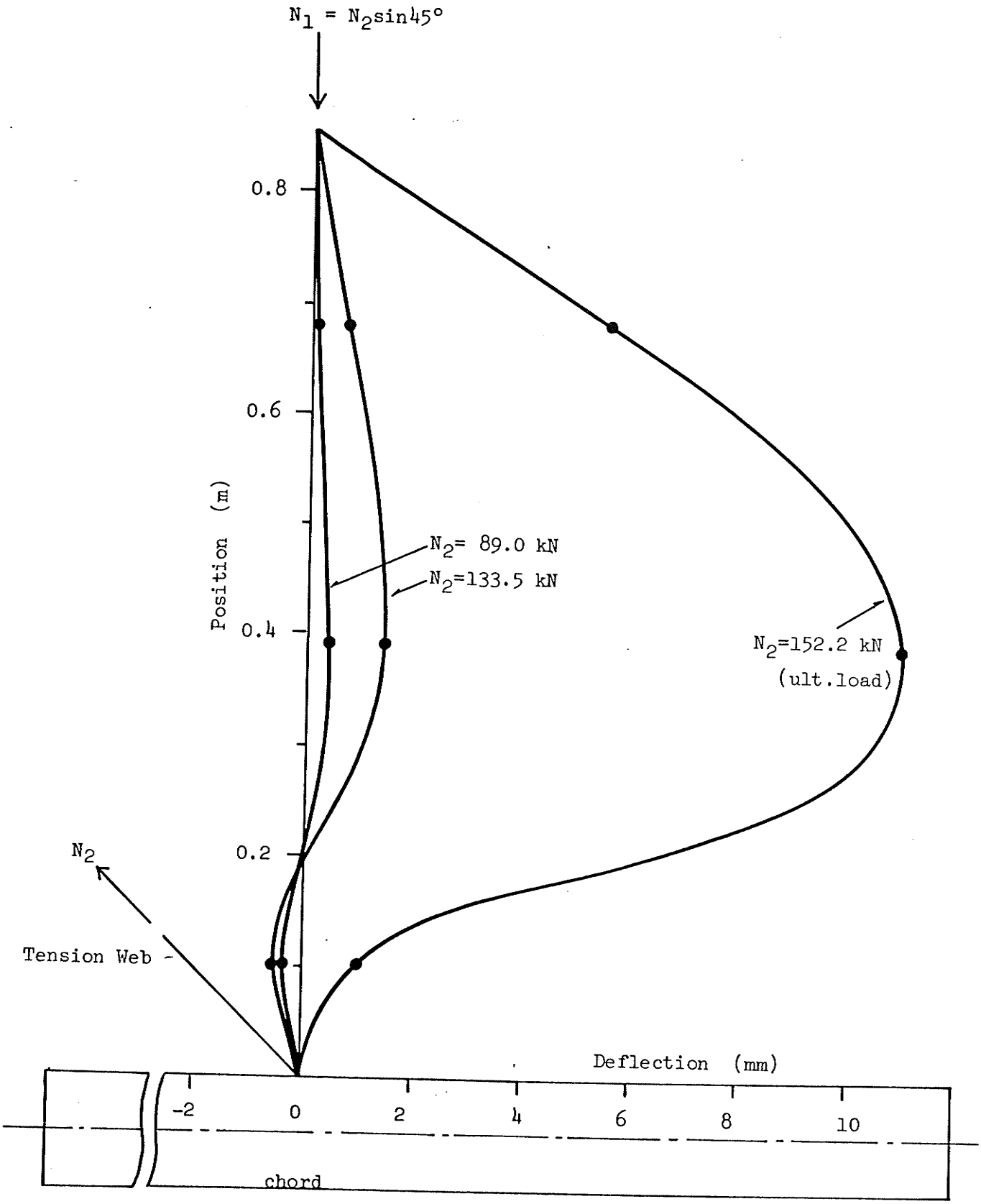

Fig. 4.30 DEFLECTION PROFILES OF COMPRESSION WEB OF SPECIMEN 4B50-IV

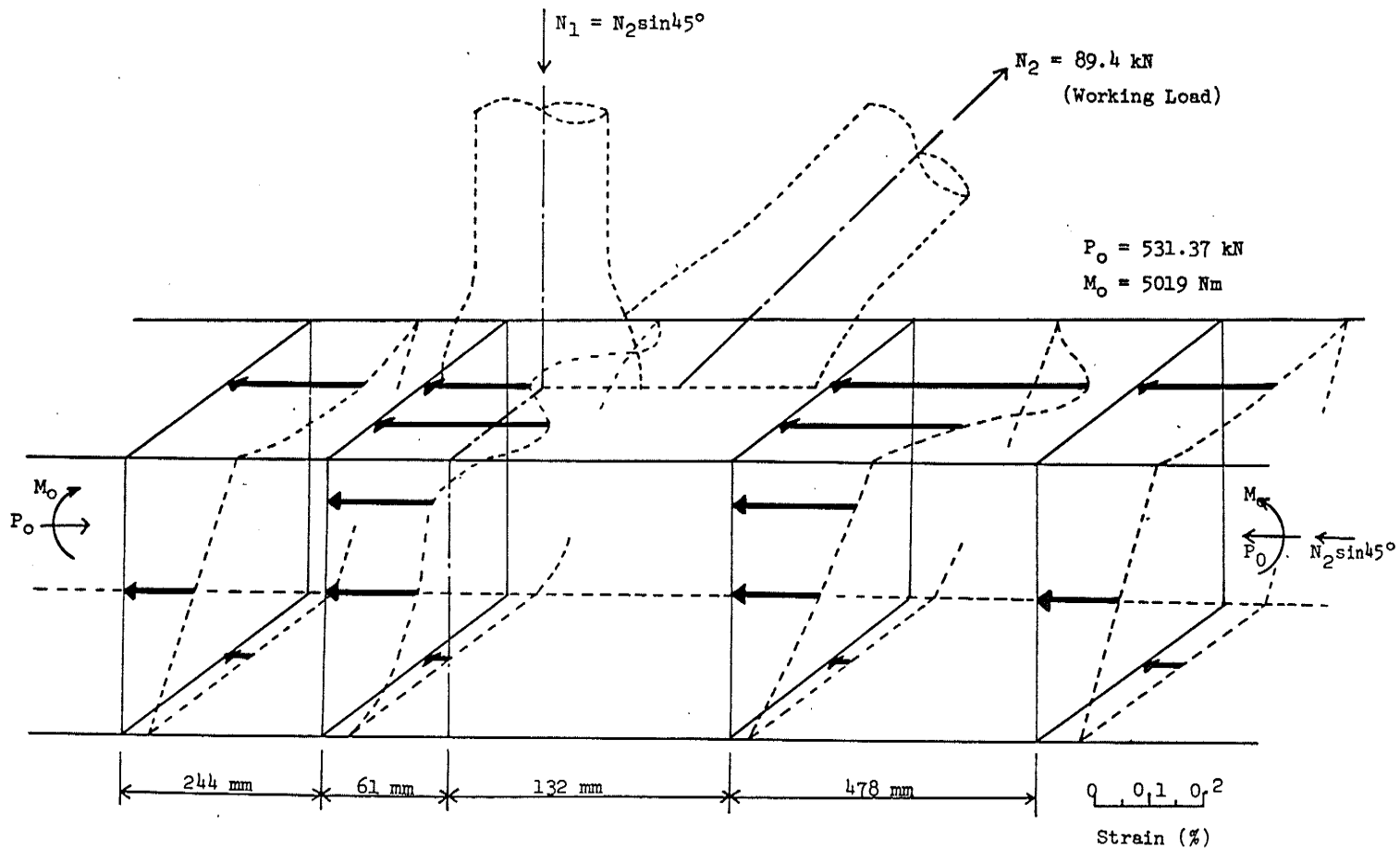

Fig. 4.31 LONGITUDINAL STRAINS ON CHORD FACE OF SPECIMEN 4B50-IV DUE TO PRELOAD AND LOAD TRANSFER BETWEEN MEMBERS

web it was about 1.2 times as large.

The transverse strains measured at the chord face of the same specimen at the working load of 89.4 kN are illustrated in Fig. 4.32. The strains were highly non-uniform. The strain at the tension web extremity was approximately equal to the corresponding longitudinal strain, about twice as large as the nominal yield strain. The strain at the compression web extremity was approximately 40 percent larger than the corresponding longitudinal strain.

4.2.4 Strains in compression web members

The longitudinal strains in the compression web of specimen 4B50-IV at loads of 44.5 kN and 89.4 kN are shown in Fig. 4.33.

The strains were fairly uniform at section D, about 0.7 m away from the joint. At the working load of 89.4 kN in the tension web, the average of the strains was 0.069 percent. This agreed very well with the average strain, 0.071 percent, obtained by dividing the axial stress by the Young's modulus of the web material. The strains at sections A and B near the lap were highly non-uniform even at about one-fourth of the ultimate load of the joint. They were relatively large on the side near the overlap and small on the opposite side.

4.2.5 Strains in tension web members

The plots of longitudinal strains in the tension web are shown in Fig. 4.34 for specimen 4B50-IV. The curves were used to plot the deformation

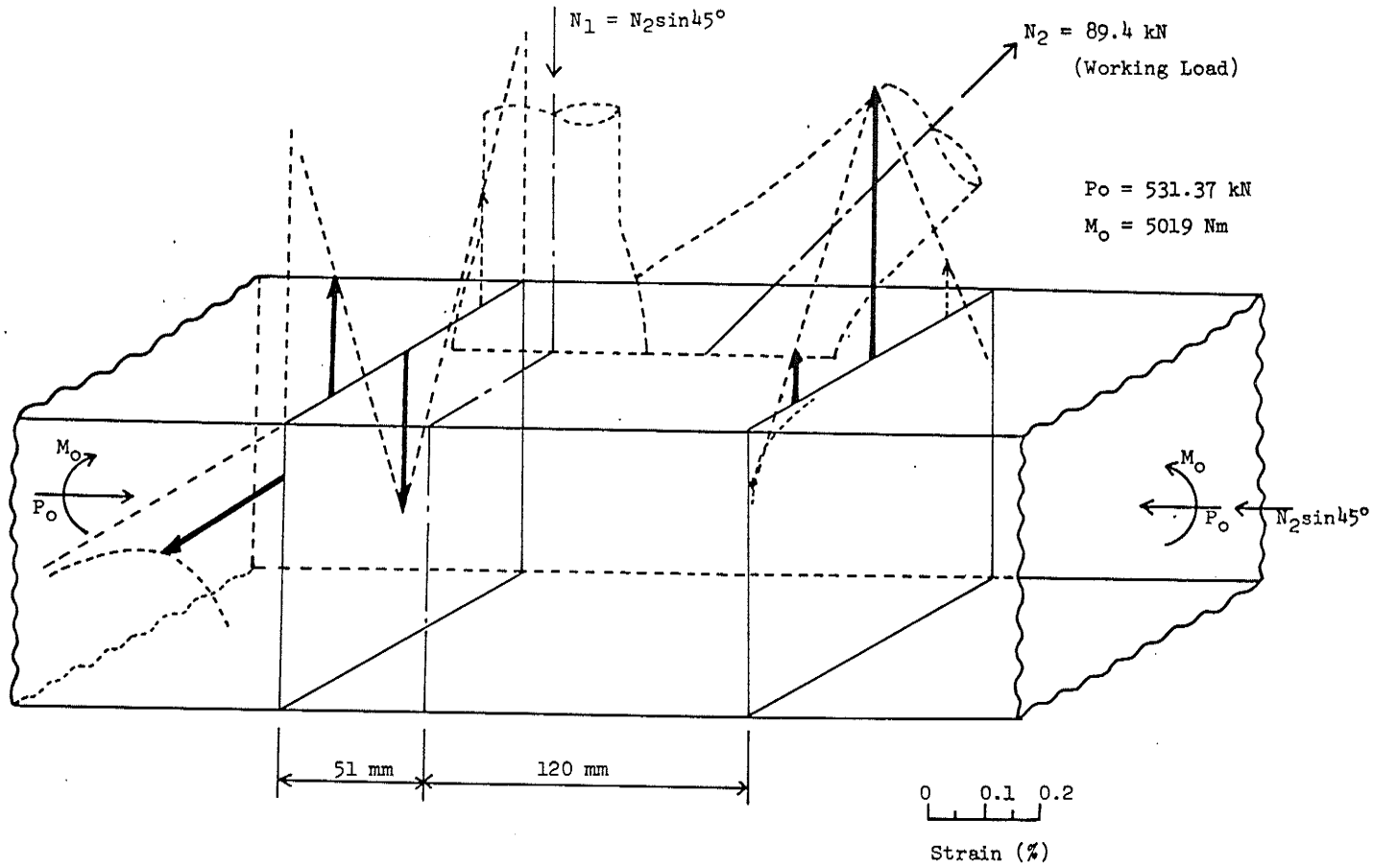

Fig.4.32 TRANSVERSE STRAINS ON LOADED CHORD FACE OF SPECIMEN 4B50-IV DUE TO PRELOAD AND LOAD TRANSFER BETWEEN MEMBERS

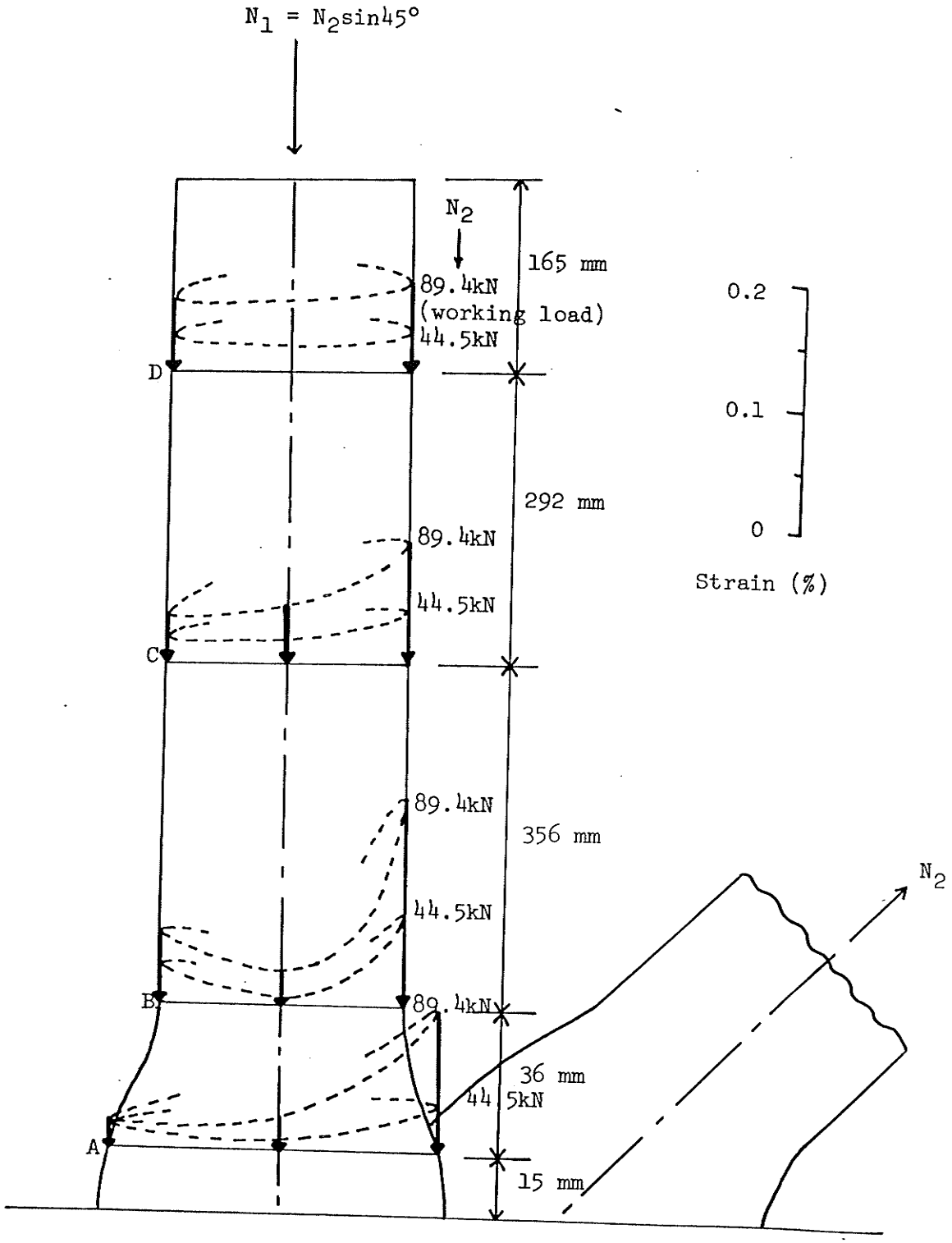

Fig. 4.33 LONGITUDINAL STRAINS ON COMPRESSION WEB MEMBER OF SPECIMEN 4B50-IV

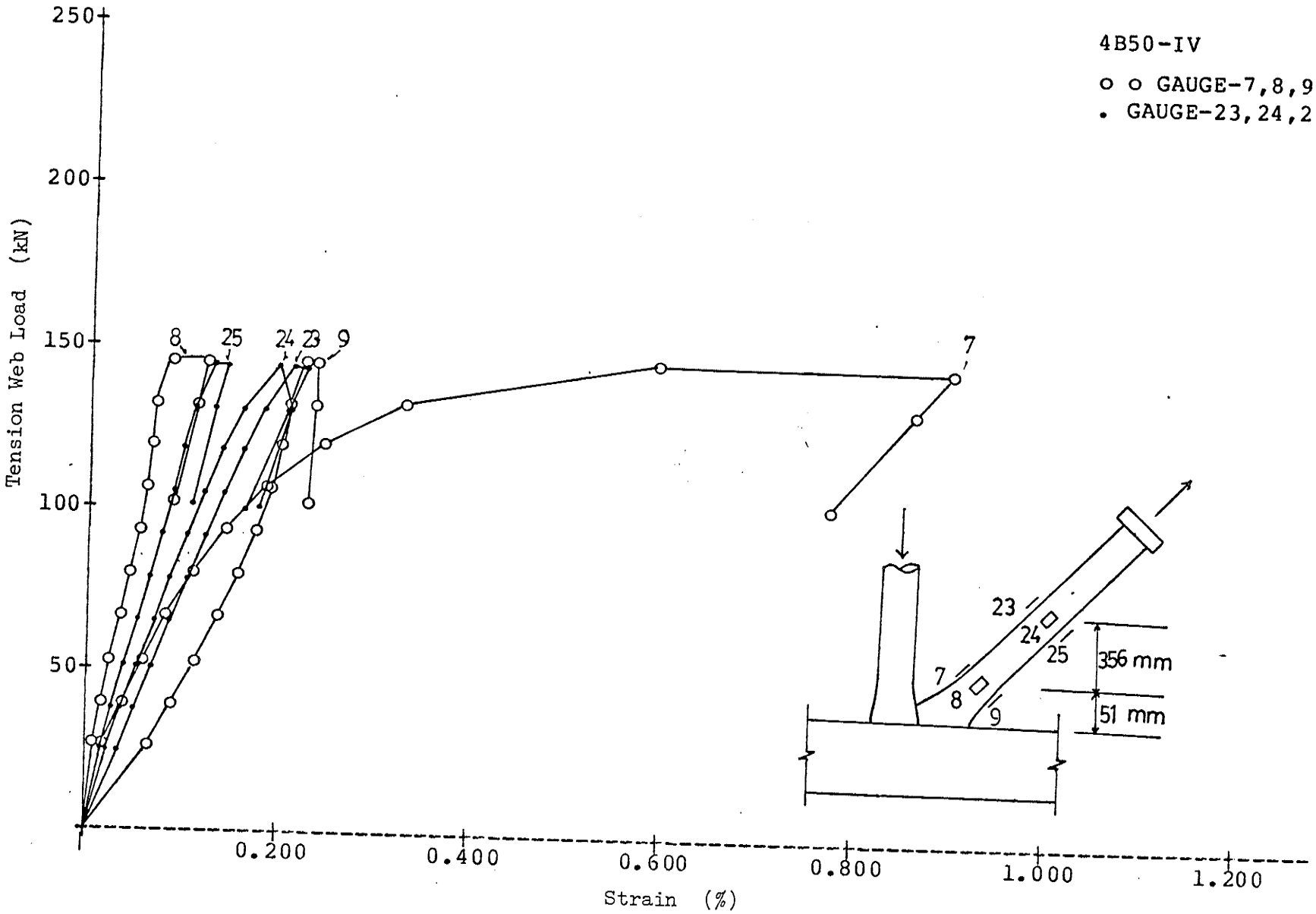

Fig.4.34 LONGITUDINAL STRAINS ON TENSION WEB MEMBER OF SPECIMEN 4B50-IV

profiles at different sections of the web, as illustrated in Fig. 4.35.

It can be seen in Fig. 4.34, that the strains at the mid-length of the web were linear up to about the ultimate load of the joint, while those at a section near the lap became non-linear at approximately one-eighth of the joint ultimate load.

It can be seen in Fig. 4.35, that the strain distributions were non-uniform, especially at the section near the lap. As the working load was reached, the tension web began to yield near its extremity (gauge 9). The average of the strains near the mid-length of the web was 0.097 percent. This agreed well with the calculated average strain of 0.100 percent.

4.2.6 Failure modes

There were five typical modes of failure in this series: excessive local deformation of the chord, buckling of the compression web, fracture of the weld at the toe of the tension web or tearing of the tension web, buckling of the chord and fracture of the compression web near the lap. Typical examples of those failure modes are given in Fig. 4.36 to Fig. 4.43. The first two modes usually occurred in combination with other modes.

Specimen 4B50-I, which had zero chord preload, failed by excessive local chord deformation and compression web buckling. In addition to these two modes, specimens 4B50-II and 4B50-III experienced fracture of weld at the toe of tension web . Specimen 4B50-IV experienced excessive chord face deformation, compression web buckling, chord buckling and

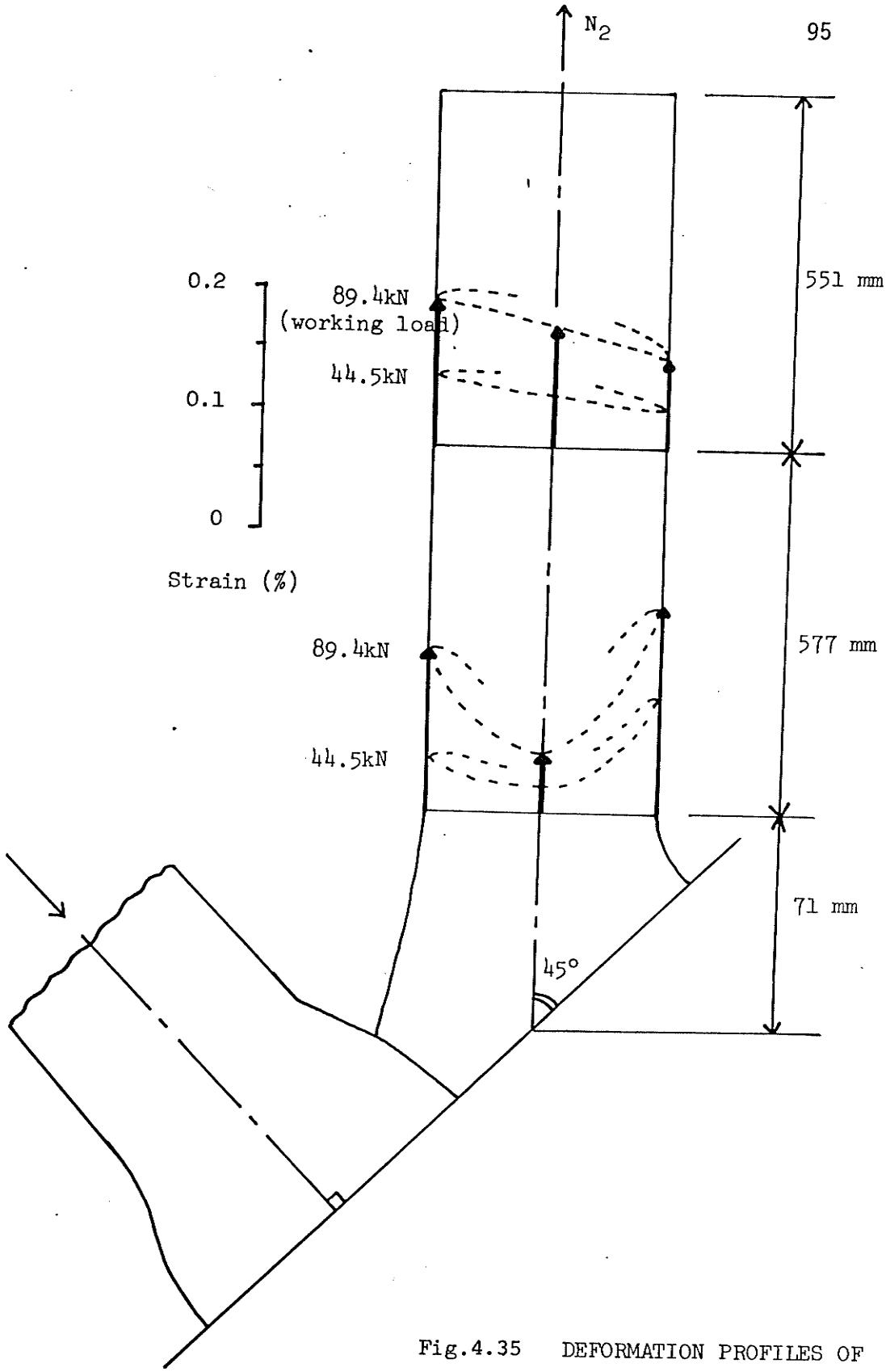

Fig.4.35 DEFORMATION PROFILES OF TENSION WEB MEMBER OF SPECIMEN 4B50-IV

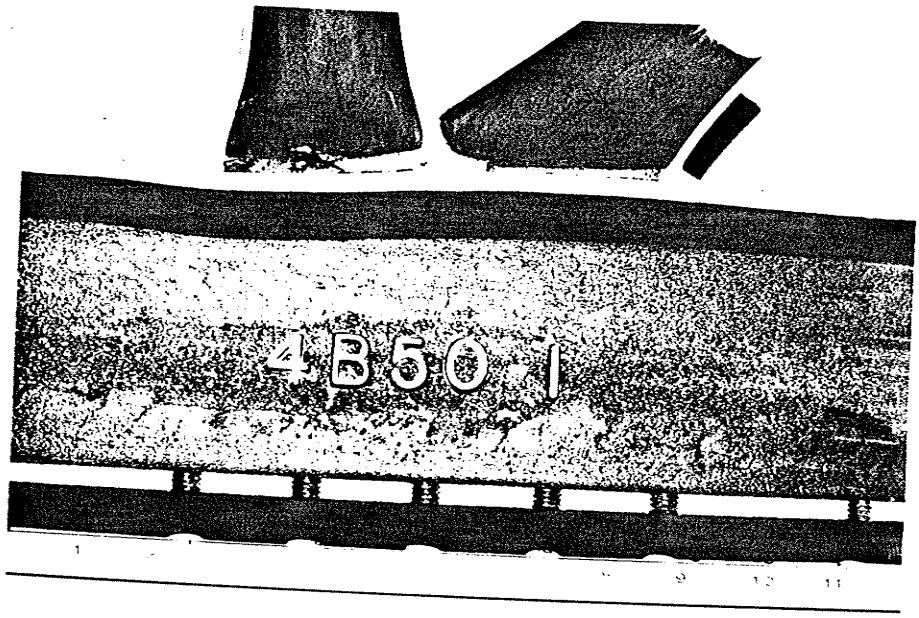

Fig. 4.36 FAILURE MODE A -- EXCESSIVE LOCAL CHORD DEFORMATION OF SPECIMEN 4B50-I

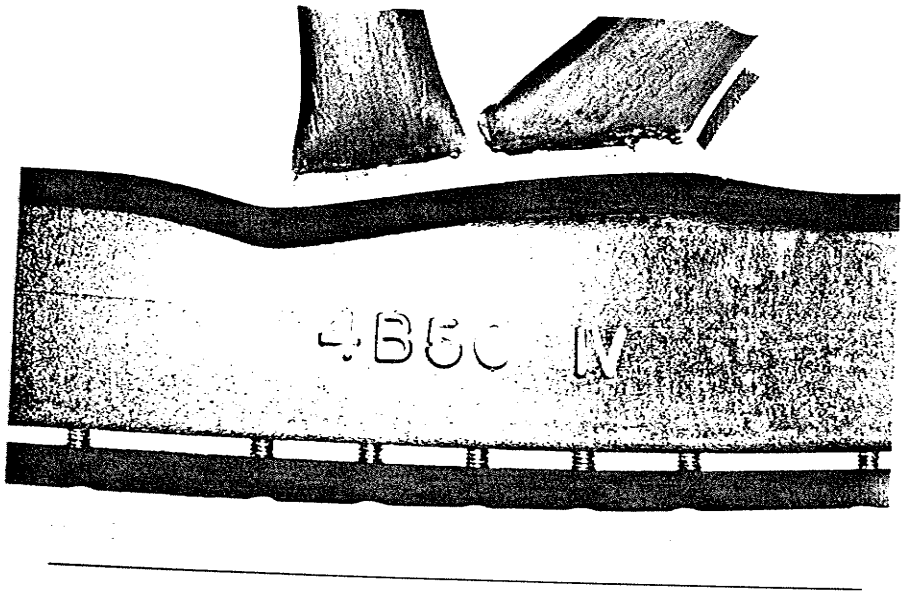

Fig. 4.37 FAILURE MODE A -- EXCESSIVE LOCAL CHORD DEFORMATION OF SPECIMEN 4B50-IV

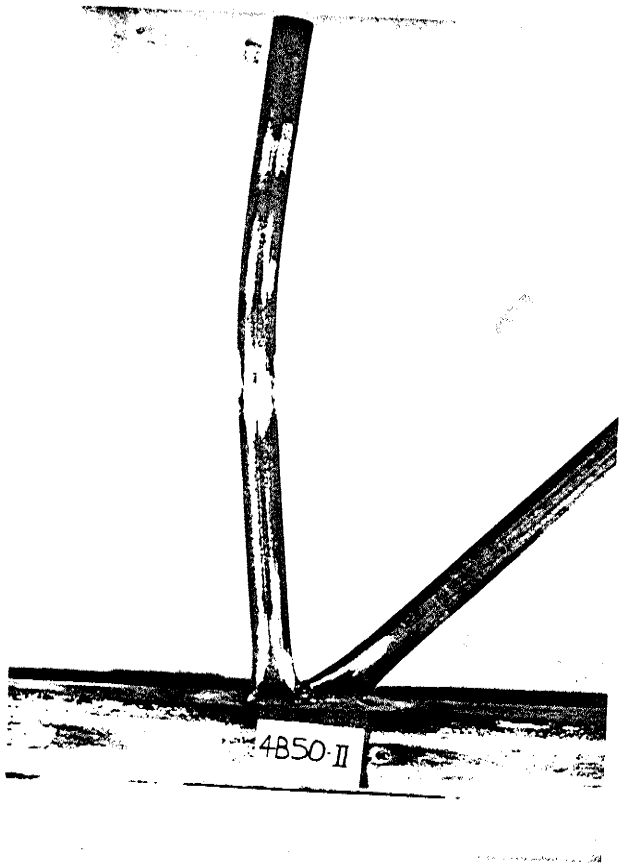

Fig. 4.38 FAILURE MODE B -- BUCKLING OF COMPRESSION WEB MEMBER OF SPECIMEN 4B50-II

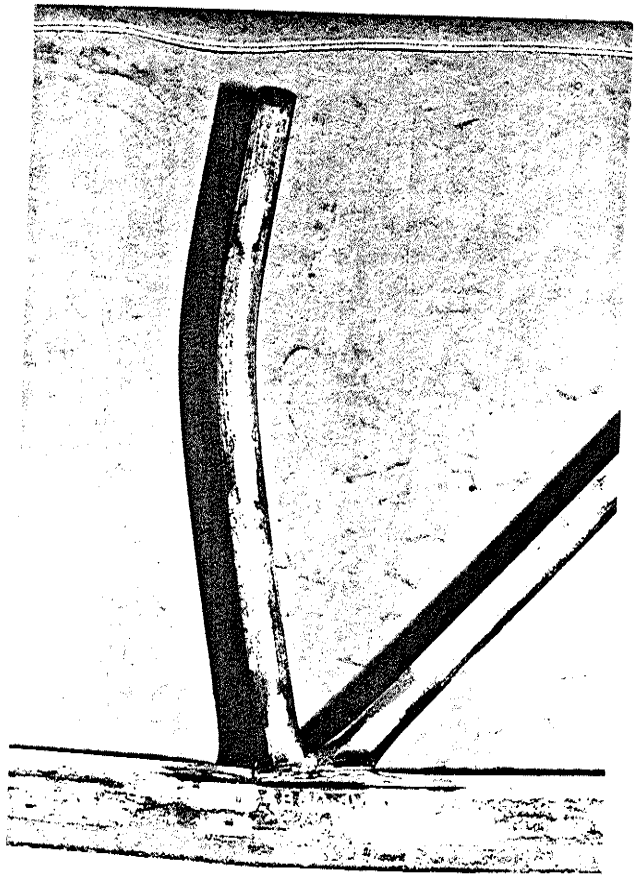

Fig. 4.39 FAILURE MODE B -- BUCKLING OF COMPRESSION WEB MEMBER OF SPECIMEN 4B50-IV

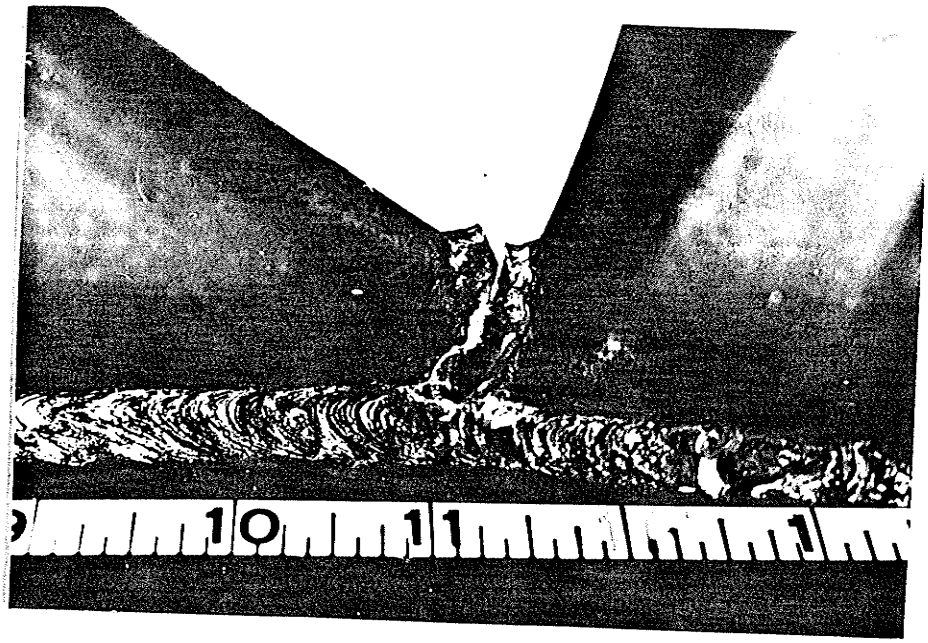

Fig. 4.40 FAILURE MODE C -- FRACTURE OF WELD AT THE TOE OF TENSION WEB MEMBER OR TEARING OF TENSION WEB MEMBER OF SPECIMEN 4B50-II

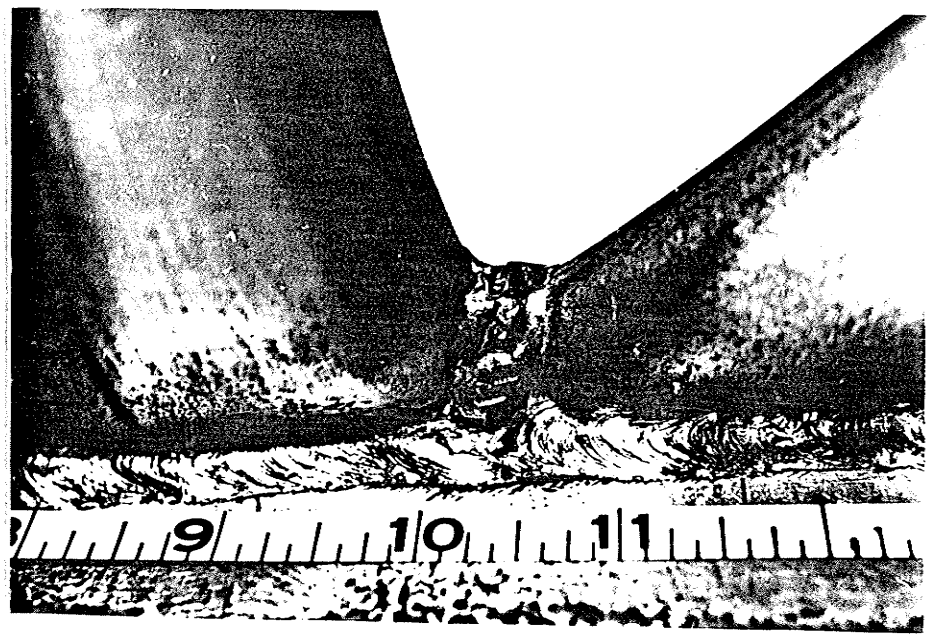

Fig. 4.41 FAILURE MODE C -- FRACTURE OF WELD AT THE TOE OF TENSION WEB MEMBER OR TEARING OF TENSION WEB MEMBER OF SPECIMEN 4B50-III

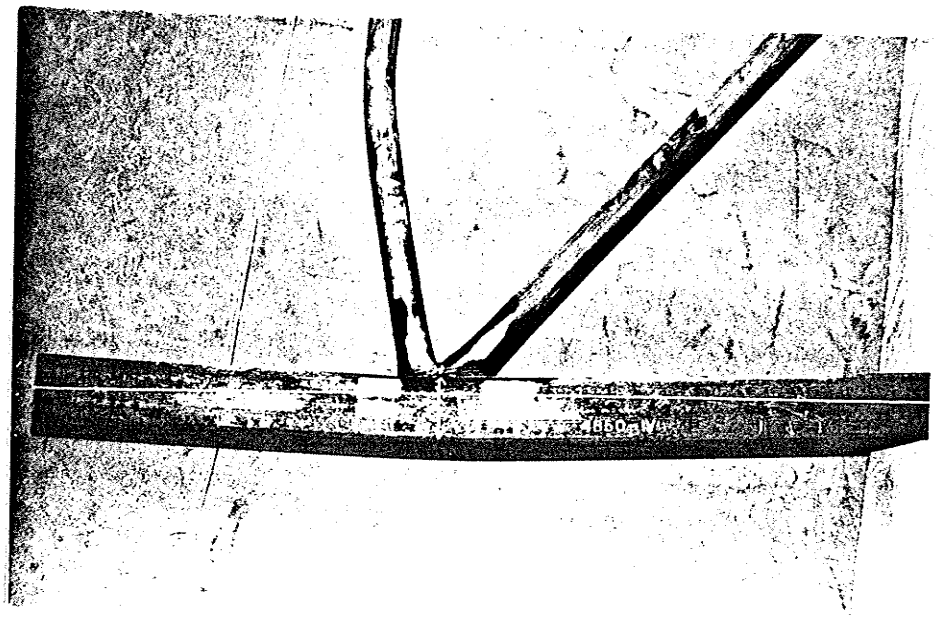

Fig. 4.42 FAILURE MODE D -- BUCKLING OF CHORD OF SPECIMEN 4B50-IV

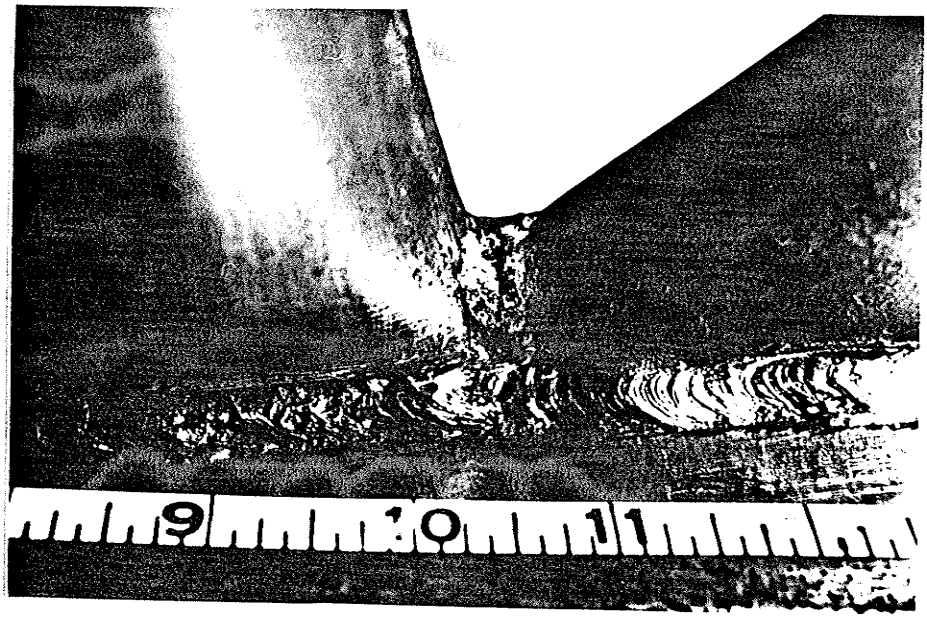

Fig. 4.43 FAILURE MODE E -- FRACTURE OF COMPRESSION WEB MEMBER OF SPECIMEN 4B50-IV

fracture of the compression web near the lap. It was thus found that the chord preload changed the failure modes significantly.

4.2.7 Joint strength

The plots of load applied to the tension web versus its movement relative to the chord axis are shown in Fig. 4.44. From those plots, the yield strengths of the joints were found using both Akiyama's and the author's methods. The results obtained, together with ultimate loads, joint efficiencies, load factors and stiffnesses are given in Table 4.2.

It can be seen that preload up to 80 percent of the chord yield load did not significantly affect the yield strengths of the joints. As the preload was increased to 90 percent, there was a sudden drop in yield strength. According to Akiyama's method, the yield strength was reduced by 15 percent, while according to the author's method, the yield strength dropped by 23 percent.

Using Akiyama's method to determine the joint yield strengths, the joint yield strength reduction coefficient was expressed in terms of chord preload as:

$$\begin{aligned} \alpha &= 1 - 0.03\ n && (0 \leq n < 80\%) \\ \alpha &= 2.02 - 1.3\ n && (80\% \leq n \leq 90\%)\ . \end{aligned} \qquad (4.6)$$

The reduction coefficient, using the author's method for yield strengths, was expressed as:

$$\begin{aligned} \alpha &= 1 - 0.06\ n && (0 \leq n < 80\%) \\ \alpha &= 2.39 - 1.8\ n && (80\% \leq n \leq 90\%)\ . \end{aligned} \qquad (4.7)$$

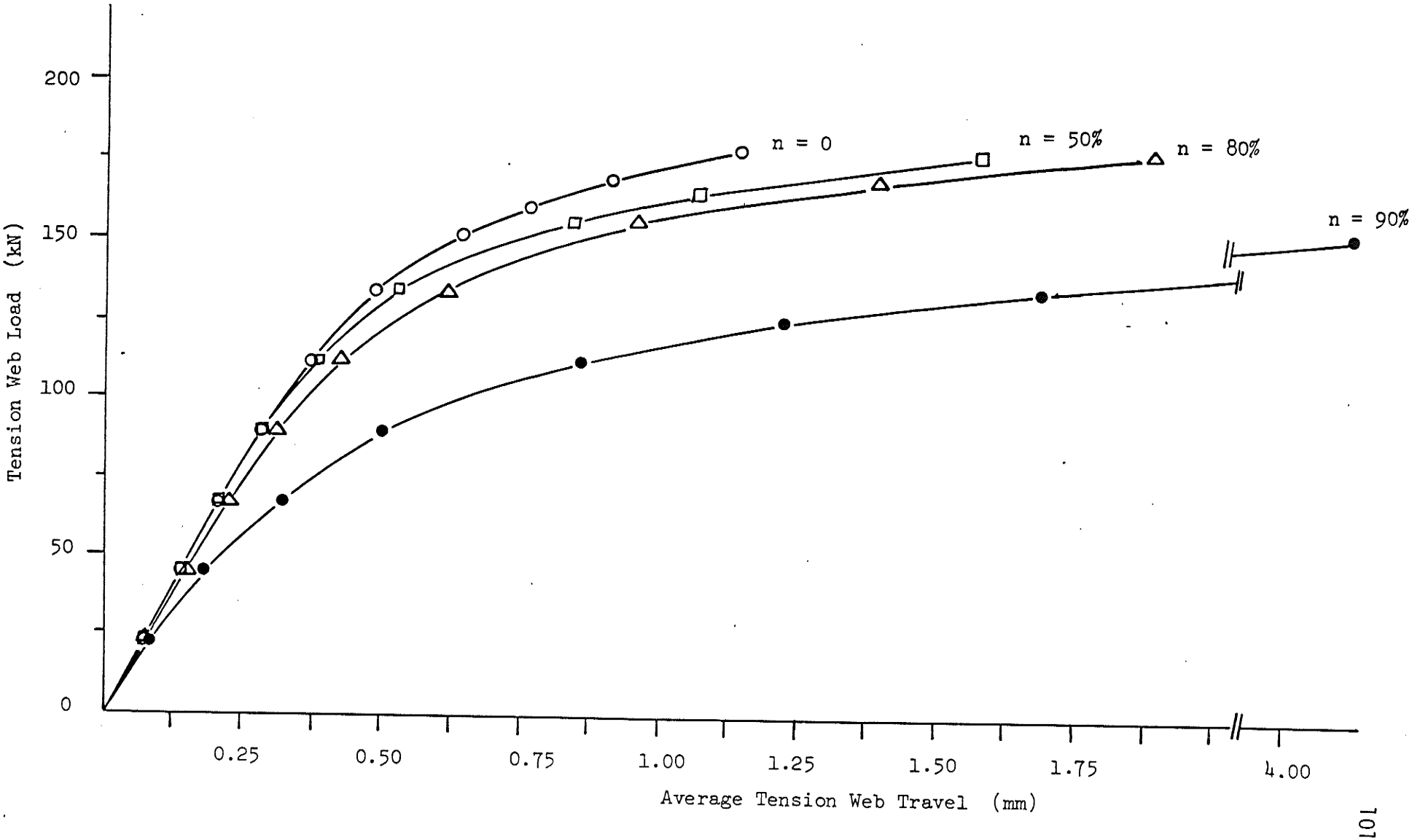

Fig. 4.44 LOAD-DEFORMATION BEHAVIOUR OF SPECIMENS 4B50-I TO 4B50-IV

TABLE 4.2: Test Results - Test Series 4B50

Specimen	Preload n %	Yield Load (The Author's Method) kN	Yield Load (Akiyama's Method) kN	Ultimate Load kN	Load Factor	Joint Efficiency	Compression Stiffness $\frac{k_1}{Ed_1}$	Tension Stiffness $\frac{k_2}{Ed_2}$	Failure Mode
4B50-I	0	135.73	153.97	179.07	2.00	120.5	0.0204	0.1130	A,B
4B50-II	50	132.61	150.86	176.62	1.97	118.8	0.0196	0.1127	A,B,C
4B50-III	80	128.61	151.30	176.93	1.98	119.0	0.0179	0.1039	A,B,C
4B50-IV	90	105.02	130.39	152.37	1.70	102.5	0.0153	0.0689	A,B,D, E

Failure Modes:

A = Excessive local deformation of chord

B = Buckling of compression web

C = Fracture of weld at the toe of tension web or tearing of tension web

D = Buckling of chord

E = Fracture of compression web at the toe

TABLE 4.2: (Continued) Test Results - Test Series 4B50

Specimen	Preload n %	Reduction Coefficient of Joint Yield Strength, α (The Author's Method)	Reduction Coefficient of Joint Yield Strength, α (Akiyama's Method)	Reduction Coefficient of Joint Ultimate Strength, β
4B50-I	0	1	1	1
4B50-II	50	0.98	0.98	0.99
4B50-III	80	0.95	0.98	0.99
4B50-IV	90	0.77	0.85	0.85

The experimental values of α were plotted against n in Fig. 4.45, together with the curves of α calculated from equations (4.6) and (4.7). The curves show that α decreased rapidly as n increased in the range of 80 to 90 percent.

As shown in Table 4.2, preload of up to 80 percent had only a minor effect on the ultimate loads of the joints. As the preload was further increased to 90 percent, the ultimate load suddenly dropped by about 15 percent. The ultimate strength reduction coefficient was expressed as:

$$\begin{aligned} \beta &= 0.99 && (0<n\leq 80\%) \\ \beta &= 2.11 - 1.4\ n && (80\%<n\leq 90\%)\ . \end{aligned} \tag{4.8}$$

The experimental values of β and equation (4.8) are plotted in Fig. 4.46. For comparison, those for test series 3B50 are also included in the figure. It can be seen that the reduction in ultimate load was much more significant for joints with thin walled chords than for those with thick walled chords. For series 3B50, the maximum preload used was 80 percent and the strength reduction for 90 percent preload was not determined. Nevertheless, it is expected that at 90 percent preload, the reduction in ultimate strength for test series 3B50 ($t_o/b_o = 0.043$) would be still larger than that for test series 4B50 ($t_o/b_o = 0.059$). This is because for a given loading and given web members, the bending stress of the chord wall is approximately proportional to the inverse of the cube of the chord thickness. Hence, higher local bending stresses occur with thinner chords.

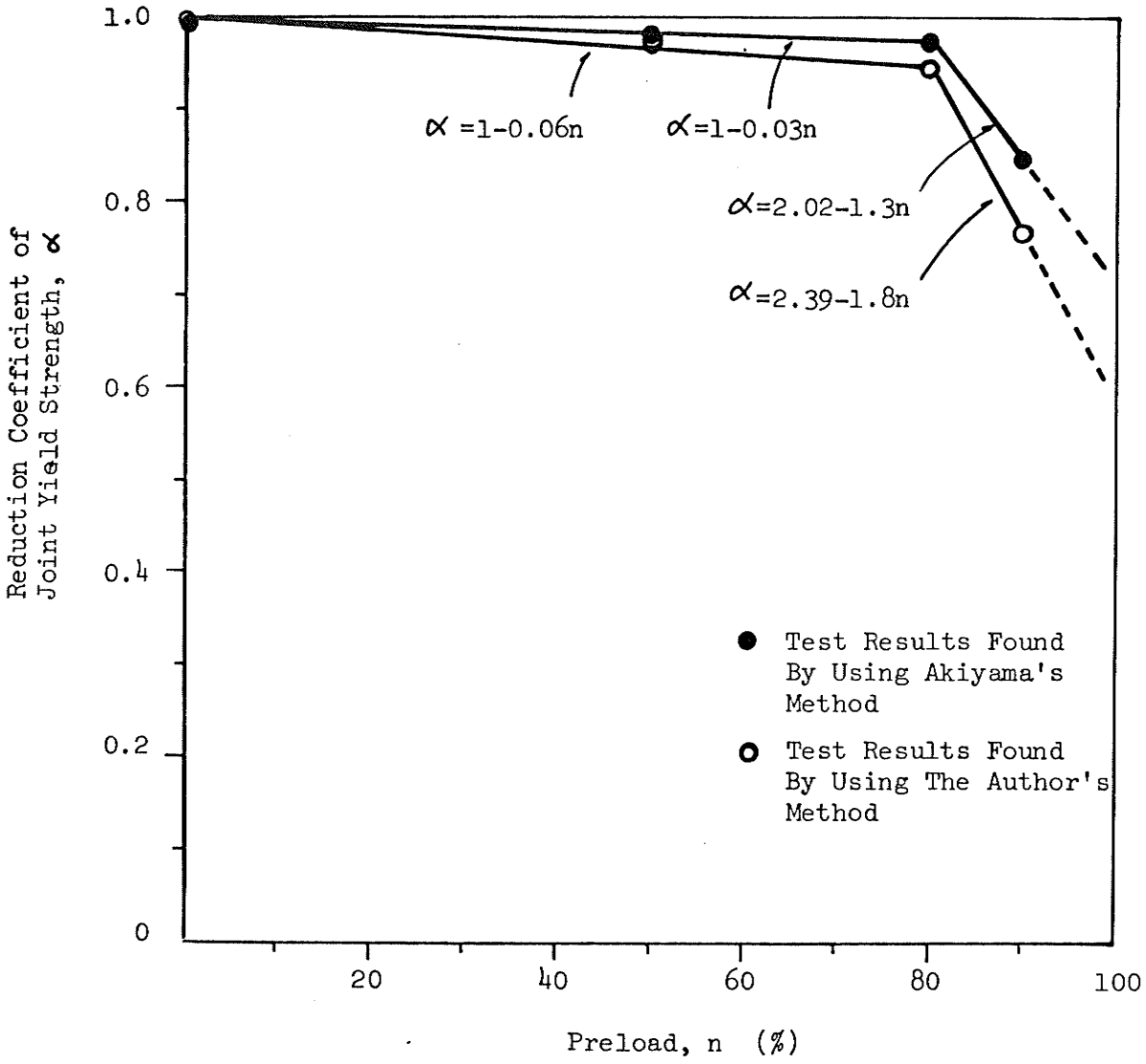

Fig. 4.45 REDUCTION COEFFICIENT OF JOINT YIELD STRENGTH

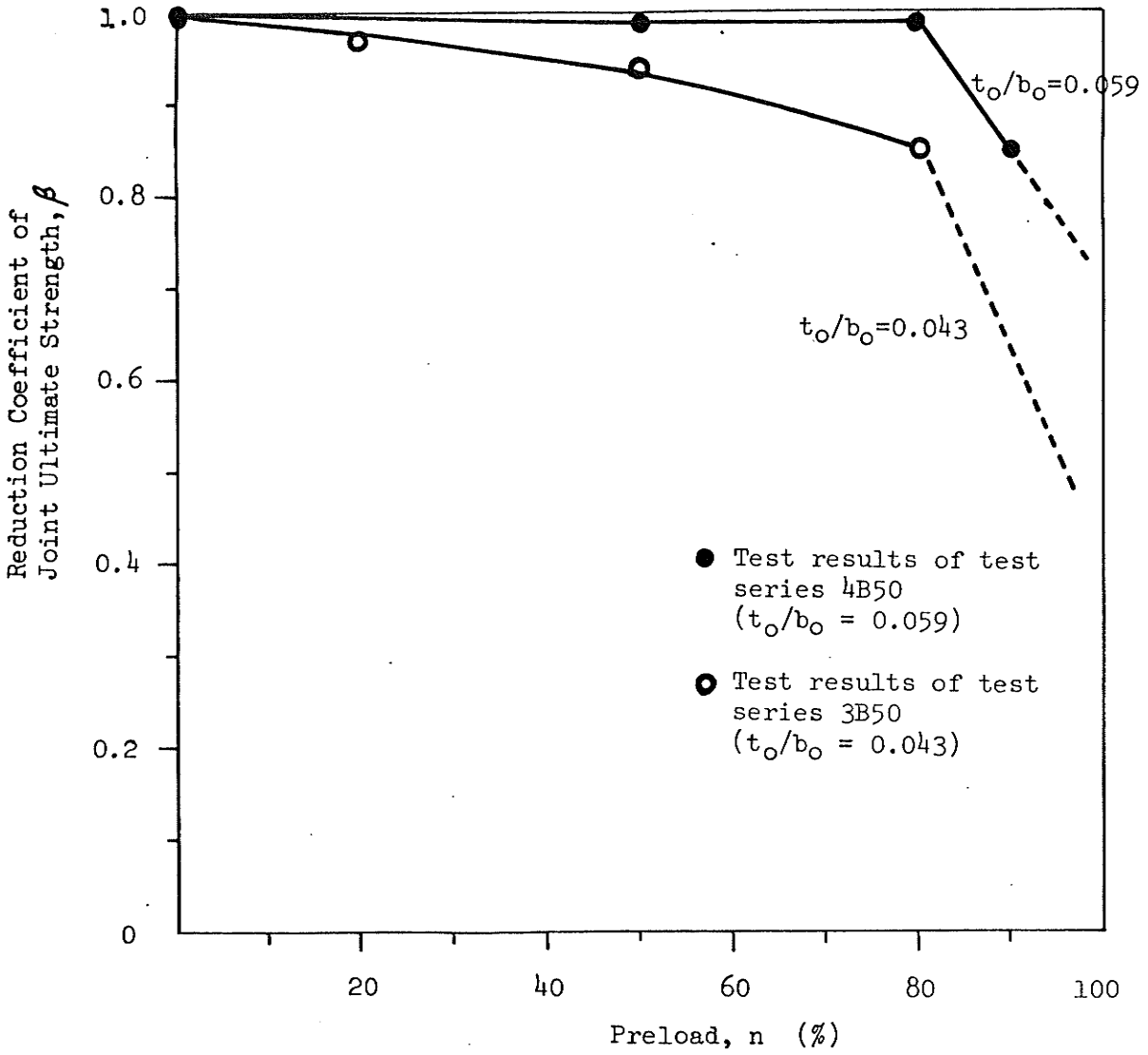

Fig. 4.46 REDUCTION COEFFICENT OF JOINT ULTIMATE STRENGTH

The joint efficiency is plotted against n in Fig. 4.47. For comparison, the corresponding values for test series 3B50 are also included in the figure. It can be seen that for the range of preload ($0 \leq n \leq 80\%$), the joint efficiency of 3B50 decreased gradually with an increase in preload, while that of 4B50 remained approximately constant and equal to 119 percent. With further increase in preload up to 90 percent, the joint efficiency for test series 4B50 dropped by approximately 15 percent. For $80\% < n \leq 90\%$, the joint efficiency of the latter can be estimated by using the following formula:

$$E_{ff} = 251 - 165\ n \tag{4.9}$$

4.2.8 Joint stiffness

The values of compression stiffness, k_1 and tension stiffness, k_2 in terms of k_1/Ed_1 and k_2/Ed_2 respectively, are given in Table 4.2 and plotted against n in Fig. 4.48. For comparison, the experimental values of k_1 and k_2 for series 3B50 are also shown in the figure.

The compression stiffness, like that for series 3B50, remained approximately constant with increase in preload.

The tension stiffness remained fairly constant up to preload of 80 percent and then abruptly dropped by about 40 percent as the preload was increased up to 90 percent. The tension stiffness for the series 3B50, on the other hand, decreased significantly with an initial increase of 20 percent in preload. It then decreased gradually with further

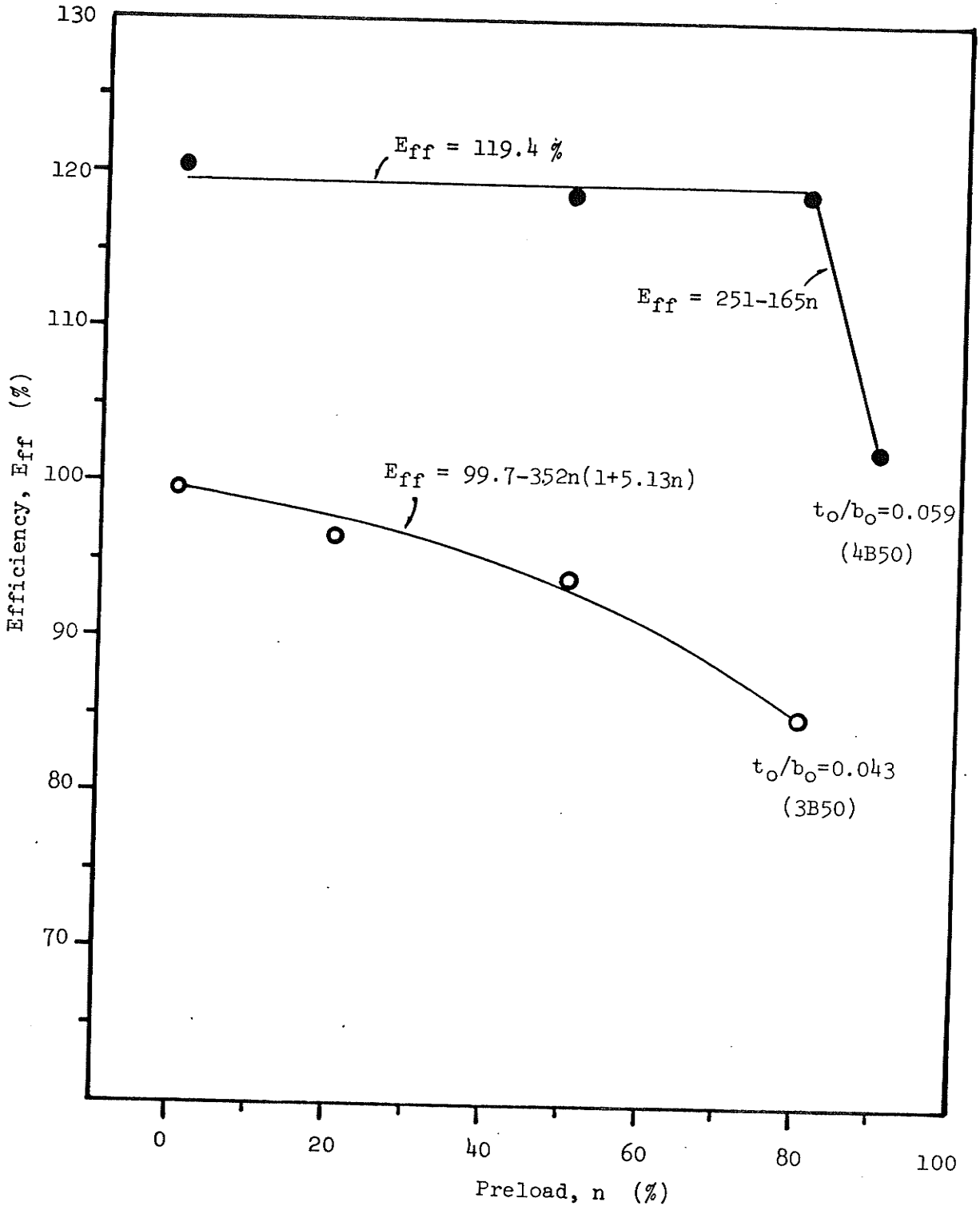

Fig. 4.47 JOINT EFFICIENCY

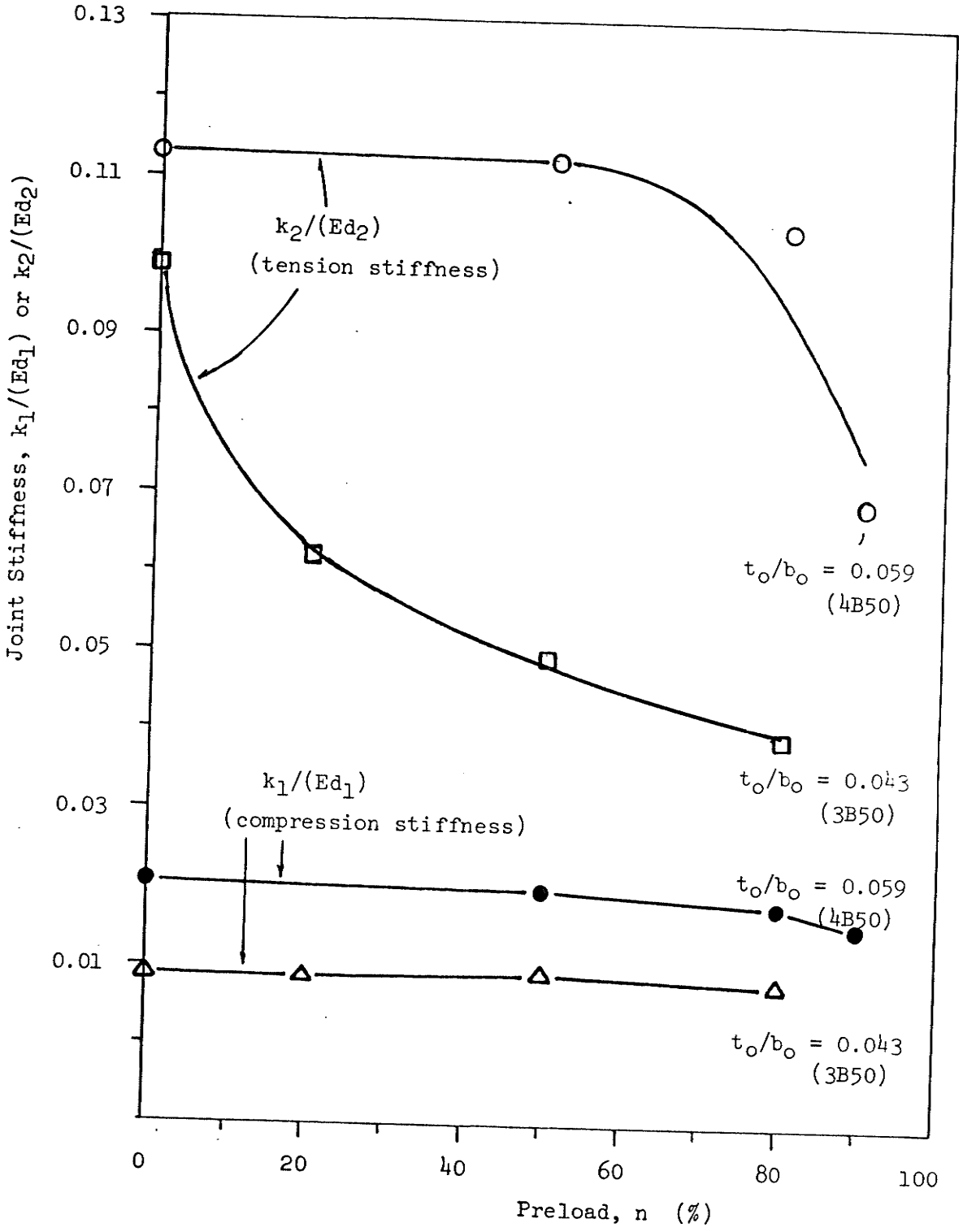

Fig. 4.48 JOINT STIFFNESS

increase in preload. The variation of tension stiffness indicated that the effect of preload was more serious at the tension web extremity. This is because the effect due to preload was additive to that due to the load transfer between tension web and chord. This is confirmed by the load-deformation behaviour of the chord wall as shown in Fig. 4.31, which shows that the maximum stress occurred near the extremity of the tension web.

It can be seen in Fig. 4.48, that the joints with the thicker chord walls were stiffer than those with the thinner chord walls. This indicated that the former offered more resistance to deformation as the thicker wall reduced the bending stresses in the chord.

The compression stiffness of series 4B50 is approximately equal to 0.0183 regardless of the level of preload, while the tension stiffness can be estimated by the following empirical formula:

$$\frac{k_2}{Ed_2} = 0.055 + 0.248\ n - 0.25\ n^2 \quad (50\% < n \leq 90\%) \tag{4.10}$$

The mean error of this formula is 0.007. The tension stiffness for the range, $0 \leq n \leq 50\%$, can be regarded as constant and equal to 0.113.

CHAPTER 5

CONCLUSIONS AND RECOMMENDATIONS

5.1 Conclusions

Based on statical load tests on 8 Pratt truss joints with square H.S.S. chords and round end-cropped H.S.S. webs, the following conclusions have been reached:

(1) The yield strength of a cropped-web joint decreases with an increase in chord preload. The yield strength can be estimated using the following formula:

$$P_y = \alpha(n)\ P_{yo}$$

where P_y is the yield strength of a preloaded joint, $\alpha(n)$ is the yield strength reduction coefficient, n the percentage of preload and P_{yo} the yield strength of a similar joint with zero preload. For joints with a chord thickness-to-width ratio of 0.043, the reduction coefficient can be computed as:

$$\alpha = 1 - 0.18\ n\ (1 + 0.94\ n) \qquad (0 \leq n \leq 80\%) \qquad (4.1)$$

where a method proposed by the author is used to determine the joint yield strengths. If a method proposed by Akiyama is used to determine joint yield strengths, the reduction coefficient can be computed as:

$$\alpha = 1 - 0.22\ n\ (1 + 0.32\ n) \qquad (0 \leq n \leq 80\%) \qquad (4.2)$$

For joints with chord thickness-to-width ratio of 0.059, the

reduction coefficient can be computed from the first or second pair of equations below. The equations are based on the author's and Akiyama's methods respectively, for determining joint yield strengths.

$$\alpha = 1 - 0.06\ n \qquad (0 \leq n < 80\%)$$
$$\alpha = 2.39 - 1.8\ n \qquad (80\% \leq n \leq 90\%)\text{(the author's method)} \quad (4.7)$$
$$\alpha = 1 - 0.03\ n \qquad (0 \leq n < 80\%)$$
$$\alpha = 2.02 - 1.3\ n \qquad (80\% \leq n \leq 90\%)\text{(Akiyama's method)} \quad (4.6)$$

(2) The ultimate strength of a cropped-web joint decreases with an increase in chord preload. The ultimate strength can be estimated by using the following formula:

$$P_u = \beta(n)\ P_{uo}$$

where P_u is the ultimate strength of a preloaded joint, $\beta(n)$ the ultimate strength reduction coefficient, and P_{uo} the ultimate strength of a similar joint with zero preload. For joints with a chord thickness-to-width ratio of 0.043, the reduction coefficient can be estimated as:

$$\beta = 1 - 0.07\ n\ (1 + 2\ n) \qquad (0 \leq n \leq 80\%) \qquad (4.3)$$

For joints with a chord thickness-to-width ratio of 0.059, the reduction coefficient is approximately 0.99 for $0 < n \leq 80\%$, while for $80\% < n \leq 90\%$, the reduction coefficient can be estimated as:

$$\beta = 2.11 - 1.4\ n \qquad (80\% < n \leq 90\%) \qquad (4.8)$$

(3) Chord preload has a smaller effect on the ultimate strength of a cropped-web joint than on the yield strength.

(4) The preload in the chord of a cropped-web joint has very little effect on the compression stiffness of the joint, while the tension stiffness of the joint decreases with an increase in chord preload.

(5) An increase in the chord thickness-to-width ratio increases both the compression and tension stiffnesses of a cropped-web joint.

(6) The local chord deformations are not significant beyond a distance of about the chord width from the extremities of the web members.

(7) Preload changes significantly the modes of failure of cropped-web joints.

(8) Three main modes of failure of cropped-web joints are: excessive local deformation of chord face, in-plane buckling of compression web and fracture of the weld at the toe of tension web or tearing of tension web.

(9) The preload, representing the overall truss action, causes high stress concentration at the joint and consequently the joint fails at a lower load. Therefore, addition of a preload consisting of a compressive axial force and a bending moment in the chord of an isolated joint simulates more closely the actual truss conditions.

5.2 Design Recommendations

Based on the test results, the following recommendations are made with regard to the design of H.S.S. truss joints with rectangular chords

and round end-cropped webs:

(1) Thiensiripipat's (1979) expression for joint strength should be reduced with respect to the loading in the chord of a joint.

(2) Joints for which t_o/b_o is less than 0.043 should be carefully checked for yield and ultimate strengths with respect to the chord loads.

(3) The welding at the toe of tension web member of a joint involving large chord loading should be sufficiently strong to preclude premature weld failure at this location.

5.3 Recommendations for Future Research

Based on the above conclusions, it is recommended that additional research be undertaken to review the influence of chord loading on joint strength so that information pertinent to design criteria may be obtained. The additional phases should include:

(1) Range of chord preload between 90 percent and 100 percent of chord yield load.

(2) Larger range of the chord thickness-to-width ratio, especially those smaller than 0.043.

(3) The ratio of web diameter to chord width as variable.

REFERENCES

REFERENCES

1. American Institute of Steel Construction (AISC) — Specification for the Design, Fabrication and Erection of Structural Steel for Buildings, Feb. 12, 1969, AISC, N.Y.

2. American Institute of Steel Construction (AISC) — Commentary on the Specification for the Design, Fabrication and Erection of Structural Steel for Buildings, Feb. 12, 1969, AISC, N. Y.

3. Akyama, N. Yajima, M. Akiyama, H. Otake, S. — Experimental Study on Strength of Joints in Steel Tubular Structures, (In Japanese). Society of Steel Construction, Japan, Vol. 10, No. 102, June, 1974.

4. Anderson, G.W. — Circumferential Stresses in a Joint Between Structural Tubes, Special Report No. 22 of Commonwealth Experimental Building Station, Sydney, May, 1961.

5. American Society for Testing and Materials (ASTM) — Steel-Bars, Forgings, Bearing, Chain, Springs. ASTM Standards Part 5, A370, 1979.

6. Beale, L.A. Toprac, A.A. — Analysis of in-plane T, Y and K Welded Tubular Connections, Welding in the World, Vol. 8, No. 2, 1970.

7. Bijlaad, P.P. — Stresses From Local Loading in Cylindrical Pressure Vessels, Transactions of the ASME, August, 1955.

8. Bouwkamp, J.G. — Concept of Tubular-Joint Design. Journal of the Structural Division, ASCE Proc. Vol. 92, ST2, April, 1964.

9. Bouwkamp, J.G. — Behaviour of Tubular Truss Joints Under Static Loads, Phase II. College of Engineering, University of California, Berkeley, California, January, 1968.

10. Canadian Institute of Steel Construction (CISC)

CSA Standards S16.1-1974, Limit States Design Steel Manual, 2nd Edition, CISC, 1978.

11. Canadian Standards Association (CSA)

Steel Structures for Buildings - Limit States Design. CAN 3-S16.1-M78, 1978.

12. Cran, J.A.
Gibson, E.B.
Stadnyckyj, S.

Hollow Structural Sections - Design Manual for Connections, The Steel Company of Canada, Ltd., 1st ed. 1971.

13. Dasgupta, A.

The Behaviour of Joints in Tubular Trusses, Ph.D. Thesis, Department of Civil Engineering, University of Nottingham, 1970.

14. Davie, J.
Giddings, T.W.

Research into the Strength of Welded Lattice Girder Joints in Structural Hollow Sections, CE 70/3, CIDECT Programme 5EC, University of Sheffield, 1971.

15. Eastwood, W.
Osgerby, C.
Wood, A. A.
Blockley, D.I.

A Theoretical Investigation into the Elastic Behaviour of Joints Between Structural Hollow Sections, Department of Civil and Structural Engineering, University of Sheffield, 1967.

16. Eastwood, W.
Osgerby, C.
Wood, A.A.
Blockley, D.I.

An Experimental Investigation into the Behaviour of Joints Between Structural Hollow Sections, Department of Civil and Structural Engineering, University of Sheffield, 1967.

17. Eastwood, W.
Osgerby, C.
Wood, A.A.
Mee, B.

An Experimental Investigation of Joints in Rectangular Hollow Section, Department of Civil and Structural Engineering, University of Sheffield, 1969.

18. Eastwood, W.
Wood, A.A.
Welded Joints in Tubular Structures Involving Rectangular Sections, Conference on Joints in Structures, Session A, Paper 2, Department of Civil and Structural Engineering, University of Sheffield, 1970.

19. Eastwood, W.
Wood, A.A.
Recent Research on Joints in Tubular Structures, Canadian Structural Engineering Conf., 1970.

20. Anonymous.
Automatic Profiling of the Tube Ends, The Engineer, April, 1961.

21. Foster, J.S.
Harington, R.
Structure and Fabric, Part 2, B.T. Batsford Ltd., London, 1976.

22. Fujimoto, M.
Abe, E.
Sado, M.
Local Stresses and Deformations of Tubular Joints (Part 1), (In Japanese), AIJ Trans. No. 89, September, 1963.

23. Ghosh, A.
Statical Behaviour of Tubular Trusses With Cropped-End Connections, M.Sc. Thesis, Department of Civil Engineering, University of Manitoba, 1978.

24. Godfrey, G.B.
Joints in Tubular Structures, The Structural Engineer, April, 1959.

25. Hlavacek, V.
Strength of Welded Tubular Joints in Lattice Girders, Building Research Institute, Technical University, Prague, 1973.

26. Jamm, W.
Form Strength of Welded Tubular Connections and Tubular Structures Under Static Loading, (Translation from German), Schweissen Und Schneiden, Vol. 3, 1951.

27. Jamm, W.
Zimmermann, G.
Duisburg, G.L.

Welded Connections of Pipe Structures - Node Points, Patent Right No. 831598, Class 37, Group 5, Republic of Germany Patent Office, 1952.

28. Kaneya, H.

Experimental Study on Local Deformations of Tubular Connections, Part 3, (In Japanese). AIJ Trans. No. 110, April, 1965.

29. Kuang, J.G.
Potvin, A.B.
Leick, R.D.

Stress Concentration in Tubular Joints, Offshore Technology Conference, Texas, Proc. Vol. 1, 1975.

30. Liaw, C.Y.

Improved Finite Elements for Analysis of Welded Tubular Joints, Offshore Technology Conference, Texas, Proceedings Vol. III, 1976.

31. Mee, B.L.

The Structural Behaviour of Joints in Rectangular Hollow Section, Ph.D. Thesis, Department of Civil and Structural Engineering, University of Sheffield, September, 1969.

32. Morris, G.A.
Frovich, L.E.
Thiensiripipat, N.

An Experimental Investigation of Flattened-End Tubular Truss Joints, Department of Civil Engineering, University of Manitoba, 1974.

33. Morris, G.A.
Thiensiripipat, N.

Behaviour of Tubular Truss Joints With End-Cropped Webs, Paper presented to the International Symposium on Hollow Structural Sections, Toronto, Canada, May, 1977.

34. Mouty, J.

Theoretical Prediction of Welded Joint Strength, Proceedings of International Symposium on Hollow Structural Sections, CIDECT, Toronto, 1977.

35. Naka, T.
Kato, B.
Kaneya, H.

Experimental Study on Joint Efficiency of Welded Tubular Trusses, (In Japanese), AIJ Trans. No. 69, October, 1961.

36. Noel, J.S.
Beale, L.A.
Toprac, A.A.

Stresses Near Tubular T-Joints, Welding in the World, Vol. 7, No. 3, 1969.

37. Okumura, T.
Murakami, E.
Akiyama, N.

Estimation of Strength of Tubular Joints, (In Japanese), Trans. of J.S.C.E., Vol. 58, No. 7, June, 1973.

38. Pan, R.B.
Plummer, F.B.
Kuang, J.G.

Ultimate Strength of Tubular Joints, Offshore Technology Conference, Texas, Proc. Vol. III, 1976.

39. Reber, B.J.

Ultimate Strength Design of Tubular Joints, Journal of Structural Division, ASCE Proceedings, ST. 6 , June, 1973.

40. Redwood, R.G.

The Bending of a Plate Loaded Through a Rigid Rectangular Inclusion, International Journal of Mechanical Sciences, Vol. 7, 1965.

41. Scordelis, A.C.
Bouwkamp, J.G.

Analytical Study of Tubular Tee-Joints Journal of Structural Division, ASCE Proceedings, ST. 1 , January, 1970.

42. Sherman, D.R.

Tentative Criteria for Structural Applications of Steel Tubing and Pipe, Committee of Steel Pipe Producers, AISI, 1976.

43. Tada, H.

Recent Trend of Tubular Steel Structures in Japan, Proceedings of the Symposium on Steel Structures, Compiled by Japan Society of Civil Engineers and Architectural Institute of Japan, October, 1961.

44. Thiensiripipat, N.
Pinkney, R.B.
Morris, G.A.
Statical Behaviour of Cropped-Web Joints in Tubular Trusses, Department of Civil Engineering, University of Manitoba, February, 1979.

45. Timoshenko, S.
Theory of Plates and Shells, First Edition, McGraw-Hill Book Co., 1940.

46. Toprac, A.A.
Johnston, L.P.
Noel, J.
Welded Tubular Connections: An Investigation of Stresses in T-Joints, American Welding Society Journal, Vol. 1, P.1-5, January, 1966.

47. Visser, W.
On the Structural Design of Tubular Joints, J. Eng. Ind. Trans., ASME, V97, SER B, N2, May, 1975.

48. Wardenier, J.
Testing and Analysis of Truss Joints in H.S.S., International Symposium on Hollow Structural Sections, Toronto, May, 1977.

49. Washio, K.
Kurobane, Y.
Kutsuno, S.
Mitsuyoshi, Y.
Research on Tubular Truss Joints, Part One, (In Japanese), AIJ Trans., No. 69, October 1961.

50. Washio, K.
Kurobane, Y.
Togo, T.
Research on Tubular Truss Joints, Part Two, (In Japanese), AIJ Trans., No. 84, April, 1963.

51. Washio, K.
Kosaka, Y.
Kurobane, Y.
Research on Tubular Truss Joints, Part Three, (In Japanese), AIJ Trans., No. 89, September, 1963.

52. Washio, K.
Togo, T.
Mitsui, Y.
Experimental Research on Local Failure of Chords in Tubular Truss Joints, (In Japanese), Trans. AIJ, No. 138, August, 1967.

53. Washio, K.
Togo, T.
Mitsui, Y.

Experimental Study on Local Failure of Chords in Tubular Truss Joints (I), Trans. AIJ, No. 850, June, 1968.

54. Washio, K.
Togo, T.
Mitsui, Y.

Experimental Study on Local Failure of Chords in Tubular Truss Joints (II), Trans. AIJ, No. 874, September, 1968.

55. Washio, K.
Mitsui, Y.
Nishida, Y.
Tanaka, T.
Hisamitsu, N.
Hozumi, S.

Study of Flat Cutting Method for End Preparation of Tube in Fabrication of Tubular Structures (1), (In Japanese), Trans. AIJ, No. 154, December, 1968.

56. Yuan, S.W.
Ting, L.

On Radial Deflections of a Cylinder Subjected to Equal and Opposite Concentrated Radial Loads, Journal of Applied Mechanics, Trans. ASME, June, 1957.

APPENDIX A

COMPREHENSIVE REVIEW OF PREVIOUS RESEARCH ON TUBULAR TRUSS JOINTS

A comprehensive review of experimental and analytical research on the behaviour of tubular truss joints is contained in this section. For clarity's sake, the past work was discussed under several different items as in the following:

A.1 Experimental Work on Conventional H.S.S. Joints

A.1.1 Joints with circular chords

Jamm (1951) tested 20 K-type tubular joints. He found that a direct connection of the tube walls was preferable to an indirect connection via gusset plates or wedges. Moreover, joints with an overlap had higher joint efficiency than joints with a gap. He indicated that a direct load transfer between web members had a favourable effect on joint strength, while the transverse force deflection due to bending of the chord wall was distinctly unfavourable.

Jamm et al. (1952) concluded that 100 percent joint efficiency could be achieved if the amount of overlap between the web members measured perpendicular to the chord face was equal to or more than 15 percent of the chord diameter. Even though the overlap might cause a negative moment, this was acceptable as long as the distance between the point of intersection of the web axes and the chord axis was less than 25 percent of the chord diameter. They considered that if d_1/d_0, the ratio of the compression web diameter to the chord diameter was large, the compression web member had to be flattened to 20 percent or 25 percent of the chord diameter in

order to localize the weld and then preserve the flexibility of the chord wall.

Anderson (1961) found that chord stresses could be reduced by increasing negative eccentricity and overlap between the web members. He also found that increasing the yield strength of the chord steel had a favourable influence on the elastic response of the entire joint.

Washio et al. (Apr. 1963) tested 65 K-type joints with profiled webs. They found that a change in the diameter of tension web member had almost no effect on the joint strength. However, joints with larger-diameter compression webs displayed high strength. They also found that negative eccentricity joints had higher strengths and smaller local bending deformation than zero or positive eccentricity joints. Like Anderson, they found that the joint strength was increased by overlapping the web members, as this allowed direct load transfer between the web members. The joint strength also increased with an increase in the thickness of chord wall.

Washio et al. (Sept. 1963) found that joints with grouted chords which failed by tearing of the tension web had higher strengths than joints with simple chords which failed by large local chord deformation.

Bouwkamp (1964), like Washio et al. (Apr. 1963) found that joints with negative eccentricity had higher strength than those with positive eccentricity. He also considered that the strength of a tubular joint was increased by overlapping the web members. He suggested that increasing the yield strength of chord steel would lead to a definite increase of the elastic load range of a tubular joint.

Kaneya (1965) found that the collapse of the chord member due to an eccentricity moment may induce the collapse of the entire truss. He recommended zero eccentricity.

Bouwkamp (1968) tested 21 N-type joints with profiled web members. He found that negative eccentricity joints had strengths superior to those of zero or positive eccentricity joints and also that joint strength increased with an increase in the thickness of chord wall as this relieved the radial bending stresses in the chord wall. Regardless of d_1/d_0 ratio, a 100 percent joint efficiency under static loads could be achieved for a zero-eccentricity joint if the chord wall thickness, t_0 was at least 5 percent of the chord diameter, while for a negative-eccentricity joint 2 percent was sufficient. He also found that additional compressive force applied to the chord did not influence the failure loads of the joints.

Washio et al. (1968) tested 33 K-type profiled gap joints. They found that joint strength increased with an increase in t_0/r_0 or d/d_0, but decreased with an increase in g/d_0 for the range of $g/d_0 < 0.2$ and remained fairly constant for the range of $g/d_0 > 0.2$. They also found that joint strength decreased with a decrease in θ_1, the angle of intersection between the compression web and the chord. On the other hand, Davie and Giddings (1971) considered that θ_1, was not a significant parameter. The joint strengths at $\theta_1 = 30°$ were found to be about 20 percent smaller than those at $\theta_1 = 90°$. Empirical formulae for calculating the effects due to different parameters were provided.

Washio et al. (1968) tested 24 K-type profiled gap joints. Unlike Bouwkamp (1968), they found that compressive loads on the chord considerably

decreased the strength of the joint, while tensile loads scarcely influenced the joint strength. They also found that the strengths of K-joints were nearly equal to those of T-joints, provided the former had large gaps between webs. However, in case of d/d_o = 0.3 to 0.6, the strengths of T-joints were 15 to 20 percent lower than those of K-joints with g/d_o = 0.2 to 0.6 which were in practical use.

Washio et al. (1968) also tested 70 X-type joints to investigate the influence of different types of end preparation on joint strength. The end preparation of the webs was carried out by an automatic gas flame cutter (the curved cutting method) and by a high speed grinder cutter (the flat cutting method). They found that the cutting method had little influence on the static strength or the low cycle fatigue strength of the joints.

Beale and Toprac (1970) tested 4 T-joints, 3 Y-joints and 4 K-joints with profiled web members. They found that the stresses around a joint were more or less uniform provided the ratio of web to chord radii (β) was large. They suggested that β = 0.5 could be taken as an optimum ratio of web to chord radii.

Reber (1973) suggested that K-joints could be treated as two independent Y-joints. Based on test results of Bouwkamp and Washio et al., he derived simple semi-empirical formulae to predict the ultimate strengths of K-joints.

Akiyama et al. (1974) tested 150 T-type, Y-type, N-type and K-type joints. Some joint stiffening methods were also investigated. Formulae for joint strength for a wide range of d_o/t_o, ($15 \leq do/to \leq 100$), were

derived. It was stressed that appropriate stiffening by increasing the chord thickness or reinforcing the chord with a stiffening ring was indispensible when d_o/t_o was large.

Pan et al. (1976) derived empirical formulae from 214 K-joint and 132 T-, T-, and X-joint load tests which included the tests done by Sammet, Nakajima, Washio, Kurobane and Kanatani. The results showed that the existing formulae of API RP 2A (1975) and Det Norske Veritas (1974), with recommended safety factors, were generally safe but might be overly conservative for some ranges of parameters.

Wardenier (1977) presented a number of empirical formulae based on experimental research on profiled joints with a gap.

A.1.2 Joints with rectangular chords

Eastwood et al. (1967) tested 60 N-type joints with circular web members and square chord members. They found that a modest overlap of the order of one-third of the web diameter resulted in a marked improvement in joint strength and substantially reduced the deformations of the joint. The complete overlap had advantages in spreading the applied load more uniformly around the web members. In addition, as for joints with round chord members, an increase in the negative eccentricity produced a marked increase in joint strength. They also found that prestressing of the chord up to the working load had little effect on ultimate strength.

Mee (1969) tested 61 N-type joints with square web members and square chord members. He found that the behaviour of the joint improved as the amount of overlap increased. Joints with partial or full overlap were more efficient than gap joints. The former had the capability to transfer

directly the axial load between the web members, the load transmitted through the chord being kept to a minimum. Joints with a gap often yielded prematurely due to the excessive local deformation of the chord wall. However, they had a large reserve of strength. The joint stiffness also increased as the degree of overlap increased up to 50 percent. However, the results showed that increasing the overlap from 50 percent to 100 percent had little effect on stiffness. The joint strength increased as the ratio of web width to chord width increased because more load was transmitted through the side walls of the chord. The joint strength also increased as the thickness of the chord increased, but only when the compression web member was wholly or partially connected to the chord, thus enabling the transmission of web forces through the chord. The overall behaviour of the joints was similar to that of joints with circular web members having the same square chord and equal ratio of web width to chord width. If there was no overlap, the latter had larger local deflection and strength. In all tests, although the chord member was severely loaded, the results were similar to those for similar joints with zero chord preload.

Eastwood and Wood (1970) found that the degree of overlap affected not only the static strength but also the low-cycle fatigue strength of the joints. The greater the degree of overlap, the smaller the deflections in the chord face and the greater the resistance to fatigue. Where the overlap was not less than 50 percent of the cross-section of the web members, the load factor was generally of the order of 2 or more. Distortion of chord face was very modest and almost unnoticeable in cases where the over-

lap was greater than 50 percent.

Davie and Giddings (1971) tested 30 N-type gap joints and one Warren joint between rectangular chord members and circular or rectangular web members. Like Mee (1969), they found that the results obtained on joints with square web members were similar to those obtained on joints with circular web members. They also found that joints with square chord members had higher strengths than joints with rectangular chord members having the same width of connected chord face.

A.2 Experimental Work on Flattened-Web and Cropped-Web Joints

A.2.1 Joints with circular chords

Jamm (1951) found that flattened joints with an overlap could achieve 100 percent joint efficiency.

Anderson (1961) tested 11 profiled and 12 cropped N-type joints. He found that the two types of joints had identical ultimate strengths, though the profiled joints displayed a more uniform distribution of chord stress and had much lower maximum stresses. For the latter, the maximum chord stress occurred in the crotches and it decreased rapidly as the region adjacent to the overlap of the web members was approached. For the former, the maximum stresses occurred adjacent to the flanks, though they were not much larger than those in the crotches. He recommended cropping as a safe and economical alternative way of joint fabrication, provided the loads were static.

Washio et al. (1961) tested 24 K-type joints. Two series of tests were conducted, each involving nine profiled joints and three flattened joints. The only difference between the two series was that the latter had smaller tension web members. Unlike Anderson (1961), they found that for the first series, the flattened joints had only about half the ultimate strength of the profiled joints with similar configurations, and that for the second series, the ultimate strength of the flattened joints was about 30% lower than that of the profiled joints. Moreover, the flattened joints had larger local deformations of chord face than the profiled joints.

Hlavacek (1973), like Washio et al. (1961) found that the ultimate strength in terms of joint efficiency of flattened joints was about 20 percent lower than that of profiled joints. He suggested that the flattened ends should be shorter than 20 to 30 mm. He also found that joint strength increased with overlap and negative eccentricity, and that compressive load in the chord had only a small effect on the strength of a joint.

A.2.2 Joints with rectangular chords

Morris et al. (1974) tested 18 N-type truss joints with flattened-end webs and round or square chords. They found that joints with square

chord members were about one third as stiff as similar joints with round chords. Moreover, the former had yield loads about 25 percent and ultimate loads about 10 percent lower than the latter. They also found that the ultimate strengths of the flattened joints with an overlap was not significantly lower than that of similar profiled joints. The direction of web member end flattening (flattening in the plane of the truss, or perpendicular to that plane) had little effect on the yield load, the ultimate load and the stiffness of joint. The joint eccentricity had a very significant effect on joint stiffness but only a minor effect on yield and ultimate load. The joint deformations contributed little to the overall truss deflection.

Morris and Thiensiripipat (1977) tested 34 N-type joints with square chords and round end-cropped webs. They found that the strengths of cropped-web joints were comparable to those for conventional profiled gap joints. Joint strength increased as overlap increased from zero to fifty percent, but further increase in overlap had no effect on joint strength. Joint stiffness on the other hand increased as overlap increased but was not affected by the change in the ratio of web diameter to chord width. They recommended 50 percent overlap joints because zero overlap joints contributed to truss deflection about four times as much as did 50 percent or 75 percent overlap joints. The contribution of joint deformation to truss deflection increased substantially when the ratio of chord thickness to chord width was smaller than 0.05.

A.3 Existing Analytical Methods

Because of the complexity of the three-dimensional geometrical configuration of tubular joints, including the abrupt discontinuities in the surface geometry at the intersection of the webs and the chord, the theoretical analysis of tubular joints becomes very complicated and laborious and sometimes unrewarding. However, a number of investigators have tackled the problem with some success.

Timoshenko (1940) provided the basic equations that govern the behaviour of a cylindrical shell subject to radial loading. The set of equations consists of three simultaneous partial differential equations which are of the second, the third and the fourth order respectively. The behaviour of a cylindrical chord when subjected to bending and shear stresses through the web members may be analysed by solving those equations. Bijlaad (1955) assumed the cylindrical shell to be simply supported at the ends and reduced those equations to an eight-order ordinary differential equation by assuming the ratios, t_o/d_o smaller than 0.1. He solved the equation by expanding the loads and displacements into double Fourier series. Fujimoto *et al.* (1963) used Bijlaad's method to analyse a T-type tubular joint and found that the stresses and displacements predicted by this method agreed very well with the experimental results. However, Noel *et al.* (1969) found that Bijlaad's stresses were not consistent with the actual stresses when $d/d_o > 0.2$.

Yuan and Ting (1957), however, considered that Bijlaad's method was tedious because the approximation by means of double Fourier series required a large number of terms. They suggested that without a digital computer,

it was necessary to avoid the method of double Fourier series. Instead, in order to solve the equations more simply, they suggested that the loads and the displacements be represented in the longitudinal direction by a Fourier integral and in the circumferential direction by a Fourier series.

Johnston (1963) used the shear area method to predict the strength of a T-type joint, in which an axial load in the web was assumed to be carried in direct shear by the chord wall. However, this method completely ignored bending and membrane stresses in the chord wall, stresses which were almost certainly the critical considerations (Toprac 1966).

Redwood (1965) used a finite difference solution of the governing thin plate equation to analyse the loaded chord face of a T-type joint with rectangular web and chord. Results obtained agreed well with experimental results which were found for brass plates.

Eastwood et al. (1967) used a beam on elastic foundation analogy to investigate the behaviour of an N-type joint. In this method, the modulus of reaction of the elastic foundation was replaced by the stiffness of the cross-section of the tube acting as a portal frame and carrying a concentrated load in the middle of the connected side. The stiffness of the beam was replaced by the stiffness in the longitudinal direction of the tube wall. This analysis suffered from the disadvantage that it was based on point loads, whereas in practice the web member load is applied around the periphery of the tube. They used the elastic theory of thin plates and a finite difference method to analyse the local deformation and stresses in N-type joints with rectangular chords and rectangular or

circular web members. The loaded chord face was considered separately from the rest of the chord member, and the boundary conditions were in the form of a moment-rotation and reaction relationship in order to simulate approximately the effects of the chord side-walls. The application was limited as deflection loadings were used rather than actual loads and there was no way to ensure that the vertical compressive load would balance the vertical tension load.

Scordelis et al. (1970) used the classical thin shell theory to analyse a T-type joint. Unlike Bijlaad (1955) and Yuan and Ting (1957), they used a Fourier series to represent the loads and the displacements in the longitudinal direction. Specified loadings or displacements were applied to a cylindrical shell tube to simulate a typical T-type joint. Results compared well with experimental results from Noel et al.'s (1965) study, but this was limited to simple geometries like T-joints and the stiffness of the web member was not considered.

Dasgupta (1970), Kuang (1975), Visser (1975), Liaw (1976) and Thiensiripipat (1979) used the finite element method to study the behaviour of tubular joints. Different types of elements were used in the analyses. Dasgupta and Thiensiripipat used a four-noded isoparametric quadrilateral flat plate element, while Kuang used both triangular and quadrilateral flat plate elements. Visser, on the other hand, used a curved plate element with quadrilateral or triangular shapes. Liaw, taking account of the variation of displacement through the thickness of the shell and the effects of transverse shear distortion, used a three-dimensional isoparametric shell element.

Dasgupta found that the secondary truss moment increased considerably with a decrease in the ratio of the web-to-chord diameter as the latter increased the axial flexibility. He also found that the secondary moments due to positive eccentricity cause unfavourable stresses at the joint, and the secondary moments due to negative eccentricity would relieve the stresses. Kuang provided formulae for estimating stress concentration factors (SCF) in simple non-reinforced tubular joints and he criticized Visser's prediction of SCF as being overly conservative in all cases. Liaw concluded that the use of three dimensional shell elements in the analysis of welded tubular connections could provide accurate modelling of the highly stressed zones near the welds. However, the practical application of this type of elements required a very general mesh generation capability, a high computational efficiency and extensive input and output data handling options. Thiensiripipat found that the finite element method could be used to predict the load-deformation behaviour and stress distribution of a cropped-web joint up to a load of about half the ultimate load of the joint. He considered that the method could be extended to include inelastic and large displacement behaviour so that the joint strength could be estimated.

Mouty (1977) used yield-line theory to predict the ultimate loads of tubular joints including T-, Y-, K- and N-type joints with or without overlap. Usually the predicted ultimate loads were smaller than or equal to the experimental values.

Analytical methods have had little success because of the geometric and computational complexities involved. The finite element method can be used to predict the elastic load-deformation behaviour of some types of

joints, but the high cost in engineering time required for preparation of mesh data and the large computer time spent on solving a large set of linear equations, say, with the Gaussian elimination method, still make its extensive use impossible. Moreover, unless a finite element model has taken account of the inelastic behaviour of the material, and the overall and local instability of the individual members at the joint, it is not applicable in predicting the plastic behaviour as well as the strength of the joint. Thus, the experimental approach seems most practical and reliable.

A.4 Summary of Past Work

From the results of previous work on tubular truss joints, the following can be summarized:

(1) The strength of a tubular truss joint is increased by:

a. an increase in the ratio of the thickness to diameter of the chord member, t_o/d_o, as this increases the stiffness of the chord member and relieves the bending stresses in the chord;

b. an increase in the ratio of the web diameter to chord diameter, d/d_o, as this improves the load transfer and the web member forces are transmitted more directly to the side walls of the chord;

c. an increase in the ratio of overlap to web diameter, q/d_2, as this allows direct load transfer between the web members, and so the load transmitted through the chord is kept to a minimum;

d. an increase in the negative eccentricity, e, as this reduces the stresses in chord;

e. an increase in the angle of intersection between the compression web member and the chord member, θ_i, as this decreases the longitudinal component of applied load, which influences the joint strength; and,

f. an increase in the yield strength of the chord steel as this delays the development of yielding in the chord member.

(2) Jamm and Anderson found that the flattened-end joints and cropped-end joints with circular chords had strengths similar to those of conventional profiled joints, while Washio et al. and Hlavacek found that flattened-end joints had lower strength than profiled joints.

(3) The strengths of overlapping flattened-end joints and cropped-end joints with rectangular chords are close to those of conventional profiled joints.

(4) Washio et al. found that compressive loads in the chord decreased the joint strength considerably and the tensile loads scarcely influenced the joint strength, while Bouwkamp, Eastwood et al. and Hlavacek found that the compressive loads on the chord had little effect on the joint strength.

(5) The strength of isolated truss joints is higher than that of the joints in an actual truss.

(6) Analysis by means of the finite element method can be used to predict the elastic load-deformation behaviour of some types of joints, but it is costly, time consuming and not practical.

APPENDIX B

EXISTING DESIGN SPECIFICATIONS

The Canadian Standard (CSA Standards S16.1-1974, S16.1-M78, 1978) and the AISC Specification (Specification for the Design, Fabrication and Erection of Structural Steel for Buildings, 1969) give little direct guidance for the design of tubular structures. Most of the design suggestions contained in the AISI publication, "Tentative Criteria for Structural Applications of Steel Tubing and Pipe (Aug. 1976)" and the Steel Company of Canada's publication, "Hollow Structural Sections Design Manual for Connections" are based on European and Canadian research which has been sponsored by CIDECT (Comite International pour le Developpement et l'Etude de la Construction Tubulaire).

The relevant British Standards (B.S. 1775, Addendum No. 1, and C.P. 113:201) and Japanese Specifications (AIJ "Specifications for Tubular Structures") give more specific design guidance for tubular structures.

Several of the provisions of the various specifications are compared in Table B.1, the data for which were obtained by making reference to the work of Bouwkamp (1964), Kaneya (1965), Mee (1969) and Cran et al. (1971). Reference was also made to CSA Standard S16.1-1974 and S16.1-M78.

TABLE B.1: Comparison of Various Design Specifications of Tubular Structures.

	U.K.	GERMANY	JAPAN	CANADA	U.S.A.
Angle of Intersection	>30°	>30°	>30°		
Minimum diameter ratio, d/d_o	>0.33	>0.40 except secondary members >0.25	>0.25		
Ratio of thickness to diameter t/d	$t \geq 0.1 \sqrt[3]{d}$			$t/d \geq \frac{f_y}{3300}$ for round hollow sections $t/b \geq \frac{\sqrt{f_y}}{255}$ for rectangular hollow sections	$t/d \geq \frac{f_y}{3300}$
Ratio of Web to chord thickness, t/t_o			$t/t_o < 1$		

N.B. The thickness t and the diameter d are both in inches.
The specified minimum yield strength f_y is in ksi.

APPENDIX C

MATERIAL TESTING

The properties of the steel in chord and web members of the joints were determined from tension tests of specimens, which were cut from the walls of sample tubes. The tension tests were carried out according to ASTM Standards A370 (1979). The dimensions of the test specimens are given in Table C.1, and the results of the tension tests in Table C.2. The load-deformation curves of the test specimens are illustrated in Fig. C.1 to Fig. C.5.

The offset method specified in ASTM Standards A370 (1979) was used to determine the yield strength.

TABLE C.1: Dimensions of Test Specimens

	Specimen No. 1	Specimen No. 2	Specimen No. 3	Specimen No. 4	Specimen No. 5
Thickness (mm)	3.02	2.92	2.92	4.22	5.89
Width (mm)	12.78	12.88	12.65	12.70	12.73
Radius of fillet (mm)	12.70	12.70	12.70	12.70	12.70
Over-all length (mm)	295.40	295.66	295.40	301.75	298.45
Length of reduced section (mm)	57.40	57.66	57.66	57.91	57.66
Length of grip section (mm)	113.03	113.03	113.03	115.57	113.79
Width of grip section (mm)	22.35	22.35	22.35	24.89	25.15

TABLE C.2: Results of Tension Tests

Specimen No.	Proportional Limit (MPa)	Yield Point (MPa)	Yield Strength at 0.2% offset(MPa)	Ultimate Strength (MPa)	Young's Modulus (MPa)
1	282.5	344.5	374.1	560.9	207,000
2	261.8	344.5	368.6	553.1	207,000
3	268.7	372.1	399.6	567.5	207,000
4	227.4	330.7	348.0	518.8	207,000
5	220.5	344.5	354.8	525.2	207,000

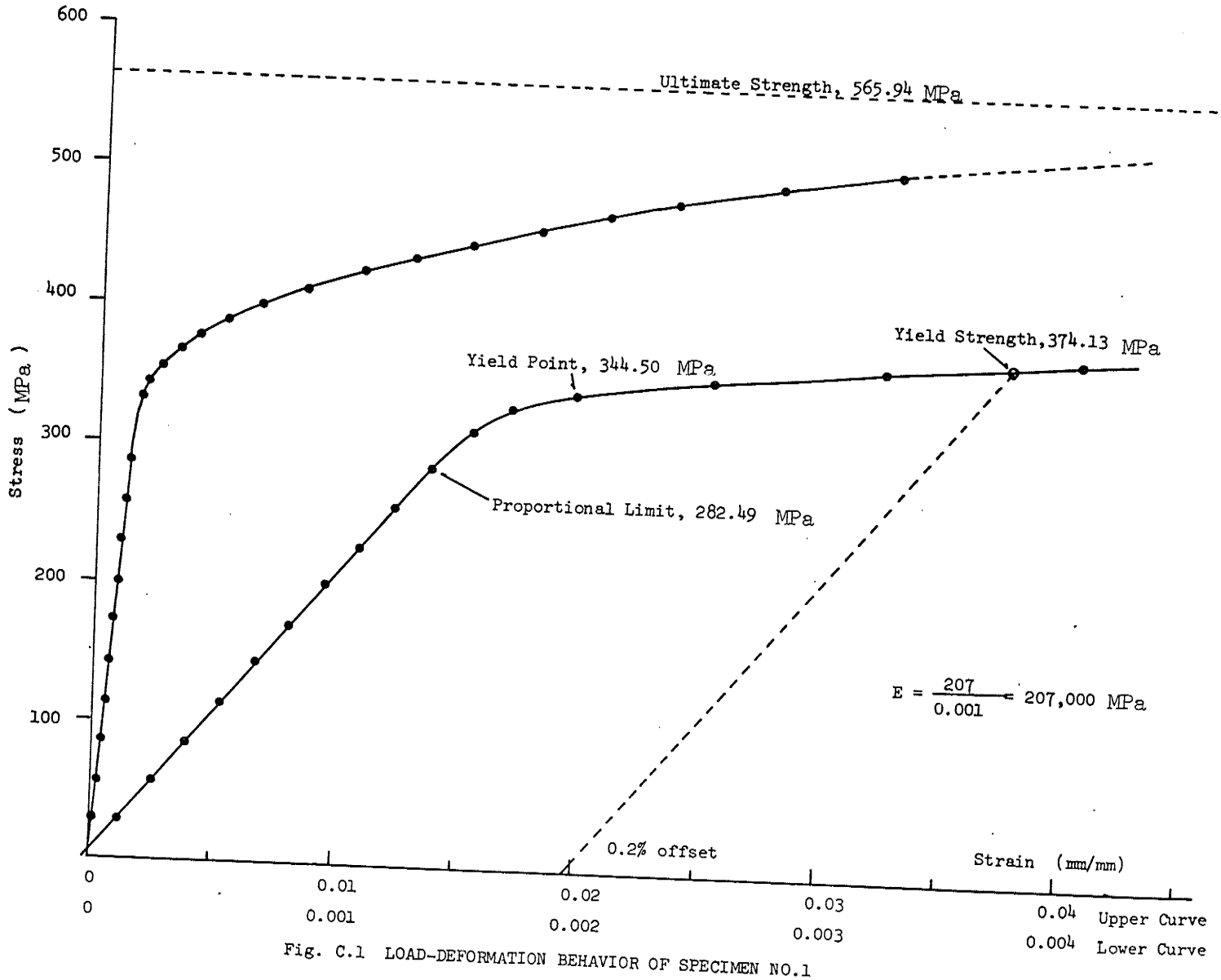

Fig. C.1 LOAD-DEFORMATION BEHAVIOR OF SPECIMEN NO.1

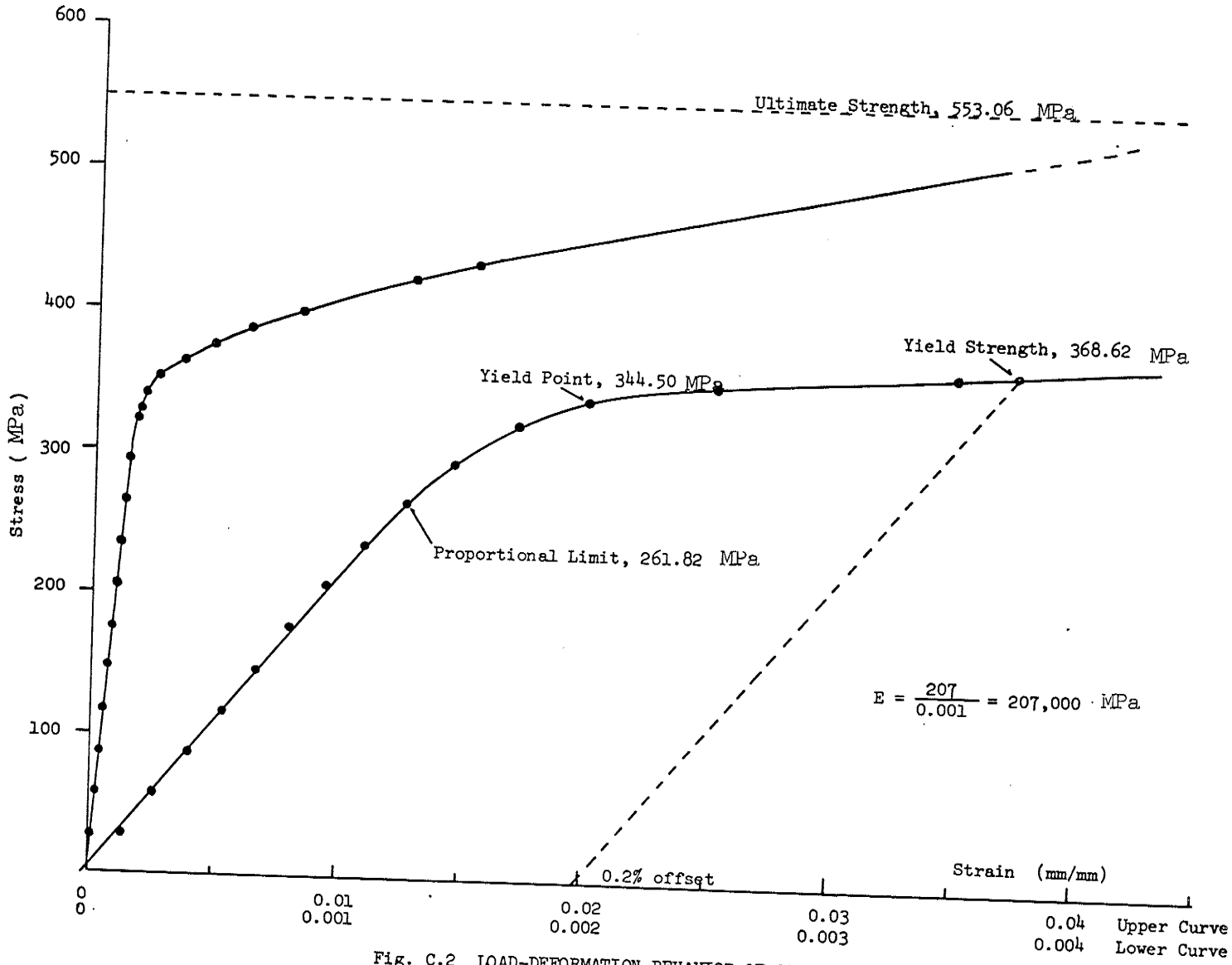

Fig. C.2 LOAD-DEFORMATION BEHAVIOR OF SPECIMEN NO.2

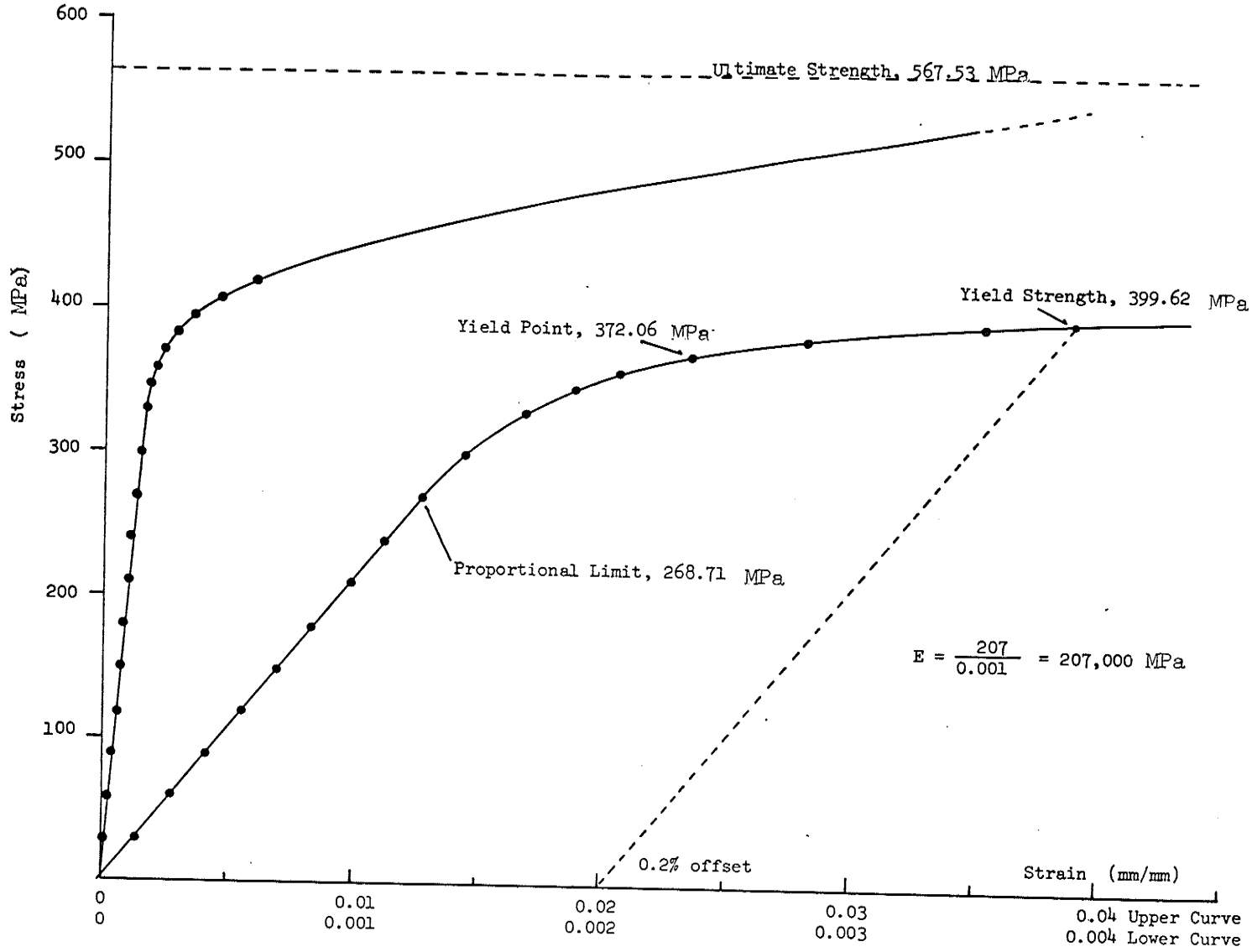

Fig. C.3 LOAD-DEFOFMATION BEHAVIOR OF SPECIMEN NO.3

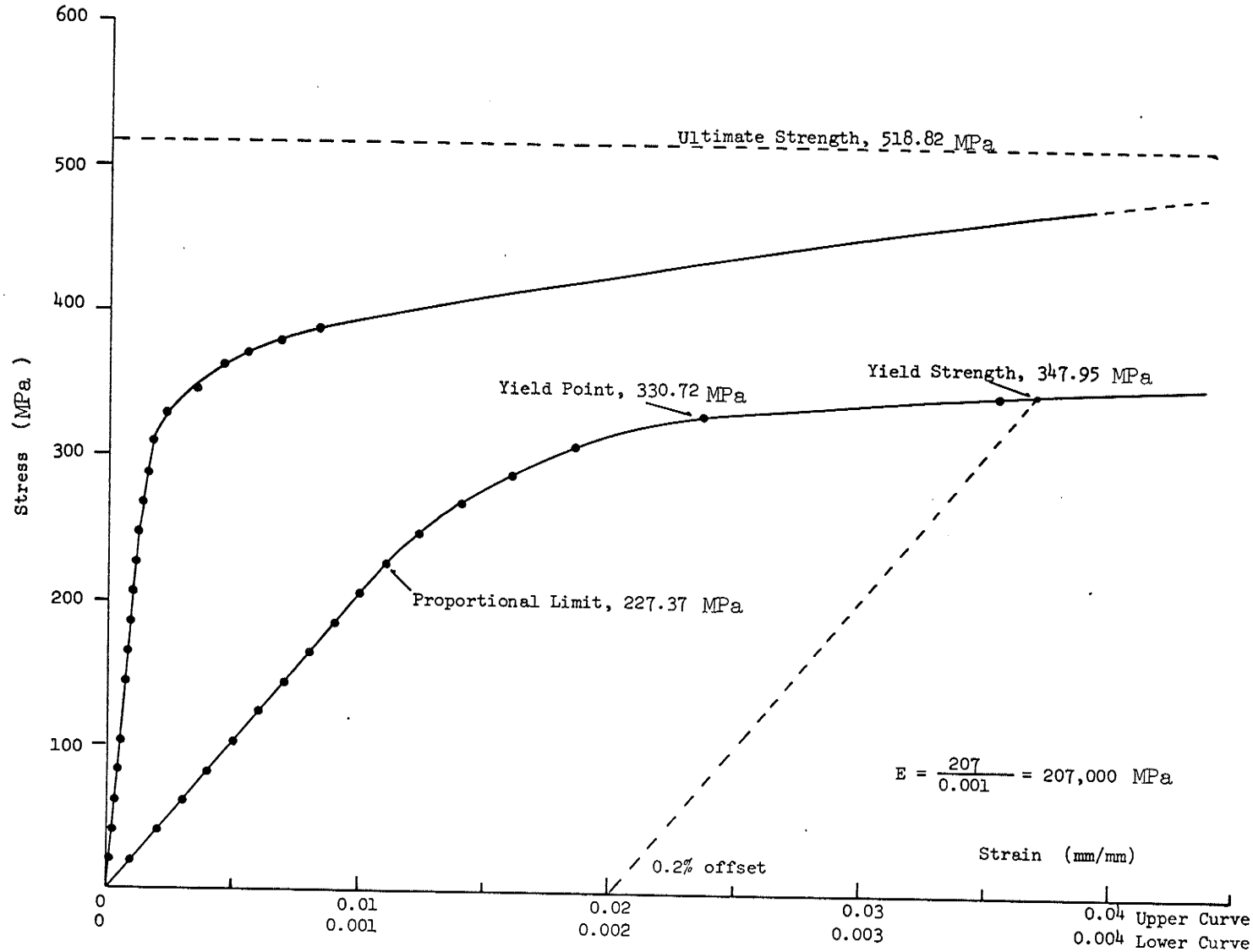

Fig. C.4 LOAD-DEFORMATION BEHAVIOR OF SPECIMEN NO.4

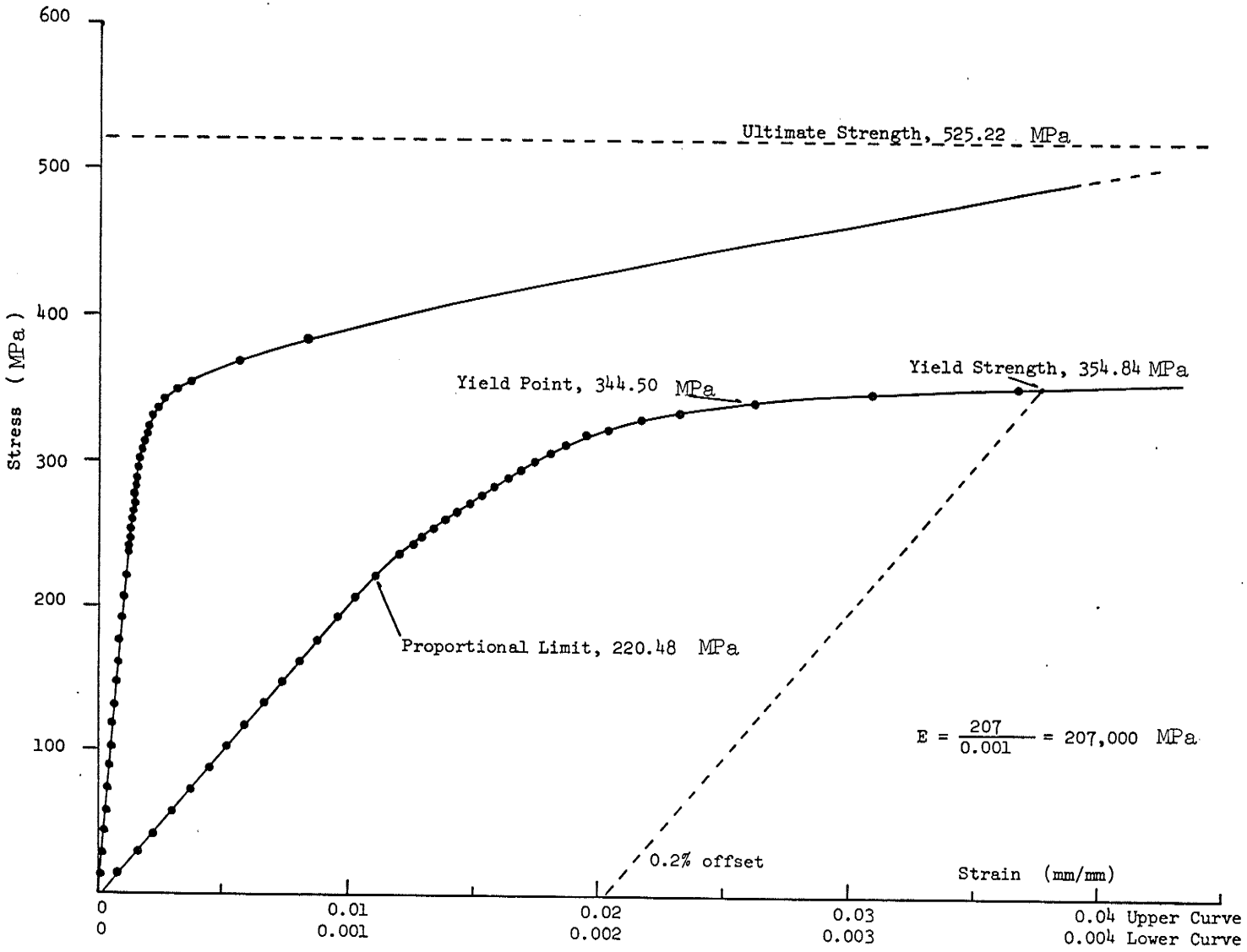

Fig. C.5 LOAD-DEFORMATION BEHAVIOR OF SPECIMEN NO.5

APPENDIX D

CALIBRATION OF PRESTRESSING BARS

REBAR LOAD CELL #1

	LOAD kN	STRAIN %
1		
2	-6.559	0.008
3	-13.006	0.015
4	-19.876	0.023
5	-26.489	0.031
6	-33.231	0.039
7	-39.847	0.046
8	-46.495	0.054
9	-53.074	0.062
10	-59.661	0.069
11	-66.293	0.077
12	-73.251	0.085
13	-79.926	0.093
14	-86.580	0.101
15	-93.212	0.108
16	-99.786	0.116
17	-106.423	0.124
18	-113.093	0.131
19	-119.715	0.139
20	-126.360	0.147
21	-133.024	0.155
22	-139.686	0.163
23	-146.316	0.170
24	-152.921	0.178
25	-159.596	0.186
26	-166.229	0.194
	-172.832	0.201

* * * * * * * * * * * *

REBAR LOAD CELL #2

	LOAD	STRAIN
	kN	%
1	-6.871	
2	-13.353	0.008
3	-19.898	0.016
4	-26.488	0.024
5	-33.265	0.031
6	-39.839	0.039
7	-46.690	0.047
8	-53.365	0.055
9	-59.989	0.062
10	-66.576	0.070
11	-73.283	0.078
12	-79.878	0.086
13	-86.508	0.093
14	-93.177	0.101
15	-99.871	0.109
16	-106.482	0.117
17	-113.082	0.124
18	-119.789	0.132
19	-126.403	0.140
20	-133.040	0.148
21	-139.673	0.155
22	-146.724	0.163
23	-153.407	0.172
24	-160.050	0.179
25	-166.728	0.187
26	-173.421	0.195
27	-180.035	0.203
		0.211

* * * * * * * * * * * *

REBAR LOAD CELL #3

	LOAD	STRAIN
	kN	%
1	-6.801	0.008
2	-13.347	0.016
3	-19.864	0.024
4	-26.480	0.032
5	-32.882	0.039
6	-39.822	0.048
7	-46.430	0.055
8	-53.084	0.063
9	-59.687	0.071
10	-66.265	0.079
11	-73.234	0.087
12	-79.893	0.095
13	-86.525	0.103
14	-93.203	0.111
15	-99.857	0.119
16	-106.457	0.127
17	-113.076	0.135
18	-119.722	0.142
19	-126.418	0.150
20	-133.010	0.158
21	-139.696	0.166
22	-146.269	0.174
23	-153.438	0.183
24	-160.063	0.191
25	-166.727	0.199
26	-173.383	0.207
27	-180.074	0.215

* * * * * * * * * * * *

REBAR LOAD CELL #4

	LOAD	STRAIN
	kN	%
1	-6.846	
2	-13.362	0.008
3	-19.873	0.016
4	-26.423	0.024
5	-32.860	0.032
6	-39.405	0.039
7	-45.954	0.047
8	-52.504	0.055
9	-59.053	0.063
10	-65.616	0.071
11	-72.165	0.079
12	-78.678	0.086
13	-85.206	0.094
14	-91.753	0.102
15	-98.275	0.110
16	-104.817	0.118
17	-111.332	0.125
18	-117.927	0.133
19	-124.516	0.141
20	-131.023	0.149
21	-137.583	0.157
22	-144.098	0.165
23	-150.639	0.173
24	-157.186	0.181
25	-163.744	0.188
26	-172.883	0.196
27	-179.526	0.207
		0.215

* * * * * * * * * * * *

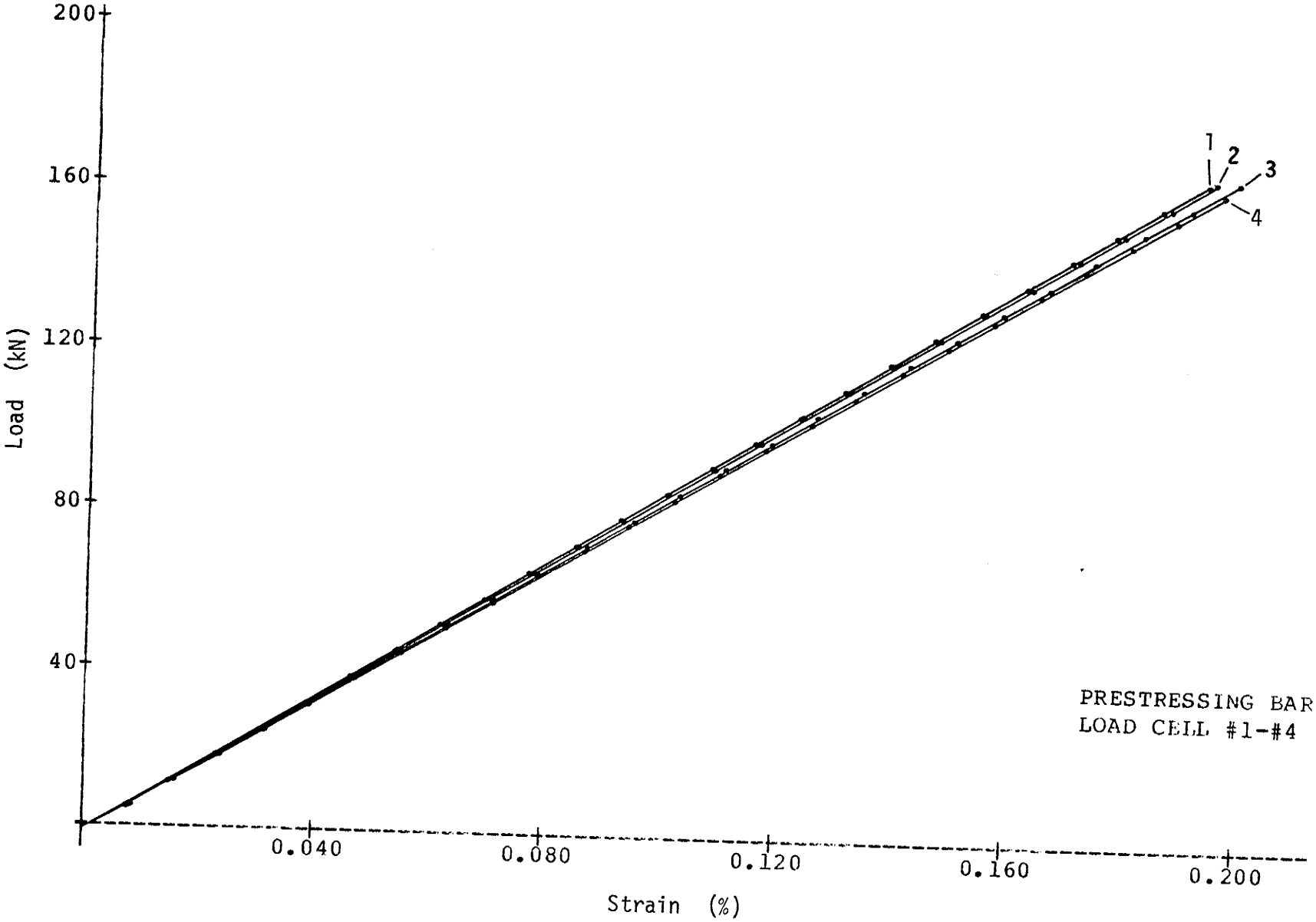

Fig. D.1 CALIBRATION OF PRESTRESSING BARS

APPENDIX E

MEASUREMENT OF TENSILE FORCES IN PRESTRESSING BARS

This appendix includes the measured values of the tensile forces, $F_i (i = 1, 2, 3, 4)$ in the prestressing bars. They were plotted against the tension web load as shown in Fig. E.1 to Fig. E.6. The specified values of F_i are also included in the figure.

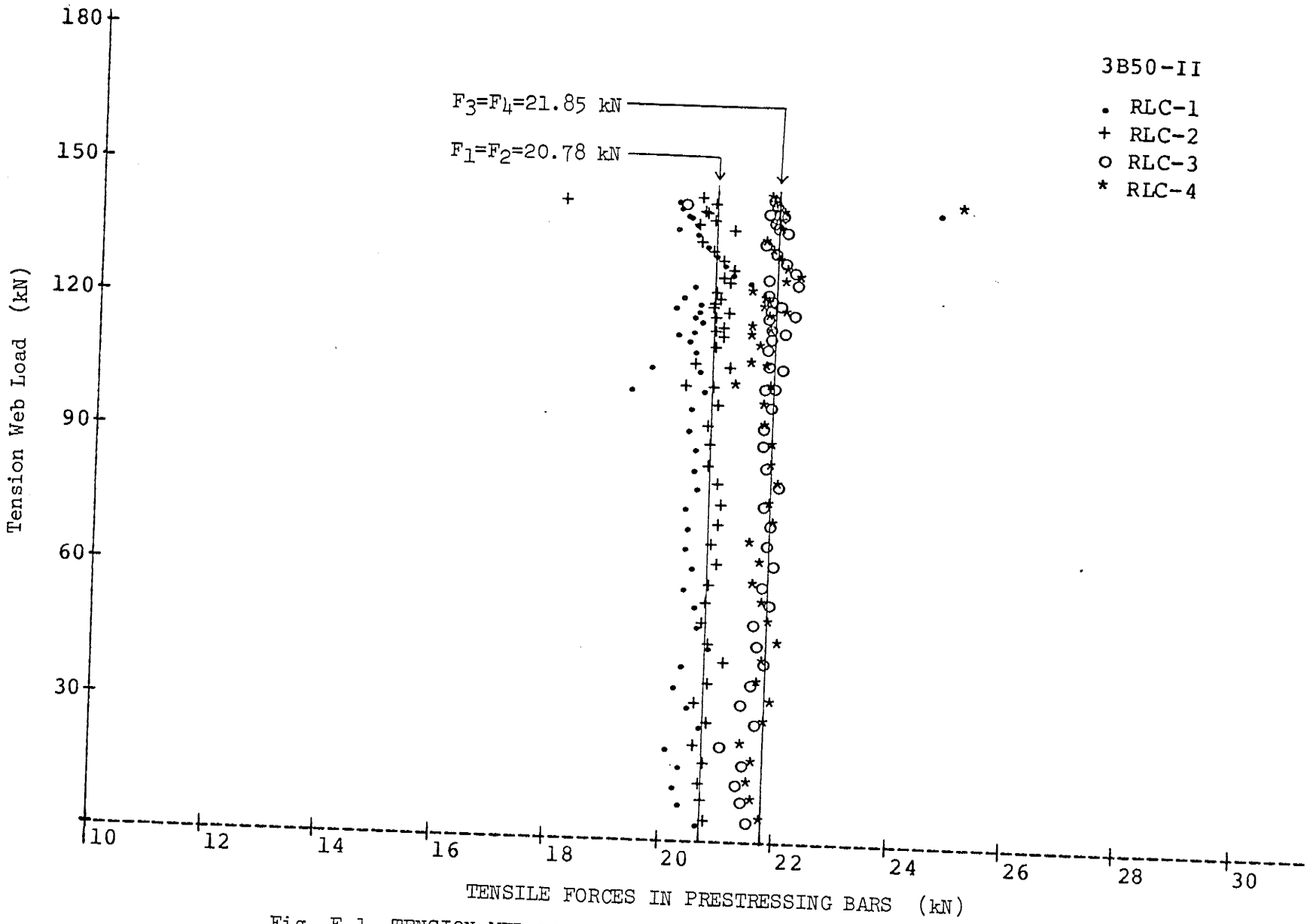

Fig. E.1 TENSION WEB LOAD VS. TENSILE FORCES IN PRESTRESSING BARS

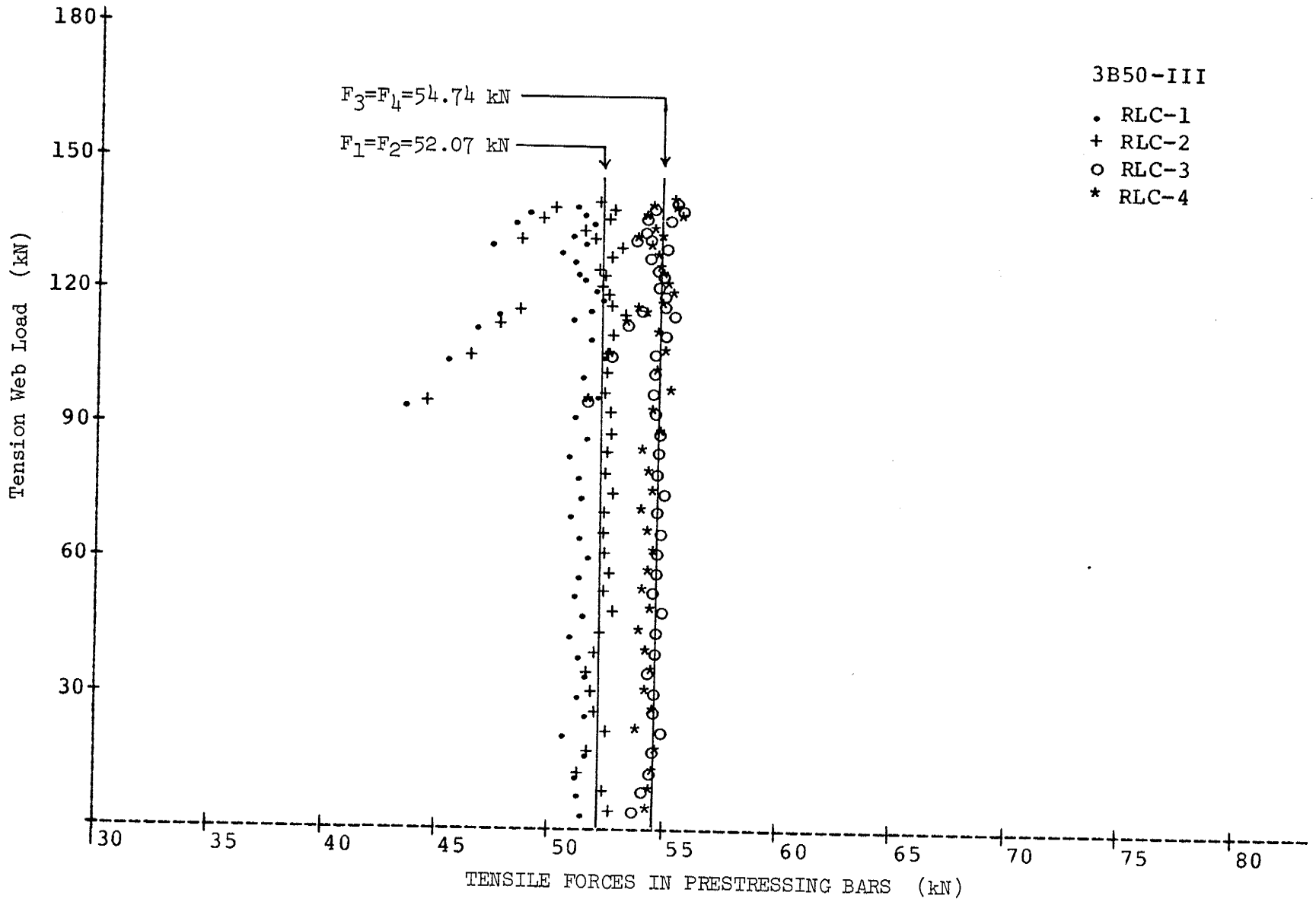

Fig. E.2 TENSION WEB LOAD VS. TENSILE FORCES IN PRESTRESSING BARS

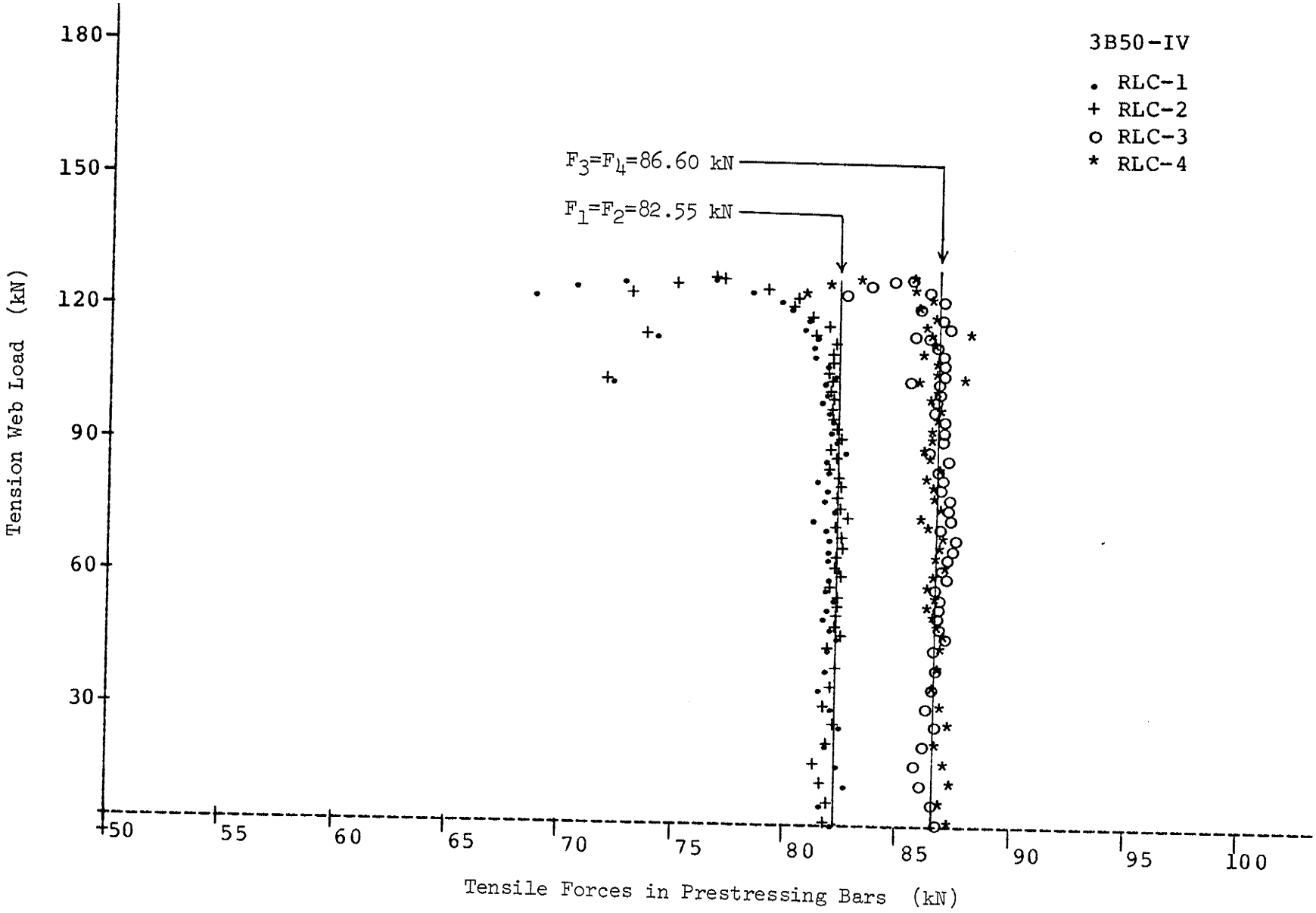

Fig. E3. TENSION WEB LOAD VS. TENSILE FORCES IN PRESTRESSING BARS

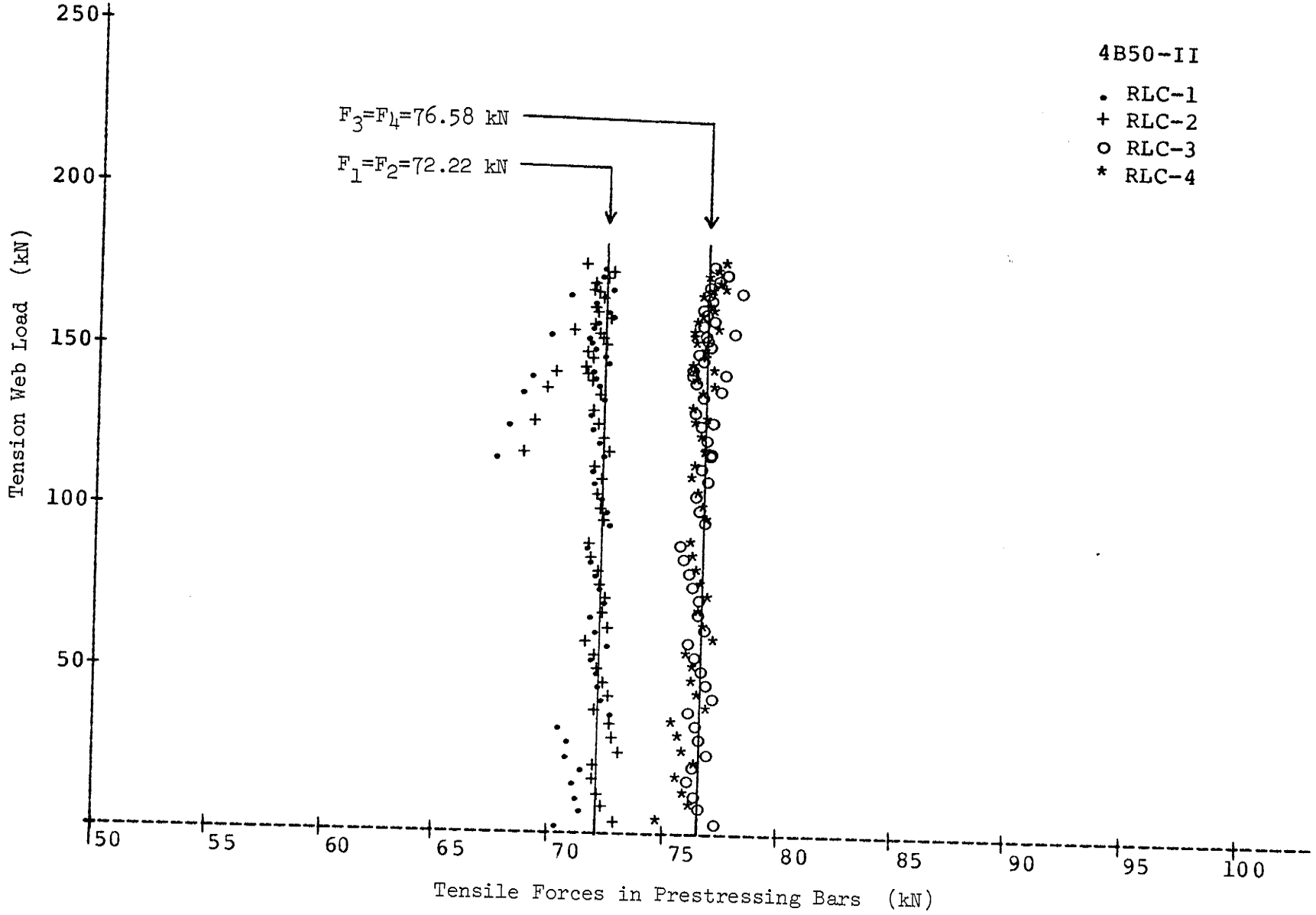

Fig. E.4 TENSION WEB LOAD VS. TENSILE FORCES IN PRESTRESSING BARS

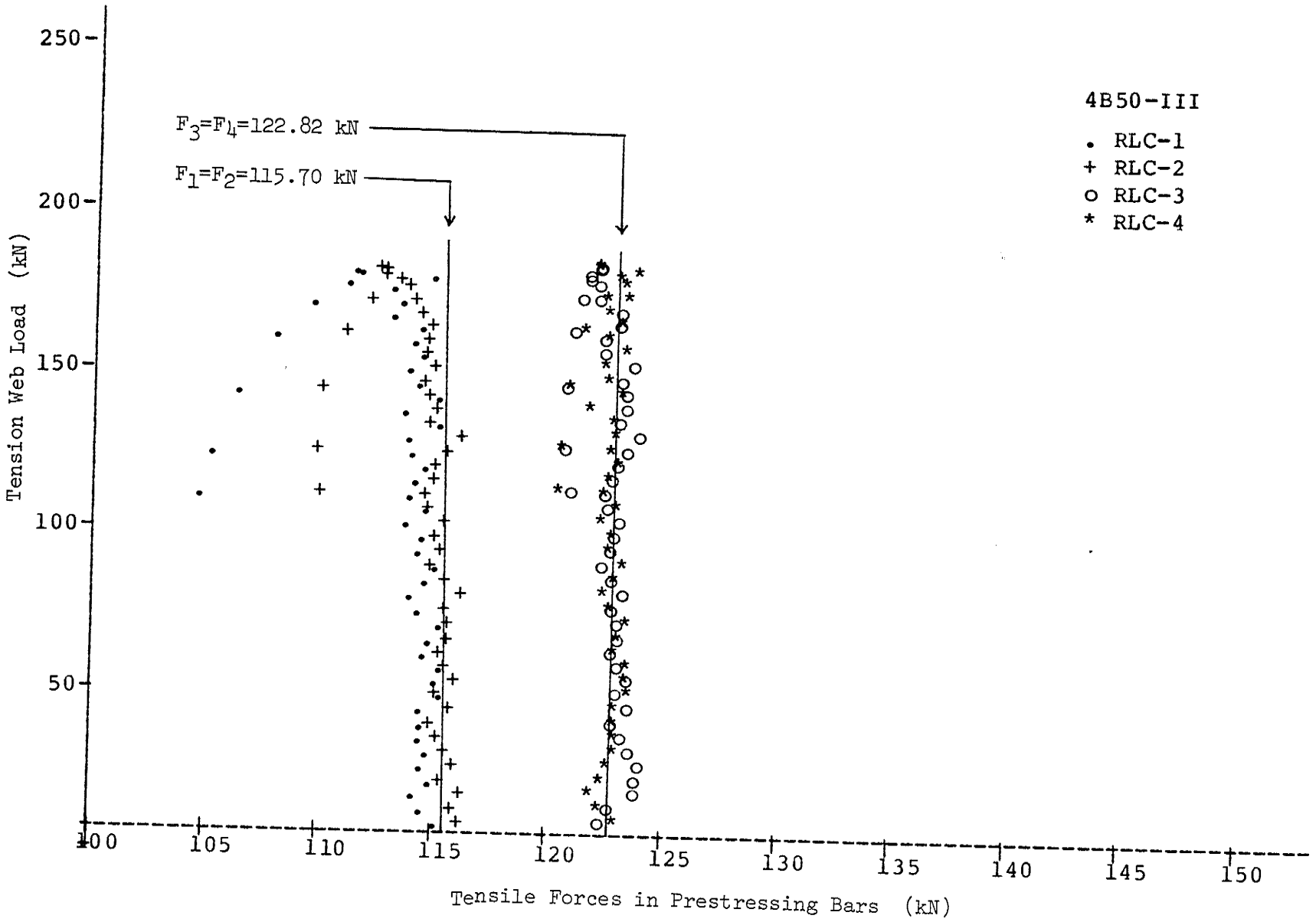

Fig. E.5 TENSION WEB LOAD VS. TENSILE FORCES IN PRESTRESSING BARS

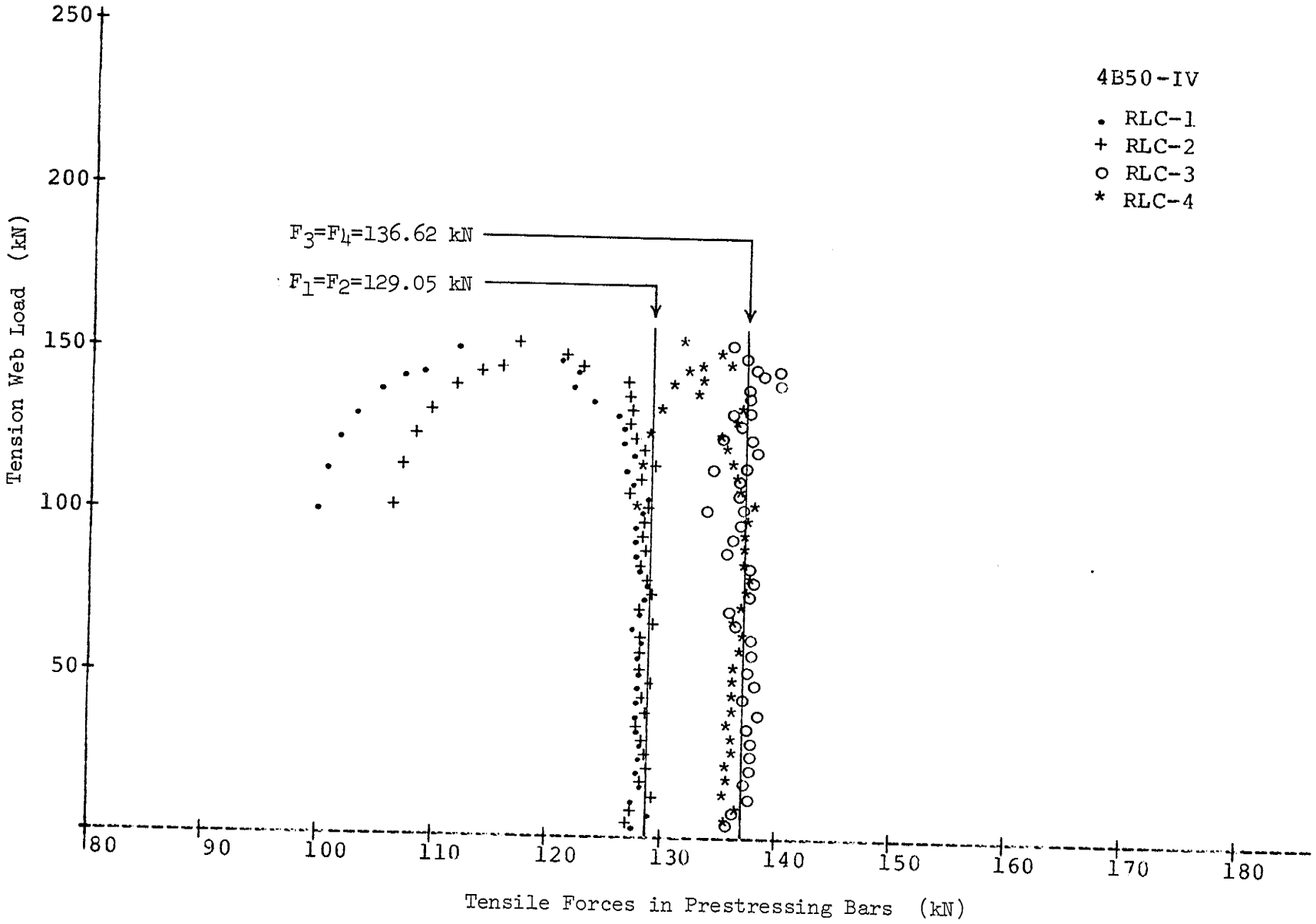

Fig. E.6 TENSION WEB LOAD VS. TENSILE FORCES IN PRESTRESSING BARS